UC Merced
UC Merced Electronic Theses and Dissertations

Title
Understanding the Role of Sclerostin in Post-Traumatic Osteoarthritis Development in Mice

Permalink
https://escholarship.org/uc/item/0dt4g2wp

Author
Chang, Jiun Chiun

Publication Date
2016

Copyright Information

Peer reviewed|Thesis/dissertation

UNIVERSITY OF CALIFORNIA, MERCED

Understanding the Role of Sclerostin in Post-Traumatic Osteoarthritis

Development in Mice

A DISSERTATION SUBMITTED IN PARTIAL SATISFACTION OF THE

REQUIREMENTS FOR THE DEGREE DOCTOR OF PHILOSOPHY

in

Quantitative and Systems Biology

by

Jiun Chiun Chang

Committee in charge:

Dr. David M. Ojcius, Chair

Dr. Miriam Barlow

Dr. Ajay Gopinathan

Dr. Gabriela G. Loots

Spring 2016

Signature Page

The Dissertation of Jiun Chiun Chang is approved, and it is acceptable in quality and form for publication on microfilm and electronically:

_____

Dr. Gabriela G. Loots

_____

Dr. Miriam Barlow

_____

Dr. Ajay Gopinathan

_____

Dr. David M. Ojcius, Chair

_____

Date

University of California, Merced

Spring 2016

Dedication

In recognition of my family, I dedicate my work to my mom, dad, brother and love. Furthermore, to a few true friends that without whom this work would not be possible. I am eternally grateful for all of your support, love and care. Thank you all for being here with me throughout this journey.

Table of Contents

LIST OF ABBREVIATIONS

AC – Articular cartilage

ACL – Anterior cruciate ligament

Agn – Aggrecan (Agn)

BMP – Bone morphogenetic protein

BV/TV – Bone Volume per Total Volume

cKO – Conditional knock-out

Col2a1 – Collagen type II

DMM – Destabilization of the Medial Meniscus

DKK1 – Dickkopf-1

ECM – Extracellular matrix

FPKM – Fragments per Kilobase of Transcript per Million Mapped Reads

Grem – Gremlin

GP – Growth plate

GWAS – Genome Wide Association Studies

HA – Hyaluronic Acid

IA – Intra-articular

IAF – Intra-articular fracture

LncRNA – Long non-coding RNA

Nog – Noggin

NSAIDs – Non-Steroidal anti-Inflammatory Drugs

PTOA – Post-traumatic steoarthritis

MMP – Matrix Metalloproteinase

LRP – Low-density lipoprotein

IHC – Immunohistochemistry

OA – Osteoarthritis

OB – Osteoblasts

OC – Osteocytes

RA – Rheumatoid Arthritis

RNASeq – RNA Sequencing

Sost – Sclerostin

SySADOAs – Symptomatic Slow Scting-Drugs for Osteoarthritis

TC – Tibial Compression

TIMPs – Tissue Inhibitors of MMPs

uCT – Micro-Computed Tomography

LIST OF FIGURES

LIST OF TABLES

ACKNOWLEDGEMENT

VITAE

2016   Doctor of Philosophy in Quantitative and Systems Biology (QSB)
University of California, Merced with Lawrence Livermore National Laboratory (LLNL) affiliation.

2009   Masters of Science, Quantitative and Systems Biology
University of California, Merced

2007   Bachelors of Science Biological Sciences, Biochemistry
University of California, Merced

Publications

<u>J Chang</u>, B Christiansen, N Collette, A Sebastian, D Murugesh, N Hum, S Hatsell, A Economides, C Blanchette and G Loots (2016 in preparation), *SOST/Sclerostin Reduces the Severity of Post Traumatic Osteoarthritis by Inhibiting MMPs.*

<u>J Chang</u>, A Sebastian, D Murugesh, S Hatsell, A Economides, B Christiansen and G Loots, *Global Molecular Changes in a Tibial Compression Induced ACL Rupture Model of Post-Traumatic Osteoarthritis.* Journal of Orthopedic Research. 2016

N Fischer, D Weilhammer, A Dunkle, C Thomas, M Hwang, M Corzett, C Lychak, W Mayer, S Urbin, N Collette, <u>J Chang</u>, G Loots, A Rasley and C Blanchette (2014), *Evaluation of Nanolipoprotein Particles (NLPs) as an in vivo Delivery Platform.* PLoS One. 2014

<u>J Chang</u>, M Szaszák, W Leng, J Rupp, D Ojcius and A Kelley, *Characterizing the Intracellular Distribution of Metabolites in Intact Chlamydia-Infected Cells by Raman and Fluorescence Microscopy.* Microbes Infect. 2013

Awards

2013-2015   *American Society for Bone and Mineral Research (ASBMR) Conference Travel Award*

2014   *Quantitative and Systems Biology Travel Award,*
University of California Merced

2013-2014   *Quantitative and Systems Biology Summer Fellowship*,
University of California Merced

2008   *Outstanding Graduate Student Teacher,*
University California Merced

Presentations

ASBMR 2015 Concurrent Oral: *Sost Protects Mouse Joints from Post Traumatic Mediated Cartilage Degradation by Inhibiting MMP-Activating Enzymes Furin and MMP14*

Lawrence Livermore National Laboratories (LLNL) 2015 Seminar for the Biosciences and Biotechnology Division: *Modulating Sost Expression Influences the Progression and Severity of Post Traumatic Osteoarthritis Development in Mice*

ASBMR 2014 Plenary Oral: *Elucidating Molecular Mechanisms leading to Post Traumatic Osteoarthritis in Sost KO mice*

QSB 2014 Fall Retreat Oral: *Modulating Sost Expression Effects the Progression and Severity of Osteoarthritis in Mice*

ASBMR 2013 Plenary Oral: *Modulating Sost Expression Influences the Progression and Severity of Post Traumatic Osteoarthritis in Mice*

University Services

2009-2010   Graduate Student Research Day Committee, Treasurer

2007-2011   Numerous Student Panels for admissions, BEST and STAR including transfer students and future graduate students

Objectives

Osteoarthritis (OA), a joint inflammatory disease commonly described by the breakdown of articular cartilage, with two major contributing factors including aging (ware and tare) or traumatic injuries to the joints. To date, OA treatments are dominated by surgical procedures that stabilize the joint and pain management; hence OA patients are anxiously awaiting the development of new pharmacologic interventions aimed at minimizing, preventing or repairing cartilage tissue damage triggered by degenerative disease or joint injury. Recent studies projected that the presence of Sclerostin (Sost) affecting Wnt signaling may modulate the metabolic processes in the articular chondrocyte. Therefore, the research conducted here is to explore whether Sost recombinant protein may be potentially used as a therapeutic to either prevent or more likely, delay OA development, subsequent to trauma. In addition, the RNASeq analysis may reveal a list of possible novel secreted molecules as possible candidate biomarkers to classify or stage the disease in asymptotic patients (i.e. through routine blood draw).

We identify the role of Sost in knee joints before and post non-invasive tibial compression (TC) OA injury by examining post traumatic OA (PTOA) development in mice over expressing SOST ($SOST^{TG}$) and lacking Sost ($Sost^{KO}$) and comparing them to the common background mouse strain C57Bl/6, as the wildtype (WT) control. I will survey the effect in bone, cartilage, synovium, and meniscus by histological, micro-computed tomography (uCT), immunohistochemistry (IHC), and quantitative real-time PCR (qPCR) validation. Our results revealed an overall retention of cartilage integrity after 16 weeks post TC OA injury in $SOST^{TG}$

comparing to $Sost^{KO}$ and WTs. In addition, SOST overexpression reduces osteophyte formation in mice after injury. Interestingly, the overall activated matrix metalloproteinases (MMPs) are significantly reduces (~2 fold) in $SOST^{TG}$ compared to $Sost^{KO}$ and WT injured joints. After further validation, MMPs 2 (Gelatinase A) and 3 (Stromelysin-1) were dramatically down-regulated in $SOST^{TG}$ injured joints. Consistent with the transgenic data, overall activated MMP levels were also reduced in WT injured joints after intra-articular administration of recombinant Sost protein shortly after the TC injury.

By taking a systems biology approach and investigating whole joint derived RNA (injured and uninjured) by RNA Sequencing (RNASeq) in hopes to identify the pathways contributing to OA development. We identified 1446 genes differentially regulated between injured and uninjured joints in WTs. The transcripts presented both know regulators (*Mmp3*, *Fn1* and *Comp*) and uninvestigated (*Suco*, *Sorcs2* and *Medag*) genes associated with OA. Moreover, we identified 18 long noncoding RNAs that are differentially expressed in the injured joints. By comparing our TC data set with genes identified using the surgical (DMM) PTOA model, we presented several common genes and shared mechanisms including signaling pathways such as Wnt and Tgfβ signal transduction pathways. This study provides the first global gene expression profile changes associated with PTOA development and progression in a TC model. Future pathways analysis, in strains of mice with varying PTOA phenotypic outcomes have the potential to unveil new possible prognostic biomarkers and therapeutic targets that may be further explored for the treatment of PTOA in humans.

Chapter 1: Introduction

Osteoarthritis Disease, Pathogenesis, Symptoms and Treatments

Osteoarthritis (OA) is a painful and debilitating joint disease that is due to degeneration or traumatic injury to the articular cartilage [1, 2]. It is the most prevalent joint disease limiting human mobility followed by Rheumatoid Arthritis (RA), an autoimmune joint disorder where chronic inflammation of the knee or synovitis causes progressive degeneration of cartilage and its underlining bone, in articulated joints [3]. According to the Center for Disease Control and Prevention (CDC), OA-associated annual burden is estimated to be over $150 billion dollars in the United States (US) and affects ~ 27 million (M) people, 12.4M of which are over the age of 65 [1]. Research has shown that major risk factors of OA include age (long term ware and tare) and trauma (injury) related incidents. Excessive high impact physical activity due to exercise or sports injury increases the risk of knee osteoarthritis [4, 5]. In particular men and women engaged in physically demanding activities such as athletes and active members of the military are at greater risk of OA due to the physically demanding nature of their jobs [6]. Because the hips and the knee joints bare the most amount of body load, those locations are the two most prevalent locations where humans develop OA, even individuals without major joint injuries still develops OA as they age [6].

In addition to the heavy burden of this disease, there are more complications associated with diagnoses and treatment options. Symptoms of knee OA include: joint pain, swelling, and stiffness eventually leading to limited

mobility [7]. OA develops slower than RA and milder phenotypes are asymptomatic; however when one feels pain or has limited mobility, treatment options for individuals with OA are generally limited. As a progressive joint disease, OA can involve either one or multiple joints, including knee, hip, and hand [8], with the knee being the most prevalent joint to develop OA [9]. While diagnosis of OA is limited to primarily clinical and radiological features [10, 11], symptoms of joint pain and stiffness lead patients to seek medical attention [12]. To date, OA treatments are based on symptom (primarily pain) management by relying on a combination of non-pharmacological and pharmacological approaches adjusted to a patient's need and risk factors. Non-pharmacological approaches include access to information (education), weight lost (diet adjustment), and moderate exercise [13]. However, it remains controversial whether these measures are effective in patience with moderate to severe OA. Patient data suggests that non-pharmacological treatments are only recommended for individuals with early symptoms of OA. When one experiences stiffness, swelling, and pain accompanied by limited mobility, non-pharmacological approaches are no longer an effective treatment option. Pharmacological treatments include: analgesic and non-steroidal anti-inflammatory drugs (NSAIDs), intra-articular supplements of hyaluronates, chondroitin and/or glucosamine sulfate usage in OA pain management [13].

NSAIDs are the most common and most widely used to reduce pain and treat early symptoms of OA. Together with painkillers, NSAIDs are highly recommended to be used in parallel with non-pharmacological regiments to

achieve the most promising effect in pain management. Though analgesics and NSAIDS are effective in low symptomatic OA individuals, however NSAIDs treatments are also known to be associated with serious side effects pertaining upper gastrointestinal (GI) complications. Reports have indicated frequent high dose users of NSAIDs were at 2~3X higher risk of GI complications [14].

Hyaluronic Acid (HA) is a high density anionic glycosaminoglycan. The molecule is abundant in joint tissues providing a lubricant property and maintaining the viscoelastic properties of articular cartilage, ligaments, tendon, and synovial fluid. Because HA gets depolymerized in the synovium of OA knee joints, intra-articular (IA) injections of HA (viscosupplementation) have demonstrated to reduce joint pain and increase mobility [15]. The efficacy between IA HA and oral NSAIDs seems to be insignificant between patients, suggesting HA replacement as an alternative to NSAIDs to reduce OA symptoms [16]. In clinical applications, corticosteroids are usually coupled with IA HA to allow higher dosage delivery, however some have reported the therapeutic effects HA and steroid combination are barely significant.

A wide range of glycosaminoglycan are cleaved and degraded by catabolic enzymes during OA development. These natural macromolecules found in cartilage are essential, and need to be replaced if the overall integrity of the cartilages is to be maintained. A class of drugs known as symptomatic slow acting-drugs for osteoarthritis (SySADOAs) were developed to battle joint pain. Chondroitin sulfate (CS) and glucosamine sulfate (GS) are SySADOAs and they were both commonly used for joint pain management. Though there are many

3

reports demonstrating the effectiveness of these drugs by assessed radiologically by an improvement in joint space of treated patients [17-19], the data is controversial, since a wide range of SySADOAs were prescribed in different countries or regions of the world, with varying results [12]. After a variety of investigations, it was suggested that prescription of GS and CS may differ in individuals due to differences in genetic factors, dietary supplements, pharmaceutical formulations (different manufactures) and quality, dosing regiments, and pharmacokinetics, therefore their use needs to be further investigated. With these concerns, further studies are underway and investigating the side effects and possible benefits and of GS and CS in the United States.

OA is typically symptomatic in human knee, hip, and hand with knee OA leading the charts causing disability in aging populations [20]. In all, it is recommended to combine both non-pharmacological and pharmacological treatments together, however an effective treatment method are still in high demand. Effective, long lasting treatment approaches with less invasive methods than reconstruction surgery of hip/knee replacements are still limited. For OA, different joint locations require similar but different treatment options. Moreover, because surgical replacements of knee and hips are the most effective, however invasive, it is the most current and effective treatment. Hence a more common and non-invasive method of treatment options may be a better therapeutic.

The Bone and Cartilage Development of the Knee Joint

In principle, all cells in the human body experience some level of physical forces such as gravity, tension, compression and shear; these mechano-forces are capable of influencing growth and remodeling at the cellular level [21]. Bone and cartilage are tissues best suited to cope with large loading forces because of the extensive extracellular matrix (ECM) composition that surrounds and embeds these highly specialized cells [22]. Before exploring the pathogenesis of OA, we must first understand the development and molecular changes associated with cartilage and bone development.

Articular cartilage (AC) is a connective and mechanosensitive tissue composed of predominantly matrix encompassing a relatively spread populations of chondrocytes (cartilage forming cells), which implements the overall matrix maintenance and functions [23]. AC is typically found at the bases of bones with a unique high capacity to bare load. The AC matrix composition is approximately 60% water, 15% collagens and 15% proteoglycans, and less than 5% chondrocytes by weight [24]. During cartilage growth and development, chondrogenesis is the active cellular process which leads to creating diverse cartilage types, including elastic, fibrous, and hyaline cartilage. Hyaline cartilage is the very prominent and susceptible to pathological stress deformation and are largely found on the surfaces of the diarthrodial (knee) joints and the growth plate (GP) of long bones. GP behaves as a barrier separating the bone growth from cartilage maintenance during pre- and postnatally [23].

By comparison, bone is another mechanosensitive high load bearing tissue that is composed of a mixture of mineral [inorganic] and organic material with three dominant cell types: osteoblasts, osteocytes, and osteoclasts [25, 26]. Osteoblasts (OB) synthesize the inorganic matrix of the bone, osteoclasts break down or resorb bone, and osteocytes maintains bone integrity by signaling osteoblasts and osteoclasts during bone modeling and remodeling. Osteocytes (OC) are derived from osteoblasts after they embedded in bone matrix [26, 27]. In In the human skeletal system, initial chondrogenesis occurs fist than followed by endochondral ossification (bone formation process). Chondrogenesis initiate by recruiting scattered mesenchyme, while factors such as bone morphogenetic protein (BMPs) condenses mesenchymal cells [28]. During this early stage, condensing mesenchyme expresses ECM and cell adhesion molecules such as collagen type II (Col2a1) [29] and N-cadherin (N-cad) [30], respectively. Meanwhile, transcription factor Sos9 leads chondrocyte differentiation at early stages of chondrogenesis [31]. Active chondrocytes begin to produce ECM rich in Col2a1 and aggrecan (Agn). Following early chondrocyte differentiation, the cells rapidly proliferate to expand the cartilage template (Fig 1A II). Cells at the center of each proliferating center starts to have reduce cell cycles and initiate hypertrophic (double in size) differentiation (Fig 1A III). During hypertrophic differentiation (chondrocyte maturation), chondrocytes enlarge in size, terminally differentiate, mineralize, and eventually undergo apoptosis. As chondrocytes perish, their residual cartilage matrix template serves as scaffold for later mineral deposition and turnover by osteoblast and osteoclast invasion. The degraded cartilage template becomes

vascularized by surrounding blood vessels to establishing the bone marrow cavity (Fig 1A IV). Finally the cartilage growth plates (GP) found at each end of a developing bone are formulated through a continual process of chondrocyte proliferation, differentiation, and replacement [23]. A complete schematic of cartilage and long bone formation is shown in Figure 1.

Unlike bone, cartilage is an avascular tissue, and with the lack direct oxygen, nutrient supplies (blood), and stem cell access, this gives AC a very low to minimal regenerative property. Hence if and when AC is eroded away in an aging individual (long term ware and tare) or by injury, the low regenerative properties prevents recovery, so currently, the only effective long term treatments are invasive reconstructive surgery or joint replacement [32]. OA as a stress-related cartilage disease also identifies with the problem of cartilage repair or maintenance. A major focus had been on investigating the cellular and molecular mechanism of regulating, preserving, enhancing chondrogenesis and chondrocyte differentiation. There are some critical insights necessary to understand the current molecular changes essential to affecting chondrogenesis and chondrocyte differentiation. These information will provide some insight on how pathological conditions such as excess mechanical loading and knee OA progression on cartilage. With an overall understanding of the basis stress influencing cartilage metabolism (molecular changes and stress triggers) may provide a baseline for therapeutic exploration on impacting the pathological stress diseases. The architecture of a knee articular cartilage and its associated bones are presented in Figure 2.

In contrast to cartilage, bones are connected to the vasculature through blood vessels that supply them with oxygen, nutrients, and stem cells [33, 34]. As a result, our bones possess a remarkable capacity to regenerate both from a metabolic (anabolism) and repair (fracture healing) point of view [35]. In sharp contrast, cartilage uniquely stands out in the human body as an avascular tissue with low intrinsic regenerative properties [35-38]. Hence cartilage structure and function is more likely to decline in response to aging or traumatic injury, since physical cellular damage from wear and tear will have a cumulative effect over an individual's life and contribute to the gradual deterioration of the joint [39].

The evidence that chondrocytes and osteoblasts are sensitive to mechanical forces and translate mechanical signals into molecular and functional outputs stems from the observation that both bone and cartilage have the ability to synthesize new matrix (make new tissue) or destroy old tissue in response to mechanical stimuli [40, 41]. AC homeostasis is maintained by a balance between ECM (collagen, proteoglycans, and water) formation carried out by chondrocytes and cartilage synthesis in response to mechano-stimulation (loading) [42]. It has been shown that moderate exercise improves the health of our skeletal system (both cartilage and bone), stimulating chondrocytes to produce more ECM and shifting the balance of cartilage formation towards higher matrix mineral density [42-44]. In aging individual, as the level of physical activity decreases, ageing chondrocytes have been shown to exhibit a decrease in anabolic activity, an increase in catabolic activity or both [45-47]. Further support to this effect

stems from the characterization of human, equine, bovine, rabbit and mouse articular cartilage explants which revealed that the intrinsic metabolism of chondrocytes and their response to external factors varied with the age of the animal [48]. It has been previously shown that the mechanical properties of cartilage also deteriorate with age, allowing the tissue to become more vulnerable to injury and less capable of withstanding joint loads [49]. Like changes in the tissue matrix, healthy aging diminishes the synthetic activity of chondrocytes [50]. These aged cells also synthesize less matrix proteins in response to mechanical stimulation, which is necessary for normal healthy function. The lack of responsiveness to mechanical loading in aged cells limits the ability of the tissue to maintain homeostasis.

Despite the fact that many of the risk factors associated with the development of OA are well established, the pathogenesis of OA is still poorly understood. It has been demonstrated that inflammation [51], abnormal subchondral bone properties [52] and loss of response to mechanical load [53, 54] all contribute to the development of OA; however, the molecular and genetic mechanisms leading to cartilage degeneration have yet to be elucidated. The lack of progress in this area has severely limited the development of effective therapeutics for the treatment of OA. Furthermore, many individuals that have or are in the process of developing OA are asymptomatic until significant joint damage has occurred [55], at which point the only available treatment options are surgical replacement of the joint and/or pain management [56]. Thus, a better understanding of OA pathogenesis to identify potential therapeutic targets to

minimize cartilage degradation is of great interest. Simultaneously, we an establishment of candidate biomarkers that can be used to track the progression of the disease in asymptomatic patients are also an active field of research.

Animal Models of Post-Traumatic Osteoarthritis

Trauma to joints often leads to post-traumatic osteoarthritis (PTOA), and more than 40% of people who suffer significant articular joint injuries will develop PTOA. Recent evidence suggests that injury to the joint initiates a sequence of events (currently unidentified) that can lead to progressive articular surface damage and subsequent PTOA. One common feature of joint injuries that is believed to cause PTOA is the sudden application of mechanical force (impact) to the articular surface. The extent of mechanical damage to any structure is a function of the intensity of the impact. Studies on explanted joints show that more severe impact also causes greater local tissue damage, as measured experimentally, by the proportion of cells releasing reactive oxygen species, chondrocyte death, and matrix disruption [57]. While some data has been generated using 3D tissue culture approaches and cartilage explants, the unique environment of the joint (bone/cartilage/synovial fluid) before and after trauma is difficult to model *in vitro*. Therefore, animal models that resemble PTOA are vital in understanding the molecular changes within the joint in response to injury. In 2008, Little *et al.* explained five essential properties of an "optimal" animal model of OA [58]:

1) Model should have high reproducibility of disease that occurs with an appropriate time frame and high throughput studies.

2) Introduce the disease that develops universally allowing early, mid, and late pathology and treatment effects.

3) Animal models should be mammalian species that is compliant, inexpensive, easy to manage and house with large enough offspring allowing multiple experimental measurements (analysis/outcome), genome wide sequencing (microarray or chip-sequencing) availability, and proteomic sequencing.

4) The ongoing disease introduced to the animal must recapitulate human disease in all tissues of the joint.

5) The model should represent effective treatments in both treating animals and humans (i.e. what works in animals also works in treating humans).

Several mouse models of OA have been previously developed with the goal of studying cartilage and bone parameters before, during and post OA development. In addition, animal models of OA are instrumental in studying the development of the disease on an accelerated timeframe relative to OA development in humans, which is slow and cumulative over a person's life time. Mice represent an ideal animal model to study OA due to the availability of numerous genetically modified mouse strains which facilitate the investigation of genetic contributions to OA development. To date, the majority of accepted mouse models of OA utilizes some form of whole joint injury or localized joint degradation, signifying post-traumatic osteoarthritis (PTOA). Unfortunately, no consensus on

11

methodology has yet been established that standardizes the methods utilized animal injury models that most effectively represent human OA disease pathogenesis. In early studies of OA, mouse joints were injected with recombinant collagenases, which cause to the breakdown of collagen over time leading to cartilage degradation [52, 59, 60]. Other methods include excessive motion through multiple bouts of mechanical loading, mimicking longer wear and tear of the joint [61]. Currently, surgical modes are the most commonly utilized method to induce PTOA in mice. These methods include either the transection of anterior cruciate ligament (ACL) and or transection of the medial meniscal ligament, or both [55, 56]. The surgical methods are more favored and more widely used because of the robustness of the OA phenotype and systemic effects on the joint, including both bone and cartilage remodeling; however, these methods may introduce artifacts due to the surgical/invasive technique itself, instead of the underlining joint injury [62]. Because of the invasive nature of enzyme injections and surgical procedures, neither one of these approaches is clinically representative of human PTOA (i.e. sports injury or military service men/women experiences on duty), therefore less invasive methods would be preferred. Thus, to better understand the process of OA development in humans, novel animal models of OA must be developed that more closely resemble human trauma and follow pathological manifestations in the joint subsequent to trauma.

There are a few non-invasive injury methods currently being utilized which avoid the complication of surgery, these techniques include: 1) intra-articular fracture of tibial subchondral bone [63]; 2) multiple cyclical bouts of short term

mechanical loading of the articular cartilage through tibial compression [61]; and 3) anterior cruciate ligament (ACL) rupture through tibial compression overload [64]. Collectively, those non-invasive mouse models are unique for studying various conditions of the effects of traumatic injury on human joints. An overview of these methods including benefits, drawbacks, clinical relevance, and methodology [apparatus, forced used, success rate (reproducibility)] are described in Table 1.

Intra-articular fracture (IAF) was the first non-invasive PTOA mouse model developed [63], where a high impact load was applied to an intact joint inducing a tibial plateau fracture. This model has a relative high reproducibility rate (87%) and PTOA develops within 2 months. The purpose of this model is to mimic human high energy impact injuries such as car accidents, military personal injury, or construction work related accidents. In addition, this injury model is adjustable in terms of the fracture severity, allowing researchers to study OA developing joints spanning a wide range of fracture severity and complexity. Regardless of the fracture severity, however this model is not ideal for low energy impact injuries, and may overemphasize the contribution of bone repair to cartilage damage and metabolism [62].

The cyclical compression of tibial articular cartilage, is a method most commonly used to study bone adaption parameters [65]. In 2011 Poulet *et al.* described a cyclical compressive load introduced to the hind legs through the ankle to the knee which causes mild to moderate OA [61]. Similar to IAF, this method is also highly reproducible (83%), the injury severity is adjustable, and OA develops

13

between two to five weeks post injury. This is a model more representative of OA driven by joint overuse rather than a high impact injury. One potential drawback of this method is the OA severity (cartilage phenotype) is generally very mild to moderate assuming the absence of ligament rupture, meniscal tear or other physical damage in the joint. The purpose of this model is to mimic the outcomes of repetitive motions applied to joints such as excessive typing, frequent participation in marathons, and repetitive pipetting. This mode of OA is ideal for studying the effect of low impact, highly repetitive overuse of joints. Though this is a reproducible and adjustable method, a major limitation this model is the OA severity which is mild. This prevents researchers from investigating the late stages of OA development in joints.

A similar tibial compression method with more severe outcomes was described by Christiansen *et al.* in 2012 [64]. Here, a single dynamic compressive overload applied to the lower hind leg, forcing the tibial condyle off the femoral condyle causes ACL rupture. Similar to other non-invasive techniques, this method is reproducible and adjustable and has several benefits over the models described above.

ACL Rupture through Tibial Compression (TC) Overload

Though TC ACL rupture PTOA model loads the knee joints similar to the cyclical tibial compression model, the initial injury events in joints are likely to be very different. Immediately post ACL tear, the applicable load on articular cartilage is a single high energy loaded (joint destabilized) compared to the cyclical loading

(no internal joint damage) injury is vastly different. Similar to the TC ACL tare model, surgical model of the ACL transection reflects a comparable OA phenotype in mice. As a consequence of ACL break, the contact points between femoral and tibial cartilages shifts unevenly and reflects more cartilage erosion and chondrocyte apoptosis in the posterior zone of the destabilized joint. A major benefit of this model is to allow studies of PTOA in a rapid developing condition. However this rapid developing PTOA model may also be a drawback. This model is consistently dramatic affecting the posterior region on the medial compartment of the joint. Over time, cartilage erosion and bone remodeling are enhanced at a focal point on the tibial surface. This clear phenotype were observed as early as 8 weeks post injury. Consequently, the TC overloading injury model may be more applicable to studying acute processes at the initial OA injury stages and not used for long term studies. Overall this model mimics ACL rupture in humans, which is one of the main causes of PTOA. Collectively, the benefits of non-invasive methods allow investigation of early adaptive OA developing events, at the initial time of injury, and may more closely of human OA injury which are typically mechanically induced.

The tibial compression (TC) induced ACL rupture model replicates a clinically relevant human knee injury, enabling one to focus on the early events of joint injury that trigger the downstream molecular changes ultimately responsible for the development of OA. TC injury represents an improvement over the animal models of OA described above, since it is non-invasive it likely overcomes some of the inflammatory side effects that may be exacerbated in surgical models. The

TC injuries are easy to perform, which enable us to design experiments with less animal-to-animal variation and obtain statistically significant results using fewer animals. In comparison to the more invasive, surgical PTOA mouse models, in TC, OA develops consistently within 4-8 weeks of injury [64, 66]. In addition, and similar to human knee injuries, we observe an initial acute inflammatory response and joint swelling that resolves in a few days, followed by extensive remodeling of subchondral bone and cartilage [67]. Also comparable to human knee injuries, a systemic inflammatory response that results in similar (although lower magnitude) structural changes in the contralateral (uninjured) knee occurs. Despite the numerous advantages of this TC injury relative to previously published models, this model has never been used to systematically evaluate the development of OA at the molecular level, or in genetically modified strains of mice.

Histological Atlas of Osteoarthritic Joints in Animal Models

Similar to humans, during OA development, there are many hallmarks an arthritic joint presents, including: 1) articular cartilage erosion; 2) underline subchondral trabecular bone remodeling; and 3) osteophyte formation in mice [68, 69]. To evaluate histological severity of murine OA joints, a variety of scoring systems were developed. However depending on the joint injury, regions of interest (medial vs lateral, and anterior vs posterior), various components and contributing factors may allow any of the OA landmarks to be more apparent or severe than the other. Nevertheless, one common parameter among all arthritic joints during OA development is cartilage erosion. Hence, to evaluate the severity

of OA in mice post injury, the most standardized mouse scoring atlas used to evaluate the severity of OA joints post injury is through the assessment of cartilage integrity [70]. Glasson *et al.* recommended a common histological assessment of OA in mice through the Osteoarthritis Research Society International (OARSI) in 2010 (Figure 3). By utilizing the ORASI scale by Glasson, OA evaluations can be standardized across all mouse OA models examined. In addition to the post-traumatic injury, there are a wide range of catabolic enzymes involved in the breakdown of cartilage and bone matrix.

Matrix Metalloproteinase (MMP) and Joint Inflammation

Metalloproteinases belong to a large family of endopeptidases (187 human genes; 194 mouse genes) that are identified by their conserved $Zn2^+$ active site and are classified into subcategories based on their structural catalytic domain [71, 72]. The mammalian matrix metalloproteinase (MMPs) comprised of 24 related extracellular endopeptidases, and all are synthesized with conserved pro- and catalytic domains [71, 72]. Pro-MMP (inactive form) catalytic domains contain the Zn2+ active site, which are hidden until the pro-domain is cleaved to obtain MMP activity [72]. In addition, MMP expression is translationally regulated by primarily pro-inflammatory cytokines [73, 74] and growth factors [71]. Their major function include remodeling of the extracellular matrix (ECM), which is comprised of organized scaffolds secreted by specialized cells. Soluble (secreted) and membrane bound MMPs are generally synthesized as an inactive pro-enzyme, which are activated by cleavage of their pro-domain. It has been previously shown

that some MMPs are activated by other proteinases including the extracellular matrix protein Furin [72, 74]. MMP activity is also negatively regulated post-translationally by tissue inhibitors of MMPs (TIMPs) which bind and inactivate most MMPs. Moreover a wide range of tissues can express MMPs, and because the enzymes can cleave a wide range of ECM components, this makes the tissue or cell-type of origin for MMPs difficult to pin point. Therefore, mRNA and protein activity do not always correlate *in vivo,* since transcription may originate in one cell type, and post-translational modifications may occur in the extracellular matrix shared by several cell types, therefore a combination of immunohistological analysis using antibodies targeting active and inactive isoforms may be more informative in interpreting function. This concept had led other research into focusing on MMP cleavage of ECM molecules in infiltrating cells and ECM remodeling processes during development and regeneration. Since MMPs are regulated both transcriptionally and post-translationally, the complex mechanisms and regulatory networks are not restricted to one biological pathway or biological trigger. Scientists have investigated the role of MMP in human diseases include cancer tumor invasion [75], bone fracture [76], and joint arthritis [77].

MMPs are utilized by mammalian chondrocytes to regulate and maintain the overall integrity of the articular cartilage and their extracellular matrix. It is known that MMPs are up-regulated both transcriptionally and through enhanced activation by pro-inflammatory triggers or excessive mechanical stimuli, and it has been suggested that elevated MMP activity has a deleterious effect on cartilage, contributing to the development of OA. In the context of OA, a group of MMPs have

18

been previously identified to be essential in maintaining the homeostasis of cartilage integrity. However in an OA developing joint, elevated levels of MMPs 2 [78], 3 [79], 9 [80], and 13 [81] were identified in focal regions of arthritic cartilage. In addition, ADAMTS4 [82] and 5 [54, 82] had also been found in parallel with MMPs in OA cartilage. Moreover, genetically modified mice lacking MMPs 2, 3, 9 and 14 along with ADAMTS4/5 had all been shown to develop less OA suggesting MMP over expression contributes to cartilage degradation in OA [83]. One of the common stimulators of these enzymes and the persistence of MMP activity in OA cartilage seems to be triggered through pro-inflammatory cytokines such as Interleukin (IL) -1, IL-6, TNFα, and NF-κB [72]. However the molecular and cellular mechanisms involved in elevating and maintaining high MMP activity in the joint remain elusive. The Wnt signaling pathway is one of few molecular pathways that has been recently shown to contribute to OA pathogenesis, in animal models of PTOA.

Wnt Signaling and Osteoarthritis

Wnt signaling is an important regulatory pathway involved in musculoskeletal bone development and it is classified into two categories: canonical, which is mediated through downstream activation of β-catenin; and non-canonical that is independent of β-catenin activation. This signaling pathway is initiated through the physical interaction of a variety of Wnt ligands with Wnt receptors and co-receptors to activate signaling via: β-catenin, calcium ($Ca2^+$), planar cell polarity (PCP), or protein kinase A (PKA) pathways and drive gene

expression [84-86]. Because of the vast collection of Wnt ligands, receptors, agonists and antagonists that form complex interactions during tissue development and homeostasis, in particular, the canonical Wnt signaling pathway (β-catenin dependent), has been of great interest in studying bone development and maintenance. Schematic of Wnt/ β-catenin signaling is presented in Figure 4.

Wnt signaling is essential in limb and joint development affecting osteoblasts (bone forming cells), osteocytes (matrix embedded osteoblasts that maintain bone) and osteoclasts (bone absorbing cells) in different context [87]. As a consequence, mutations in several members of canonical Wnt signaling pathways result in skeletal defects in mice and humans. After mouse models of Wnt associated genes have been identified in modifying bone formation, Wnt antagonists such as secreted frizzled-related protein 1 (sFRP), Dickkopf-1 (DKK1), and Sclerostin (Sost) were also previously investigated. For example, mutant mice with decreased expression of Wnt antagonists sFRP-1 [88], DKK1 [89], and Sost [90, 91] all have a higher developing bone mass phenotype. Conversely, Sost transgenics (overexpression) display a low bone mass phenotype [92]. Similarly, sFRP, low-density lipoprotein (LRP) 5/6, and DKK1 mutant mice have also revealed a cartilage phenotype with respect to OA development in a surgical model of OA. Though a wide range of Wnt signaling targets had been investigated in the context of bone remodeling, however much focus are lacking in understanding its role in cartilage metabolism.

In humans, a variety of mutations had been identified to cause alterations in bone density along the canonical WNT signaling pathway. For example,

homozygous null mutations in LRP5 cause osteoporosis-pseudoglioma syndrome (OPPG) in humans [93]. Conversely, a gain of function mutation in LRP5 causes high bone mass [94, 95]. Similarly in mice, a comparable LRP5 conditional knock-out (KO) in osteocytes presented an attenuated bone formation in the appendicular skeleton [96]. In addition to LRP5 mutation, mutations in Wnt inhibitors have also been shown to cause skeletal dysplasia in to humans. Sclerostin (Sost) is a Wnt antagonist secreted by osteocytes, that inhibits Wnt signaling by physically interacting with LRP 5/6 co-receptors [97, 98]. Patients carrying homozygous mutations in the gene SOST or its transcriptional regulatory region develop Sclerosteosis [99] and Van Buchem disease [92, 100], two rare but closely related high bone mass genetic disorders. In Sost KO mice, they also develop high bone mass phenotype in their appendicular skeleton [90, 101, 102]. Conversely, transgenic mice overexpressing SOST are osteopenic (low bone mass) [92]. Taken together, deletions in Wnt receptor (LRP5 [96]) and its signaling antagonists (Sost [103] or DKK1 [104]) in mice all present high bone mass, this tightly supports the link between Wnt signaling and bone metabolism.

Initially, major focuses on Wnt signaling had been on regulators of bone formation and regeneration [105], proposing the possibility that altering of Wnt signaling may be beneficial in treating skeletal disorders such as osteoporosis [106]. For over the past 2 decades, the role of Wnt signaling had been established to affect cartilage development and function as well. In animal OA models, Wnt signaling has been implicated in cartilage and its underlining bone remodeling during OA development [107], hinting at potentially new molecular explorations for

treatment of human OA. Unlike genetic mutations that are known to alter bone metabolism, very few genes have been associated with early onset osteoarthritis and mouse genetic models have not yet been fully explored to expand our repertoire of candidate genes contributing to cartilage degradation and OA. To date, a few Wnt associated target genes have been explored in the context of OA development. Genetically altered mice including: LRP5$^{-/-}$ [108], LRP6$^{-/+}$ [109], Col2a1-DKK1 [110, 111], and sFRP3$^{-/-}$ mice [112] all presented more severe PTOA phenotypes compared to controls in surgical mouse models of PTOA. Interestingly, Sost has been implicated to play a protective role in OA development in both a sheep and a mouse surgical model of PTOA [113], however antibody competitive inhibition of Sost treatment suggested that Sost depletion may not negatively affect the joint cartilage [114]. The role of Sost in OA cartilage remains a controversy to be elicit and are of interest in recent OA research. With the advancement of technologies today including RNA sequencing and ability to generate tissue specific conditional KO mice, an active area of research today focuses on the inter-communication between multiple joint tissues including the articular cartilage, underlining bone and the synovium to elucidate the contributions of each tissue. Though it is still unclear the role of bone in communicating with cartilage before and during OA development, to address the conflicting results of the role of Sost, I aim to resolve this conflict and attempt to clarify the mechanism involved in cartilage metabolism during OA with its underling bone.

Hypothesis

Unlike many other human tissues with regenerative capacities, articular cartilage is unique in that is hypocellular and avascular, therefore once cartilage damage has occurred, the cartilage lacks the ability to repair, and accumulated erosion lead to the development of OA. In particular, excessive high impact physical activity due to exercise, combat, or sports injury increases the risk of knee OA. Despite the fact that many of the risk factors associated with the development of OA are well established, the pathogenesis of OA is still poorly understood. In addition, the molecular and genetic mechanisms leading to cartilage degeneration have yet to be elucidated. We have been investigating the role of Wnt signaling in post-traumatic OA (PTOA) joints and others have implicated elevated Wnt signaling in affecting chondrocyte metabolism [24, 115, 116]. While the role of Sost has been thoroughly investigated in bone, its role in the articular cartilage and in OA pathogenesis remains poorly understood.

It was previously hypothesized by Chen *et al.* that Sost may play a protective role in OA cartilage in both sheep and mouse, when they documented elevated levels of Sost in focal areas of cartilage damage [113]. These results were further supported by the finding that SOST is also transcriptional up-regulation in human OA cartilage obtained from hip replacement surgeries (gathered through biopsy) [117]. **We therefore hypothesized that mechanistically, Sost plays a protective role in PTOA articular cartilage by decreasing the catabolic activity of cartilage degrading enzymes such as MMPs.** However Rudier *et al.* had showed that Sost inhibition through Sost antibody administration does not

23

negatively affect the articular cartilage, but rather favorably impacts the subchondral bone by elevating bone formation [114]. Conversely, Bouaziz *et al.* more recently suggested that lack of Sost in mouse KOs subjected to a surgical model of PTOA develop a more severe OA cartilage phenotype than controls, through the up-regulation of osteophyte regulating genes [118]. In an attempt to resolve this discrepancy and provide experimental support for our hypothesis, we investigated the role of Sost in injured and uninjured joints of genetically modified mice with varying levels of Sost expression: SOST transgenics (overexpressing human SOST from a bacterial artificial chromosome) and global Sost KO mice by utilizing the TC OA injury model.

Significance

To date, OA treatments are dominated by surgical procedures that stabilize the joint and pain management; therefore OA patients are anxiously awaiting the development of new pharmacologic interventions aimed at minimizing, preventing or repairing cartilage tissue damage triggered by degenerative disease or joint injury. While many individuals have or are developing OA, most are asymptomatic until significant deterioration in the joint has occurred; severe and easy to diagnose OA results in debilitating pain and decreased mobility [55]. Early detection and prevention of cartilage damage remain a major challenges today. When one becomes symptomatic, the time for non-invasive treatment are not optimal and minimally effective. At this time, the only long term treatment of OA is surgical replacement of the joint, hip or knee [56]. Seizing the potential for progress in the

24

treatment of joint injuries to prevent PTOA will depend on advances in (1) developing quantitative methods for evaluating the severity of the injury, ideally where the damage is assessed both structurally and through the use of biomarkers that classify the molecular stage of the damage; (2) understanding the molecular mechanisms that lead to post-traumatic OA subsequent to an injury at the systems biology level where the architecture of the joint and the various cellular components which include examining the chondrocytes within the articular cartilage; and finally (3) validating the molecular correlation between aging and trauma induced OA. Presumably, the presence of Sclerostin (Sost) affecting Wnt signaling may modulate the metabolic processes in the articular chondrocyte. Therefore, the ultimate goal of this research is to explore whether Sost recombinant protein may be potentially used as a therapeutic to either prevent or more likely, delay OA development, subsequent to trauma. In addition, the RNASeq analysis may reveal a list of possible novel secreted molecules as possible candidate biomarker s to classify or stage the disease in asymptotic patients. One would look for secreted molecules identifiable from serum (routine blood draw) as an early detection method for asymptomatic individuals.

Figure 1. Schematic of Long Bone and Articular Cartilage Development
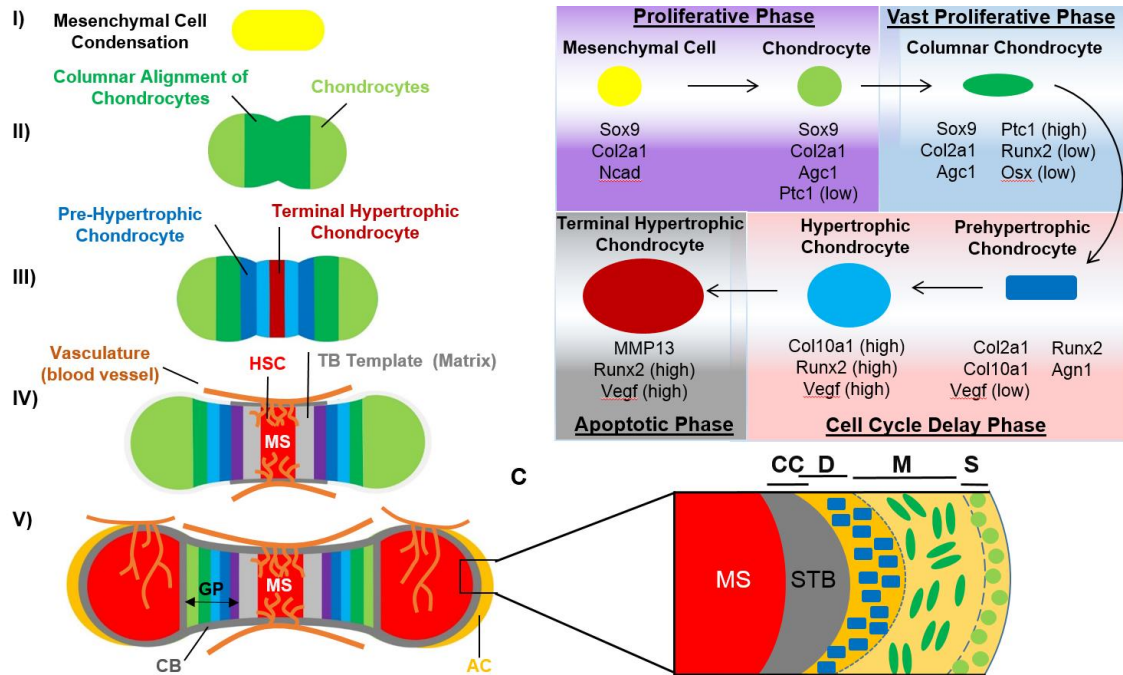
Figure 1. Molecular markers and cellular events of chondrogenesis and articular cartilage (AC) development. (A) Layout of endochondral bone formation leading to mature bone starting with condensation of mesenchyme (I); chondrocyte differentiation and formulate cartilage template (II); chondrocyte maturation and initiate hypertrophy (III); cartilage expansion allowing vascularization (orange lines) and initiate both trabecular and cortical bone formation (IV); and finally secondary ossification centers are formed separating AC and GP cartilage (V). (B) Brief model of cellular events during chondrogenesis. Important signaling factors are indicated at each stage of chondrocyte differentiation. Brackets show the levels of gene expression. (C) Magnified compartment of AC revealing four distinct cellular resigns: S, superficial zone; M, mid zone; D, deep zone; and CC, zone of calcified cartilage. Other abbreviations include: MS, marrow space; GP, growth plate; TB, trabecular bone; CB, cortical bone; and HSC, hematopoietic stem cells.

Figure 2. Architecture of Human Knee Join

A

B
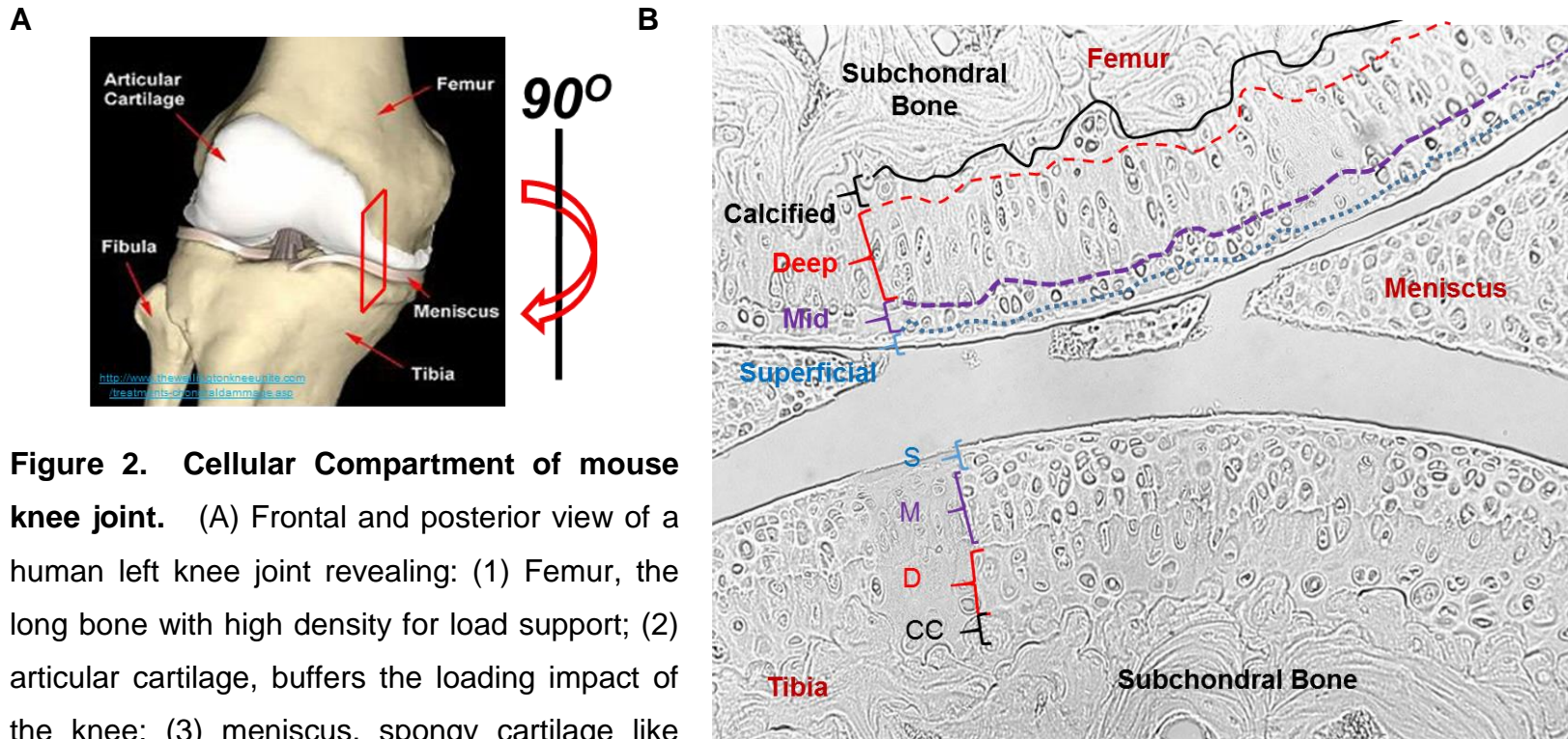
Figure 2.   Cellular Compartment of mouse knee joint.   (A) Frontal and posterior view of a human left knee joint revealing: (1) Femur, the long bone with high density for load support; (2) articular cartilage, buffers the loading impact of the knee; (3) meniscus, spongy cartilage like tissue that holds the joint in place, along with synthesizing lubricant to provide smooth joint movement; and (4) tibia (thicker) and fibula (thinner) lower leg bone. A 90° sagittal view of red box (B) reveals a bright field (20X magnification) image of a mouse knee joint including femoral and tibial articular cartilage. The division of superficial (S), mid (M), deep (D) and calcified cartilage (CC) regions along with its underlining subchondral bone.

Figure 3. Grading Scale of OA Severity using Cartilage Landmarks
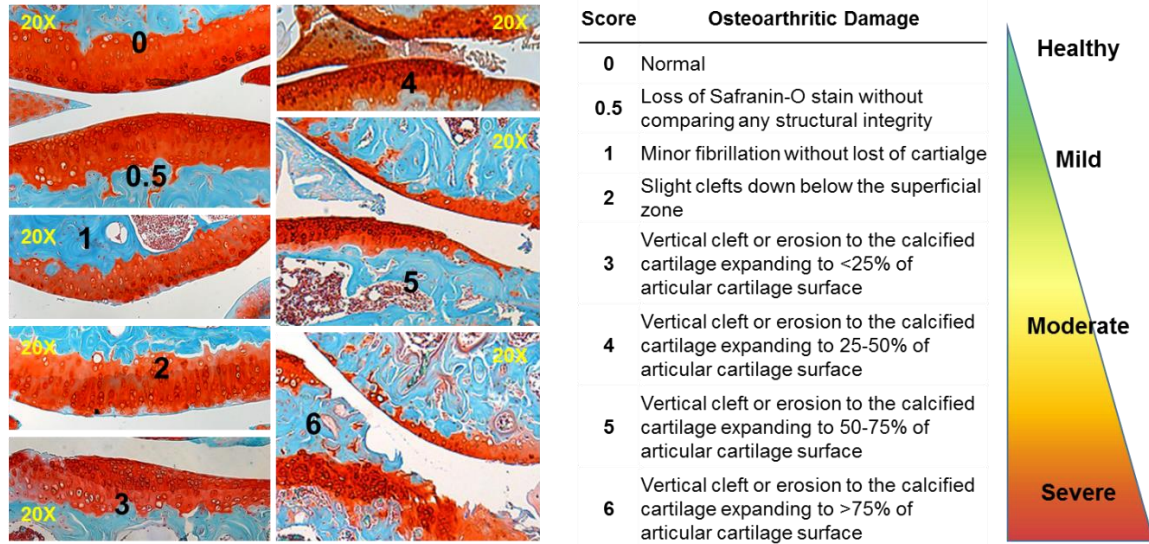
Figure 3.   Recommended histological atlas of OA severity in mice through OARSI by Glasson *et al.* 2010 [70]. (A) Safranin-O and Fast Green histological stains presenting a variety of OA severity and semi-quantitative scores. (B) The evaluation standards were similarly adopted [70] however modified using sagittal instead of frontal views of injured cartilage. (C) Standard reference of healthy (score 0~0.5), mild (1~2), moderate (3~4), and severe (5~6) scores. All images were taken at 20X magnification.

Figure 4. Schematic of Wnt/ β-catenin signaling
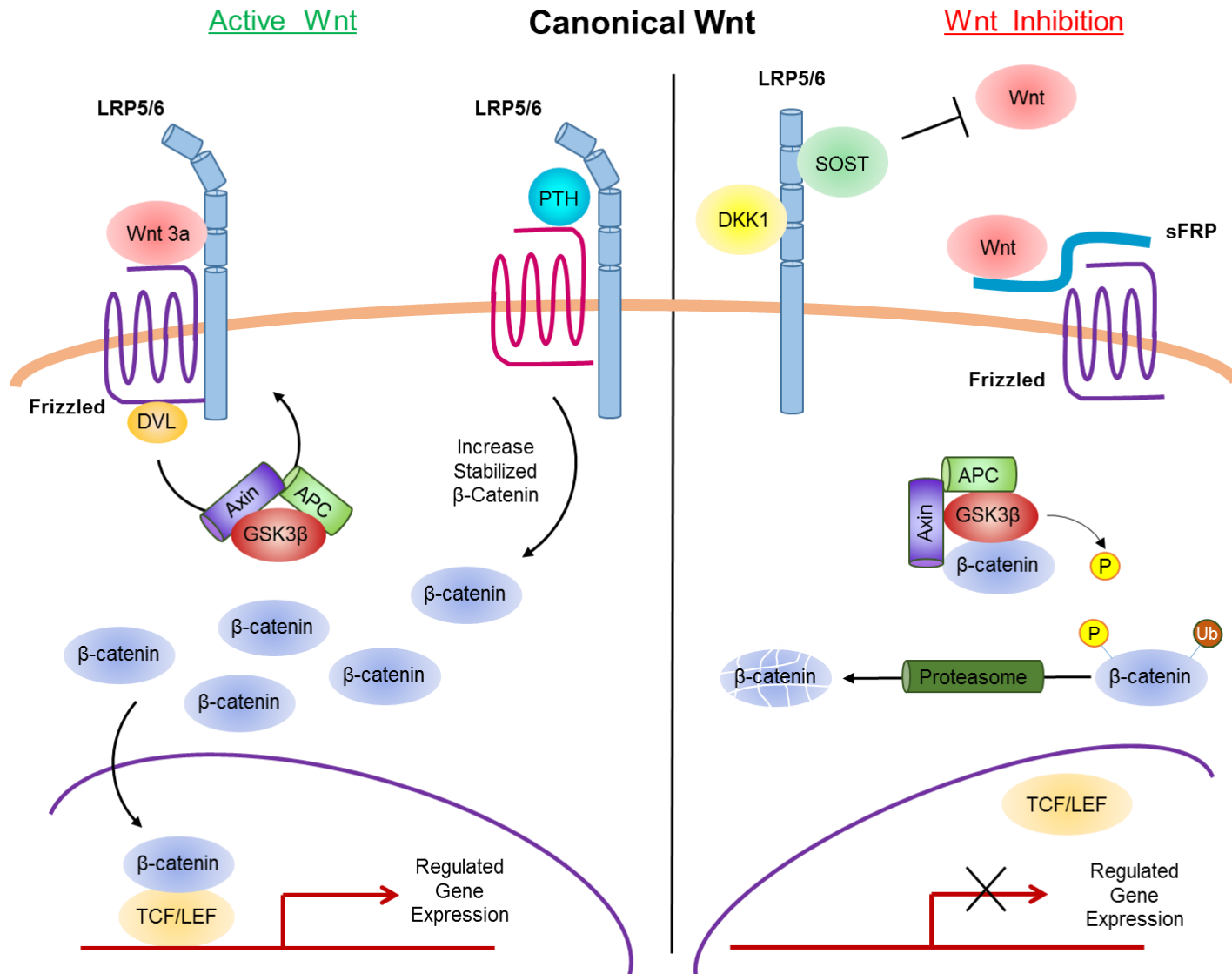
Figure 4. Schematic of Wnt/ β-catenin signaling. In absence of WNT triggers, baseline level of β-catenin are relatively low, with the exceptions of cell-cell adherent junctions (not shown). However in presence of tumor suppressors Axin, adenomatous polyposis (APC) brings to GSK-3β and consequently phosphorylates (yellow circle of Ps) β-catenin (right). Phosphorylated β-catenin is then polyubiquitinated (Ub) and subsequently marked for proteasomal degradation. In the nucleus, T cell factor (TCF) and lymphoid enhancer factor (LEF) are suppressed and targeted gene expression is limited. Conversely, in presence of a canonical WNT ligand (i.e. Wnt 3a), it binds Frizzled (a member of the seven transmembrane protein family) receptors (FRZ) and subsequently interacts with co-receptors lipoprotein receptor-related proteins 5 or 6 (LRP5/6) to initiate WNT–β-catenin signaling (left). Dishevelled (DVL) is then recruited by FRZ and interacts with Axin and draws GSK3β to close proximity of LRP5/6. This prevents β-catenin phosphorylation and ultimately its fate of proteasomal degradation. The accumulated cytoplasmic β-catenin is the translocated into the nucleus, where interactions with TCF/LEF transcription factors initiates targeted gene expression. In addition to a WNT ligands, parathyroid hormone (PTH) can also activate the pathway independently of Wnts by interacting and forming a complex with LRP5/6, to list just one example. Moreover, WNT signaling is not only modulated by its ligands and PTH, it may also be altered by extracellular antagonists including DKK1 and SOST, which competitively binds to LRP5/6 (right). In addition to secreted antagonists, secreted frizzled-related proteins (sFRPs) are a class of ligand specific competitive inhibitors that isolates WNTs from interacting with its receptors. Alternative non-canonical WNT pathways including calcium ($Ca2^+$), planar cell polarity (PCP), or protein kinase A (PKA) associated pathways are not shown.

Table 1. Currently available Non-Invasive OA Injury Models

Model	Fracture/Injury Method	Forces Used	OA Time Frame	Benefits	Drawbacks
Intra-Articular Fracture (IAF)	➢ Mimics high energy impact injury in human such as car accidents, military personal injury or construction work accidents ➢ Method: High impact fracture of tibial plateau	➢ 10N pre-load, ➢ 55N fracture load at 20M/s (adjustable)	➢ 8~50 Weeks ➢ 87% (27/31) success	➢ Nice to be used in larger mice strains ➢ Mimics high impact joint injury	➢ High energy impact
Cyclical Compression of Tibial Cartilage	➢ Representative of OA driven by overexerting the capacity of cartilage sustainability in joints ➢ (Cyclical compressive load to the lower legs through the ankle to the knee)	➢ 4.5N~9N ➢ adjustable Force various depending on the study	➢ 2~5 Weeks ➢ 83% success, however OA's not easily achieved	➢ OA development without major injuries to surrounding joint tissues ➢ Mimics extensive or repetitive use of cartilage	➢ Mild to moderate OA cartilage phenotype, limiting late stages of OA studies
Tibial Compression (TC) Overload	➢ Mimics the human ACL rupture, one of the top leading knee OA contributors and reveals new insights on rapid developing OA conditions ➢ (Single dynamic compressive overload applied to the lower hind leg, to induce rupture)	➢ 1N pre-load ➢ 12~16N overload at • 1mm/s "avulsion fracture" • 500mm/s "rapid tare"	➢ 4~8 Weeks (published) ➢ 2~4 weeks (observed, unpublished)	➢ Rapid OA developing condition; applicable to studying acute processes at the initial injury ➢ Mimics ACL injury	➢ Rapid OA developing conditions enhances erosion making it a severe OA model

Table 1. Non-invasive OA mouse Models. The intra-articular fracture (IAF) of tibial subchondral bone is the most sever of the three models [63]. By sharp contrast, cyclical short term mechanical loading on the articular cartilage through tibial compression leads to mild to moderate OA [61]. The tibial compression (TC) overload inducing anterior cruciate ligament (ACL) rupture [64] may be utilized to study early stages of OA developing joint after faithfully recapitulate human post-traumatic OA in mice. All the non-invasive OA injury models have two common benefits: 1) adjustable injury force and regiment and 2) high reproducibility. A common drawback, is that all three models are not suitable to study all three stages (initial, during, and terminal) of OA developing joint.

Chapter 2: Sclerostin Reduces the Severity of Post Traumatic Osteoarthritis

Abstract

Sclerostin (Sost), a Wnt antagonist and a potent negative regulator of bone formation has recently been implicated in regulating chondrocyte function in osteoarthritis (OA). To determine whether elevated levels of Sclerostin play a protective role in post-traumatic osteoarthritis (PTOA), we examined the progression of OA using a noninvasive tibial compression overload model in SOST transgenic ($SOST^{TG}$ or TG) and Sost knockout ($Sost^{KO}$ or KO) mice. Here we report that $SOST^{TG}$ mice develop moderate OA and display significantly less advanced OA phenotypes at 16 weeks post injury compared to wildtype (*WT*) controls and $Sost^{KO}$. In addition, TGs built 50% less osteophyte volume than *WTs,* at 16 weeks post injury. Quantification of matrix metalloproteinases (MMPs) activity revealed that TGs had ~2-fold less MMP activation, than WTs or KOs, at 3 days post injury, suggesting that elevated levels of Sclerostin inhibit the activity of proteolytic enzymes known to degrade articular cartilage matrix. Intra-articular administration of recombinant Sost protein, immediately post injury, also significantly decreased MMP activity levels relative to PBS treated controls, highlighting the protective role of Sost in articular chondrocytes through the inhibition of catabolic enzymes.

Introduction

The increased risk of developing knee osteoarthritis (OA) after injury to the anterior cruciate ligament (ACL) has been well documented both clinically and in experimental models [64, 119]. Clinical manifestation of post traumatic osteoarthritis (PTOA) is characterized by narrowing of the joint space, emergence of osteophytes through osteoarthritic remodeling, cartilage erosion and fibrillation [119]. Biomechanical disturbances in the joint such as lateral subluxation of the tibia further the development of osteophytes in the lateral tibial-femoral compartment and cause misalignment, rotation and anterior subluxation of the joint; all these physical manifestations contribute to the emergence of intra-articular lesions. Cartilage lesions become further exacerbated through molecular changes in the joint including the increase in the production of matrix-degrading enzymes, such as aggrecanases and matrix metalloproteinases (MMPs). Elevated levels of catabolic enzymes enhance the loss of articular cartilage, increase the amount of pain experienced and cause impaired joint mobility in >50% of individuals that sustained an ACL tear [120]. While undoubtedly the joint architecture, type of surgical intervention and biomechanical disturbance greatly contribute to the progression of PTOA, the individual susceptibilities to inflammatory responses, enzymatic cartilage destruction and osteophyte formation will also determine subsequent osteoarthritic outcomes.

Recent studies have implicated Wnt/β-catenin signaling in OA pathogenesis [118]. Conditional activation of β-catenin in the articular chondrocytes of adult mice resulted in reduced articular cartilage area, increase surface fibrillation, vertical

clefting and osteophyte formation, independent of trauma, suggesting that activation of Wnt signaling in the articular cartilage causes OA-like phenotypes [121]. Furthermore, activated β-catenin has been shown to stimulate the activity of catabolic enzymes in the extracellular matrix (ECM) of the cartilage [122]. These findings suggest that bone and cartilage are regulated by similar but functionally opposing mechanisms, where Wnt signaling is anabolic in bone but catabolic in the cartilage. Sclerostin (Sost) is a potent negative regulator of bone mass, where it normally inhibits Wnt signaling by physically interacting with low density lipoprotein receptor-related protein (LRP) 5/6 co-receptors [97, 98]. In the absence of Sost protein, patients develop two types of hyperostosis, sclerosteosis and van Buchem disease [100, 123]. Consistent with the human hyperosteosis, Sost deficient mice ($Sost^{KO}$ or KO) also acquire a generalized high bone mass phenotype [90, 102]. Conversely, transgenic mice overexpressing SOST ($SOST^{TG}$ or TG) are osteopenic [92].

Until recently, $Sost$ expression has been described as osteocyte-specific, but several reports have now shown that $Sost$ is also expressed in the articular cartilage. The elevated levels of Sost were observed in chondrocytes near damaged sites in the articular cartilage of sheep and mice that were subjected to surgical models of OA [113, 118]. Similarly, transcriptional analysis found $SOST$ to be up-regulated ~14-fold in cartilage derived from biopsies of OA patients undergoing joint replacement surgery [117], suggesting that up-regulation of $SOST$ in cartilage may have a protective role. While these observations have been correlative, in $vivo$ evidence has been lacking in support of $Sost$ as an anti-

catabolic agent, in the joint. Here we investigated the role of Sost in the articular cartilage and found SOST to inhibit cartilage degradation subsequence to traumatic injury by down-regulating catabolic enzymes. These findings suggest that elevated levels of Sost, immediately post injury, can aid the joint in maintaining its articular cartilage integrity in PTOA.

Material and Methods

Mice Strains and Tibial Compression OA injury. $Sost^{KO}$ and $SOST^{TG}$ have been previously described [92, 102]. In brief, $Sost^{KO}$ mice were generated by homologous recombination where a *LacZ* reporter cassette replaces the Sost open reading frame (ORF). $SOST^{TG}$ mice contain an 158-kb human bacterial artificial chromosomes (BAC) transgene of SOST through standard transgenic procedures [124]. Age matched C57/BL6 (*WT*), $Sost^{KO}$ and $SOST^{TG}$ were bred in parallel as controls. Male mice were genotyped by polymerase chain reaction (PCR) and were injured at 16 weeks of age using a previously described tibial compression OA injury model [92]. In short, a continuous dynamic compressive load was applied to the stationary (right) knee joint displacing the tibial condyle over the femoral condyle to render an anterior cruciate ligament (ACL) rupture. The contralateral (left) and age matched (uninjured) joints were utilized as internal and reference controls, respectively. All the mice injured in this experiment were males ($n \geq 5$ per genotype). All animal procedures were carried out in accordance with guidelines under the Institutional Animal Care and Use Committees at Lawrence Livermore National Laboratory and University of California, Davis.

Histology and OA Evaluation. Experimental and control mice were euthanized humanely at 1 day, 6-, 12-, and 16-weeks post injury. Injured (right) and uninjured contralateral (left) joints we dissected free of soft tissue; fixed in 4% paraformaldehyde (PFA) between 36~48 hours; and stored in 70% ethanol (EtOH)

for later processing of micro-computed tomography (µCT) scans (refer later section for details). After the µCT scan, joint samples were dehydrated in plastic cassettes in increasing concentrations of isopropanol (IPA) (70%, 80%, 90%, 95% and 100%) under vacuum pressure -50kPa (kilopascal) for 1 hr each. Fully dehydrated samples were then equilibrated into mineral oil (MO) using 1:5, 1:2, (MO: IPA) and 100% pure MO under vacuum pressure -50kPa for 2 hrs each.   MO equilibrated samples were subsequently infiltrated with 4 changes of paraffin (wax) 1 hr each change with the first two hrs under vacuum (-50kPa). Each joint was embedded with the medial compartment facing the surface of the stainless steel cassette mold (bottom of mold) and adjusted to an approximate 90° bent. Finally, serial sections of knee joints were collected after facing off the first 300µm of joint until completely through knee joint (containing both medial and lateral sections of knee joint). A visual validation of joint landmarks was done using temporal sections on regular microscopes slides.

To visualize the cartilage, bone and other joint tissues, 6µm paraffin sections were stained with Safranin-O (0.1%, Sigma; S8884) and counterstained with Fast Green (0.05%, Sigma; F7252) using standard protocol from IHC world website. Consistent Safranin-O coloration presented in the growth plate were used as an internal stain control. Sections were collected on regular glass slides for histological stains, while charged slides (Fisher; 12-550-17) were used for immunohistochemistry (IHC). OA severity was evaluated at 1 day, 6-, 12-, and 16-weeks post injury on sagittal sections by two field experts and one none expert using a modified OARSI scoring scale (Supp. Fig 1) as previously described [125].

After each step of joint preservation (4% PFA fixation, 70% EtOH storage, and 0.5M EDTA decalcification) samples were thoroughly washed with 3 changes of 1X PBS (40mL each). All solutions were prepared at pH between 7.3~7.4 unless otherwise mentioned. More detailed protocol for paraffin embedded and sectioned may be found in previously published [102, 126].

Immunohistochemistry (IHC). Serial sectioned samples on charged slides were dewaxed on a slide warmer at 65°C for 5 min followed by serial washes of 3X Xylene, 2X 100% EtOH, and 1X 90% EtOH, for 5 minutes each, in a coplin jar. Dewaxed slides were next rehydrated in water, by washing 2X 10 min each and subsequent antigen retrieval step took place for 30 min (specific details below). Slides were gently rinsed with water for 1 min and incubated with blocking agent (Rodent Block (Lab Vision Corp.; TA-125-RB) or Background Buster (Innovox; NB306)) for 30 min. Two subsequent PBS and PBS+0.1%Tween20 (PBST) solution washes followed, for 10 min each. Primary antibodies were resuspended in PBST+5% bovine serum albumin (BSA) and were pipette directly onto sections circled by wax pen and were incubated overnight (minimal 8 hrs). Next day, the slides were washed thoroughly 3X in PBS, for 20 min each. Slides were prepared in PBS+0.1%Tween20 for 10 minutes and were incubated with the secondary antibody for 2 hrs. Post incubation, slides were washed 3X in PBS, for 20 min each. Next, the slides were incubated in PBST for 10 min, followed by addition of 10mM copper sulfate (CuSO4) in 50mM ammonium acetate (pH 5.0) and a subsequent incubation of 5~10 min. This step aids in decreasing tissue auto-

fluorescence. Finally, 2 subsequent washes of PBS for 10 min each and mount with Prolong Gold and DAPI (Life Tech; P36935) on cover slides. Slides were allowed to curate for at least 12 hrs before imaging. The following primary antibodies were used in this study: mouse Sost [R&D; AF1589 (1:200)], human SOST [Abcam; ab75914 (1:20)], collagen II [Col II, Abcam; ab21291 (1:100)], mouse MMP 2 [Abcam; ab110186 (1:100)], mouse MMP 3 [Abcam; EP11867 1:50)] mouse MMP9 [Abcam; ab137867 [EP1255Y] (1:100)], mouse MMP14 [Abcam; ab53712 (1:100)], Furin [Abcam; ab3467 (1:100)], and activated β-catenin [Millipore; 05-665 (1:100)]. Trypsin/EDTA (0.25%) was used for antigen retrieval in 37°C for 30 minutes for all primary antibody except for activated β-catenin and MMPs 2, 3, 9, and Furin which required Uni-trieve (Innovex) in 65°C for 30 minutes. Following Uni-trieve, activated β-catenin and Furin requires an additional retrieval with Proteinase K (20ug/ml) for 20 min. The presence of protein expression was determined by Alexa-Fluor 488 (green) or 594 (red) (Molecular Probes) using a Leica DM5299 compound microscope. Unless otherwise mentioned, all samples were stained and prepared at room temperature (RT).

Micro-Computed Tomography (μCT). Quantification of subchondral bone, 3D reconstruction, and quantification of the osteophyte volume were carried out as previously described [66]. To summarize, injured and contralateral joints fixed in 70% EtOH were extracted and casted into agarose gel to a desire angle and scanned with μCT (SCANCO μCT 35, Bassersdorf, Switzerland) to quantify and image the subchondral trabecular bone of distal femoral epiphysis and osteophyte

40

formation surrounding the joint. Joints were imaged utilizing the guidelines for µCT analysis for rodent bone structure (energy¼55kVp, intensity¼114mA, 10mm nominal voxel size, integration time¼900ms) [127]. Trabecular bone in the distal femoral epiphysis was evaluated by manually outlining the desired regions for analysis on a 2D transverse image, and the region of interest was designated between the growth plate and subchondral cortical bone plate. The quantification of trabecular bone volume per total volume (BV/TV) was done using the tools provided by the manufacturer [64]. Our study focused on exploring only the femoral epiphysis, because of its large volume and therefore providing the most accurate trabecular bone parameters. Lastly, osteophyte volume was calculated at terminal time pointes including all mineralized tissues in and surrounding the joint space while excluding naturally ossified structures (patella, fabella, and anterior/posterior edges of the menisci).

RNA Sequencing (RNASeq). *WT* mice at 16 week of age were injured and euthanized 24 hours post injury. Whole joints (0.25~0.3g of total weight) were dissected where incisions were made at the base of the femoral and tibial joint regions, retaining an intact joint (with some residual muscles encapsulating the joint). Dissected whole joints were next chopped into small chunks and were stored in 3ml of RNAlater (Qiagen) at 4° until processing. Within a week, the RNAlater was replaced with 3ml of Qiazol (79306, Qiagen) lysis solution. Joints were homogenized (Pro Scientific; Bio-Gen PRO200) in Qiazol until samples were completely pulverized. On average, a volume of 1ml of the joint homogenate was

used per RNA isolation reaction and the remaining homogenate was stored at -80C^O, for future use. The quality of isolated RNA was assessed by nano drop (cut off ratio of A260/280 is between 1.9~2.1), where samples with high protein contamination or low RNA yield (minimal of 0.9 ug/ml) were not used for sequencing. Isolated RNA (between 1~2ug) was sequenced using an Illumina HiSeq 2000 platform. After RNA Sequencing a hierarchal clustering of samples identified a few injured and uninjured datasets that were very different from the rest; these samples were not included in the subsequent analysis. Therefore, 2 of 3 male (n=3) injured joint RNA were analyzed to identify possible candidate genes for further analysis. One set of sample was excluded from analyses due to RNA degradation and inconsistent RNA library prep. The contralateral joints were analyzed in the same manner. Sequence data quality was checked using FastQC (http://www.bioinformatics.bbsrc.ac.uk/projects/fastqc) [128]. High quality reads were mapped to mouse genome (mm10) using TopHat [129]. Cufflinks aligned reads were then assembled into transcripts and transcript abundances were estimated in Fragments Per Kilobase of transcript per Million mapped reads (FPKM). Subsequently, differentially expressed genes were identified using Cuffdiff [130]. Genes that were found to be > 1.5 fold up- or down-regulated in injured samples compared to uninjured samples with a false discovery rate (FDR) corrected *p*-value < 0.05 were considered significantly differentially expressed. A functional analysis of differentially expressed genes was performed using DAVID functional annotation software [131].

MMPSense and rmSost Administration. MMPSense (PerkinElmer, NEV10168),
was administered intravenously, 5 hours post injury [1 nmol (100µl)]. Animals were
euthanized 3 days post injury, where the skin was removed, and the joints were
scanned for 90 seconds using a Kodak image station 4000R digital imaging system
(Rochester, NY) at excitation and emission wavelengths of 750 +/- 20 nm and 790
+/- 20 nm, respectively. The fluorescent intensity of the uninjured knee joint was
used as background and its value was subtracted from the fluorescent intensity of
the injured knee. Ten week old *WT* mice were injured, received 3 independent
doses of recombinant Sost (rmSost, R&D 1589-ST-025/CF; 1µg/kg) intra-
articularly (10µl volume) at 5 hours, 1- and 2-days post injury, and *in vivo* imaging
were taken in the same manner as MMPSense. Refer Fig. 4A for time line. For
every genotype, at least 5 mice (n≥5) were used for statistical analysis.

Results

Less Severe PTOA is observed in *SOST^TG*. Using a tibial compression PTOA mouse model (Fig. 1*A*) [64], we examined whether chronic exposure to elevated levels of SOST would impact OA outcomes, post injury. *SOST^TG*, *Sost^KO* and *C57Bl6* control (*WT*) mice were examined histologically and by micro-computed tomography (µCT) at 1 day, 6-, 12- and 16- weeks post injury. While the lateral compartments of the knees were relatively normal in all genotypes, significant differences were observed in the medial compartments, at all times examined (Fig. 1*B*). Injured and contralateral joints were indistinguishable, across all genotypes, at 1-day post injury (Fig. 1*C*), indicating that the cartilage and bone were not damaged by the injury. No significant differences were observed among all genotypes at 6- and 12- weeks post injury consistent with the development of a PTOA phenotype previously described for *WT* mice at 8 weeks post injury [64]. (Fig. 1*D*). The biomechanical destabilization and lateral subluxation of the joint promoted significant erosion of both cartilage and bone on the tibial posterior side (Fig 1*C*, Region C) of the medial compartment of the joint in all genotypes. However, at 16 weeks post injury, *SOST^TG* retained significantly more of the articular cartilage integrity throughout the joint whereas *WT* and *Sost^KO* joints displayed significant erosion below the growth plate of the posterior tibial plateaus (Fig 1*C*, Region C). Examination of the sagittal views of the joints by a modified OARSI grading scale determined that *SOST^TG* had a significantly less severe cartilage loss than either *Sost^KO* or *WT* phenotype joints (Fig. 1*D*). *SOST^TG* had a

44

relatively normal articular surface on both femoral and tibial surfaces, and the meniscus remained non-calcified. The erosion on the posterior side of the tibia preceded beyond the growth plate in both *WT* and *Sost^{KO}* injured joints, while the growth plate was relatively intact in *SOST^{TG}*. These results imply that chronic exposure to high SOST levels preserves cartilage thickness, suggesting that inhibiting Wnt signaling in the joint improves subsequent OA outcomes in response to ACL rupture.

Sost is Upregulated in the Articular Cartilage at 1 Day Post Injury. Since *Sost* is not robustly expressed in the articular cartilage, and *Sost^{KO}* mice do not exhibit a dramatic PTOA phenotype [92, 114], we examined whether *Sost* expression is inducible in *WT* and *SOST^{TG}* joints post injury. Low levels of *Sost* positive chondrocytes were observed in the deep zone of femoral articular cartilage for both *WT* (Fig. 2*A*) and *SOST^{TG}* (Fig. 2*F and L*) uninjured contralateral joints. Consistent with previous reports by Chan *et al.* [113] in a sheep surgical model of OA, we found endogenous levels of Sost (Fig. 2*B-C* and *H-I*) as well as transgenic levels of SOST (Fig. 2*N-O*) to be dramatically elevated in the articular cartilage, at 1 day post injury, primarily in the deep zone of the articular cartilage. Osteocyte expression of Sost in the femoral and tibial cortices was unaffected by injury (Fig. 2*D, J, P*). These findings suggest that Sost/SOST expression is inducible in the articular chondrocytes by traumatic joint injury, and confirms the tissue-specific overexpression of SOST in *SOST^{TG}* which collectively express higher levels of Sost/SOST proteins in the articular chondrocytes than *WT* injured joints.

Consistent with its role in Wnt signaling, with response to injury, elevated levels on Sost/SOST in *WT* and *SOST^{TG}* injured joints revealed a decreased in activated β-catenin (Fig. 3*B and J*). *Sost^{KO}*s presented no alteration of activated β-catenin due to the lack of Sost protein (Fig. 3*E and F)*. These results suggest the role of Sost affecting Wnt signaling in chondrocytes (Fig. 3*B and J*). The expression of activated β-catenin doesn't seem to be altered in osteocytes (Fig. 3*C, G and K*) of injured joints. These results support the notion that Wnt signaling is directly altered in chondrocytes by Sost in the cartilage.

Overexpression of SOST Reduced Osteophyte Formation in PTOA. Since *Sost* modulates bone formation [90, 92], we next examined osteoarthritic remodeling by quantifying the loss in subchondral trabecular bone and the gain in osteophyte volume at 6-, 12- and 16- weeks post injury by μCT (Fig. 4). Consistent with the established catabolic role of *Sost* in bone, *Sost^{KO}* injured joints proceeded to synthesize 50% and 28% more ectopic bone than *WT* by 12-, and 16- weeks post injury, respectively (Fig. 4*A-B*). While no significant differences were observed between *SOST^{TG}* and *WT* joints at both 6- and 12- weeks post injury, 50% less osteophyte volume was measured in *SOST^{TG}* injured joints, at 16 weeks post injury (Fig. 4*B*). Osteophytes were most noticeable, which presents the region of focus were on the medial compartment of injured joints because physiologically have more dramatically affected by ACL rupture (Supp. Fig 2). Between 12- and 16- weeks post injury, both *WT* and *Sost^{KO}* joints built significant amount of osteophytes, while *SOST^{TG}* injured joints did not acquire any significant new

osteophyte volume. Whereas both *WT* (27.2±3%) and *SOST^TG* (21.5±10%) injured

joints lost significant subchondral bone volume in the femoral epiphysis relative to

the uninjured contralateral joints, *Sost^KO* injured joints were protected from bone

loss (Fig. 4*C*). These findings suggest that *SOST* overexpression protects the

injured joint from excessive osteophyte formation, while lack of Sost protects the

femur from bone loss due to disuse or injury mediated by elevated catabolic activity

in the subchondral bone.

SOST Inhibits the Activation of Matrix Metalloproteinases (MMP) in Injured

Joints. In animal models of OA, macroscopic and radiological changes in the joint

are preceded by early changes in cartilage metabolism. In patients with OA, the

synovial fluid contains increased levels of cartilage oligomeric matrix protein

(COMP), aggrecan fragments and high levels of MMPs, indicating increased

degradation of joint tissue post traumatic injury [132]. MMPs play a key role in

normal and pathological cartilage remodeling, and comprehensively, members of

the MMP family are able to degrade all components of the extracellular matrix

[133]. In addition, broad-range MMP inhibitors have been previously shown to

abrogate cartilage erosion in animal models of OA [134]. To determine whether

Sost/SOST modulates MMP activity in injured joints, we visualized and quantified

MMP activity using a fluorescent substrate of MMPs *in vivo*, (MMPSense750) 3

days post injury (Fig. 5*A*). Both *WT* (Fig. 5*D*) and *Sost^KO* (Fig. 5*E*) injured joints

displayed similar levels of MMP activity while *SOST^TG* injured joints had a

significant reduction (>2-fold) in MMP activity (Fig. 5*B, F*), suggesting that *SOST*

inhibits the activation of proteolytic enzymes known to degrade the articular cartilage matrix. Similarly, when *WT* injured joints were dosed with recombinant mouse Sost protein (rmSost) intra-articularly, immediately post injury (Fig. 5*A*), a significant decrease in activated MMPs (35.8$\pm$17%) was observed compare to PBS controls (Fig 5*B, G-H*).

MMPSense is a universal substrate for a wide range of MMPs, we assessed changes in specific MMP levels by both immunohistochemical staining with antibodies targeting single activated MMP proteins and whole joint RNA sequencing analysis, to assess the transcripts altered in joints after injury. In comparison, injured joints revealed a series of catabolic enzymes, including MMP transcripts that were upregulated including: MMPs 2, 3, 9, 14 Furin at 1 day post injury in both WT and KOs (Table 1). Both activated MMP2 and MMP3 were found to be dramatically upregulated in injured cartilage in both *WT* (Fig 5 *I-L*) and *Sost^{KO}* (Fig *5 M-P*). In contrast, no obvious changes in the expression levels of activated MMP2 and MMP3 were obvious in chondrocytes, between the injured and uninjured cartilage of *SOST^{TG}* (Fig *5 Q-T*). Interestingly, other MMPs including MMPs 9, 14 and Furin appears to be altered transcriptionally, however seems to be unaffected translationally between all genotypes (Table 1 and Supp. Fig 3).

Discussion

Significant evidence exists that implicates Wnt signaling to have opposing effects on bone and cartilage, hence modulation of Wnt signaling in the musculoskeletal system can contribute to both osteoporosis and OA outcomes. The multitude of Wnt signaling participants, including ligands, receptors, co-receptors and inhibitors has painted a picture of a pleiotropic Wnt signaling with many possibly redundant roles. This has hindered us from clearly delineating the role of specific Wnt molecules in the development of degenerative disorders like OP and OA. Since the discovery by *Chan et al.* [113] that Sost is upregulated in focal areas of damaged cartilage in a sheep and mouse model of OA. Conflicting reports have emerged about the impact loss of Sost has on the development of OA [118]. Here we argue that while the Sost loss of function may only slightly increase the severity of PTOA, gain of function or ectopic administration of Sost does indeed have a significant beneficial effect on the progression and outcome of PTOA. We reasoned that elevated levels of SOST in the joint (either in transgenic mice or through intra-articular administration) significantly reduce the expression and hence the activity of catabolic enzymes known to degrade the cartilage extracellular matrix. High levels of Sost in the joint therefore help the articular cartilage maintain its integrity subsequent to trauma by combating the normal upregulation of cartilage metabolic enzymes activated by inflammation. Since Wnt ligands have been shown to increase the expression of a large number of matrix metalloproteinases in the human synovium and to stimulate the

chondrocyte metabolic action in rabbit models of OA. We propose a mechanism by which high levels of Sost inhibit MMPs by preventing their Wnt-dependent activation. Though only activate MMPs 2 and 3 proteins were distinctly up-regulated in injured joint, while MMPs 9, 14 and Furin were unaffected among all characterized genotypes suggests that elevated levels of SOST in $SOST^{TG}$ joints inhibit cartilage degradation post injury, through the selective inhibition of MMPs 2 and 3 expression. Interestingly, Sost appears to only modulate MMPs 2 and 3 at the initial stages post injury. The seemingly higher upregulation of MMP activation we observed in the $Sost^{KO}$ joints may have been masked by the maximum threshold of the MMPSense limitation.

While prior work had primarily referred to Sost as an exclusively osteocyte-derived protein, our work further builds upon findings by Chan *et al.* where they observed Sost activation in chondrocytes, 2-weeks post injury. Here we show that Sost does not activate exclusively in damaged focal areas of articular cartilage, but is activated in the deep zone, immediately after the injury (Fig. 2). We also know that subchondral bone loss represents a consequence of knee injury, and since $Sost^{KO}$ joints are protected from significant subchondral bone loss, we can conclude that up-regulation of Sost in the articular cartilage post injury may also be a contributing factor to the rapid bone loss post joint injury. Though, to conclusively map out the cell autonomous and non-autonomous roles of Sost in bone and cartilage, similar studies will have to be conducted in conditional mice with inactivated alleles in chondrocytes or osteocytes.

The opposing effects of Sost on bone and cartilage are further supported by clinical data that correlates high levels of plasma sclerostin with increased fracture risk [135], and low levels of Sost in both OA patient derived plasma and synovial fluid [136]. The mechanism by which sclerostin levels are reduced in circulation and in the synovial fluid of OA patients is unknown, but our results, where intra-articular administration of Sost significantly reduced MMP activity shortly post injury, suggests that Sost may represents a biomarker of OP and OA, but may also have a therapeutic benefit in injured joints. While we didn't observe significant differences in the PTOA damage among the *WT*, *Sost^{KO}* and *SOST^{TG}* joints at initial time point (1 day) post injury, we may infer that the cartilage damage observed at 6, 12, and 16 week time points, in all genotypes, may be due exclusively to the outcome of joint destabilization, and mechanical wear of the joint in the absence of an ACL. Yet at 16 weeks post injury, primarily in regions away from the misaligned joint, it is evident that SOST overexpression preserved the integrity of the articular cartilage [Fig. 1*C*; regions A and B]. This observation combined with the MMP results post Sost-intra-articular administrations, suggest that Sost may greatly contribute to PTOA outcome, if administered to the synovium immediately post injury, and after surgical stabilization of the injured joint. Lastly, Sost administration to the injured joint may also prevent osteophyte chondrocyte formation and the accumulation of ectopic bone that may reduce mobility and increase pain in the joint, therefore a balance between the anabolic role of Sost in cartilage and the catabolic role of Sost in bone may be beneficially manipulated to promote favorable outcomes of PTOA.

Figure 1. Histological Evaluation of *WT*, *Sost^KO^* and *SOST^TG^* after TC OA Injury

Region "a"   Region "b"   Region "c"
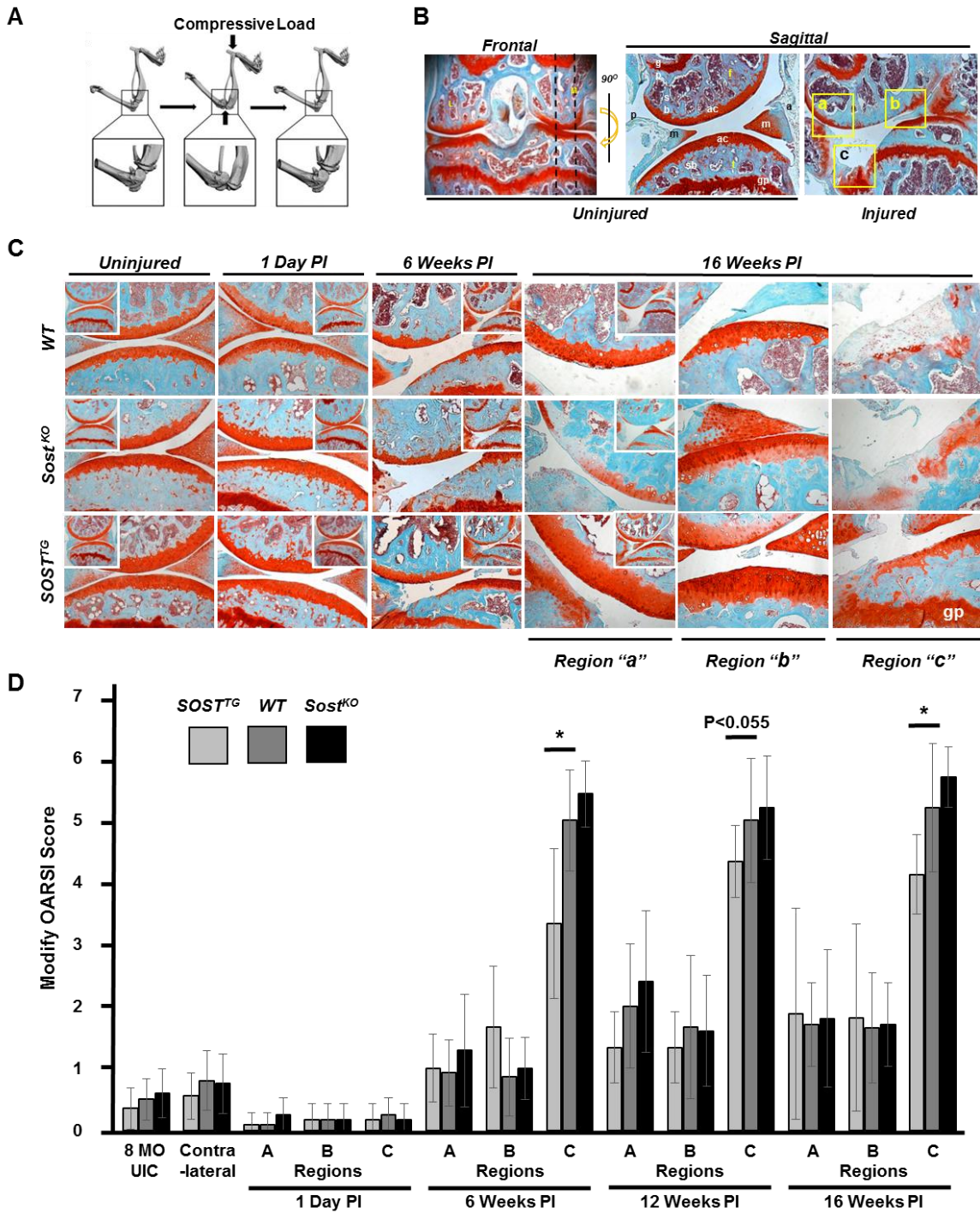
Figure 1. Moderate OA phenotype in *SOST^TG* compared to *WT* and *Sost^KO*. A compressive load was applied to *WT*, *Sost^KO* and *SOST^TG* joints to promote dislocation and ACL rupture [62] (A). Safranin-O and Fast Green stains were performed on frontal and sagittal sections (B). Sagittal sections were examined in the medial condyle between dashed lines, scoring 3 distinct regions: femoral surface (a); anterior tibial surface (b); and the posterior tibial surface (c). (C) Representative sagittal histological sections of injured joints at 1 day (early) and 16 weeks (late) post injury (C). Joints injured at 16 weeks were examined (C) and scored (D) in 3 distinct regions using a modified OARSI scoring method [OA severity: 0~2 (mild); 3~4 (moderate); and 5~6 (severe)]. 5X magnification vies are provided at the corners of each image; all other histological images are at 20X magnification. $^*p < 0.05$

Figure 2. Immunohistochemical identification of localized Sclerostin in Articular Cartilage after Injury
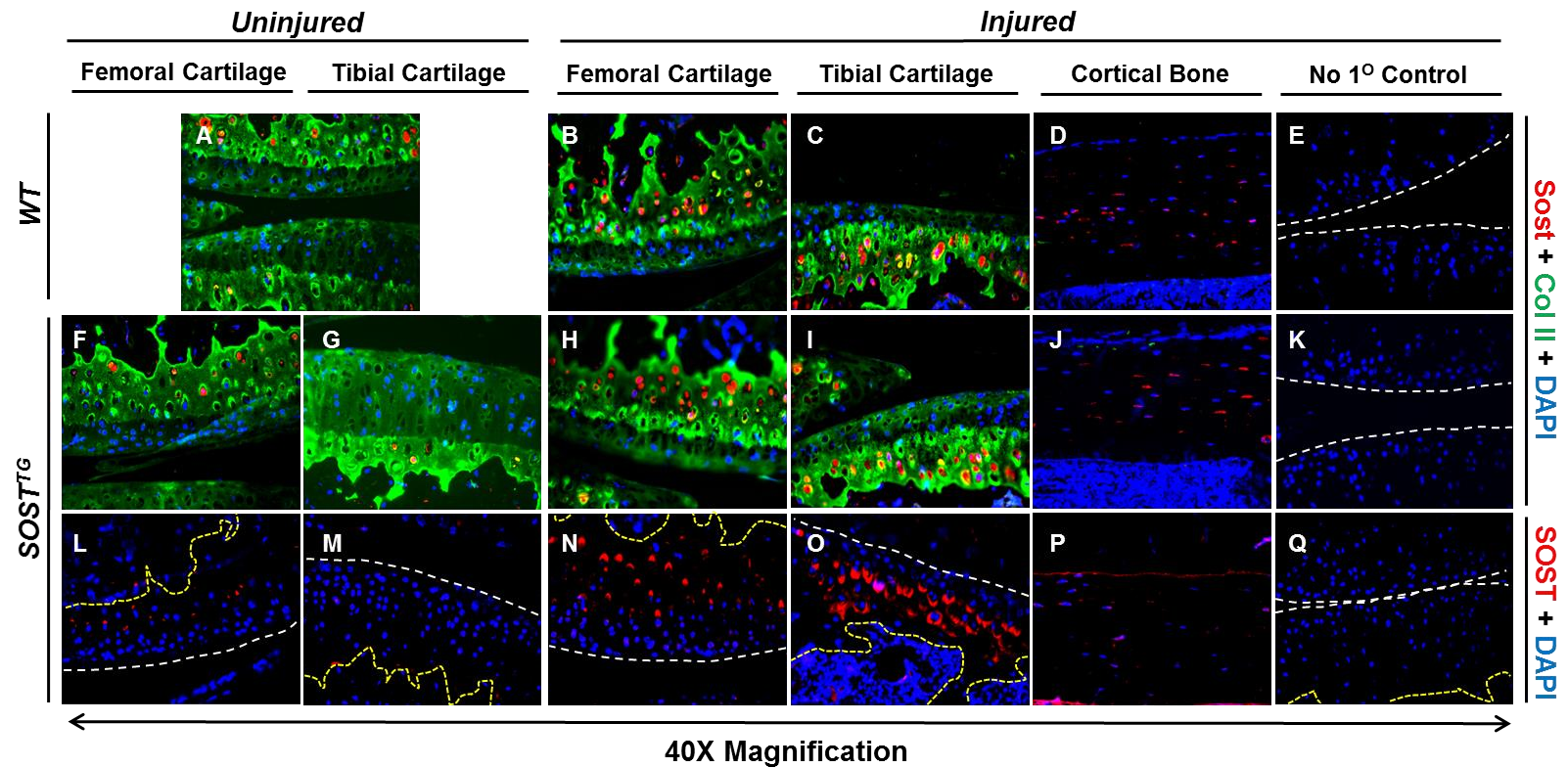
Figure 2. **Sclerostin expression upregulates in the articular cartilage, post injury.** Sost immunostaining was conducted on uninjured *WT* (*A*) and *SOST^TG* (*F, G, L, and M*) joints at 1 day post injury. Injured *WT* joints had elevated levels of Sost (*B* and *C*) while injured *SOST^TG* joints had elevated expression of both mouse (*H and I*) and human Sclerostin (N and O), 1 day post injury. No differences were observed in Sclerostin expression, in the osteocytes of injured animals (*D*, J, and P). All Images taken at 40X magnification. The white dash lines separate joint space and AC surface; and yellow dash lines separates the subchondral trabecular bone borders between calcified cartilages.

Figure 3. Reduction of Activated β-catenin in injured articular cartilage
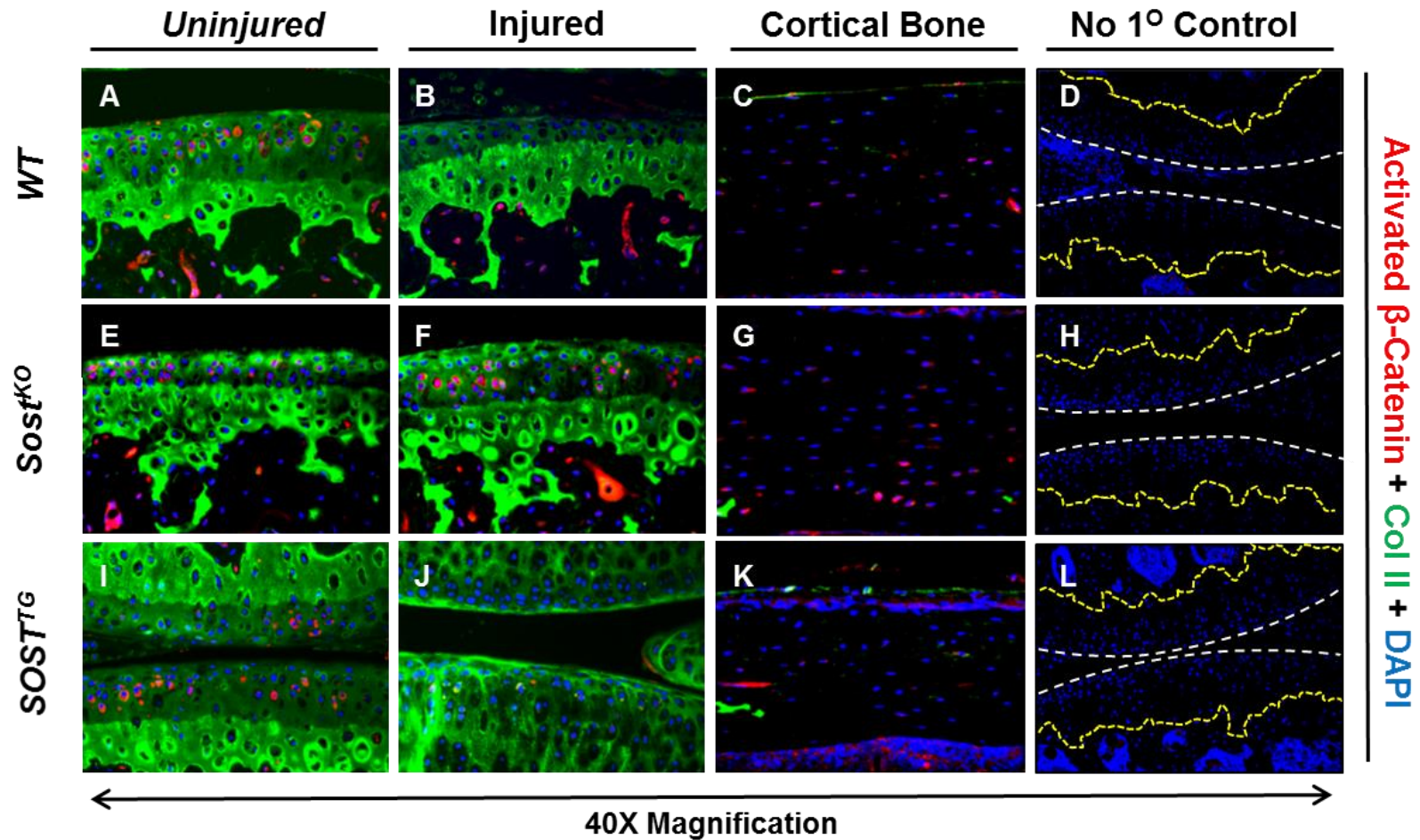
Figure 3. **Activated β-catenin expression are diminished in injured articular cartilage.** Activated β-catenin immunostaining was conducted on uninjured *WT* (*A~D*), *Sost^{KO}* (*E~H*) and *SOST^{TG}* (*I~L*) joints at 1 day post injury. Injured *WT* and *SOST^{TG}* joints had decreased levels of *SOST^{TG}* (*B* and *J*) while injured *Sost^{KO}* joints had no obvious

change compared to its contralateral joint, 1 day post injury. No differences were observed in Sclerostin expression, in the osteocytes of injured animals (*C, G, and K*). All Images taken at 40X magnification. The white dash lines separate joint space and articular cartilage surface; and yellow dash lines separates the subchondral trabecular bone borders between calcified cartilages

Figure 4. Bone and Osteophyte Parameters in SOSTTG and SostKO after TC OA Injury
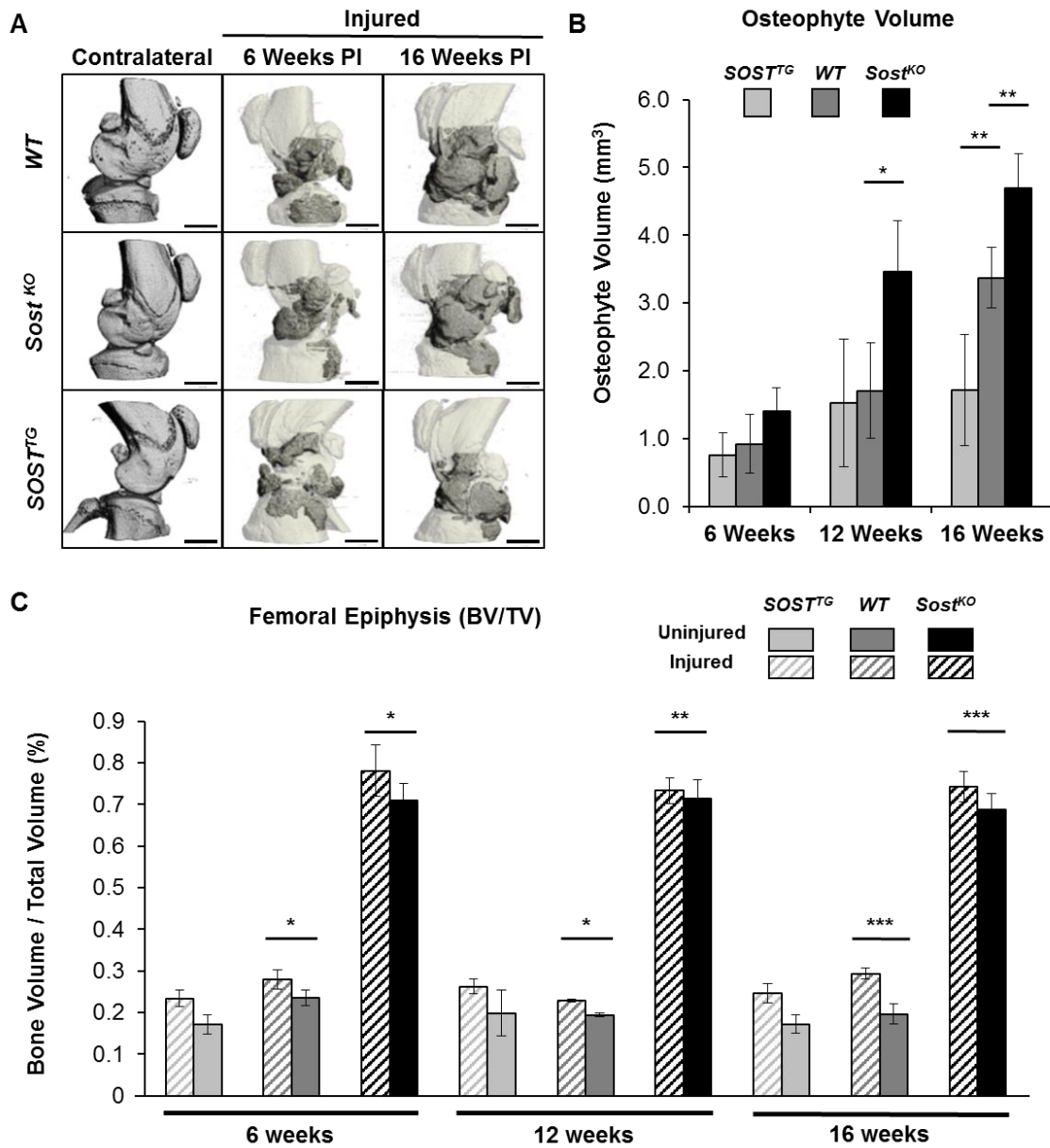
Figure 4. *SOST^{TG}* joints are protected from excessive osteophyte formation, while *Sost^{KO}* joints are protected from subchondral bone loss in injured joints. μCT representation of mouse injured joints at 6- and 16- weeks post-injury. Darker regions in the inured scans depict ectopic bone nodules (*A*). Osteophyte volume (gray area in *A*) was quantified at 6-, 12-, and 16-weeks post injury and

compared between genotypes (*B*). Subchondral trabecular bone volume to total volume ratio was quantification and analyzed between injured and uninjured joints at 6-, 12-, and 16-weeks post injury (C). Scale bar = 1mm. *$p < 0.05$, ** $p < 0.01$, *** $p < 0.001$

Figure 5. Sclerostin Effect on Activated MMPs at Early Stages Post Injury
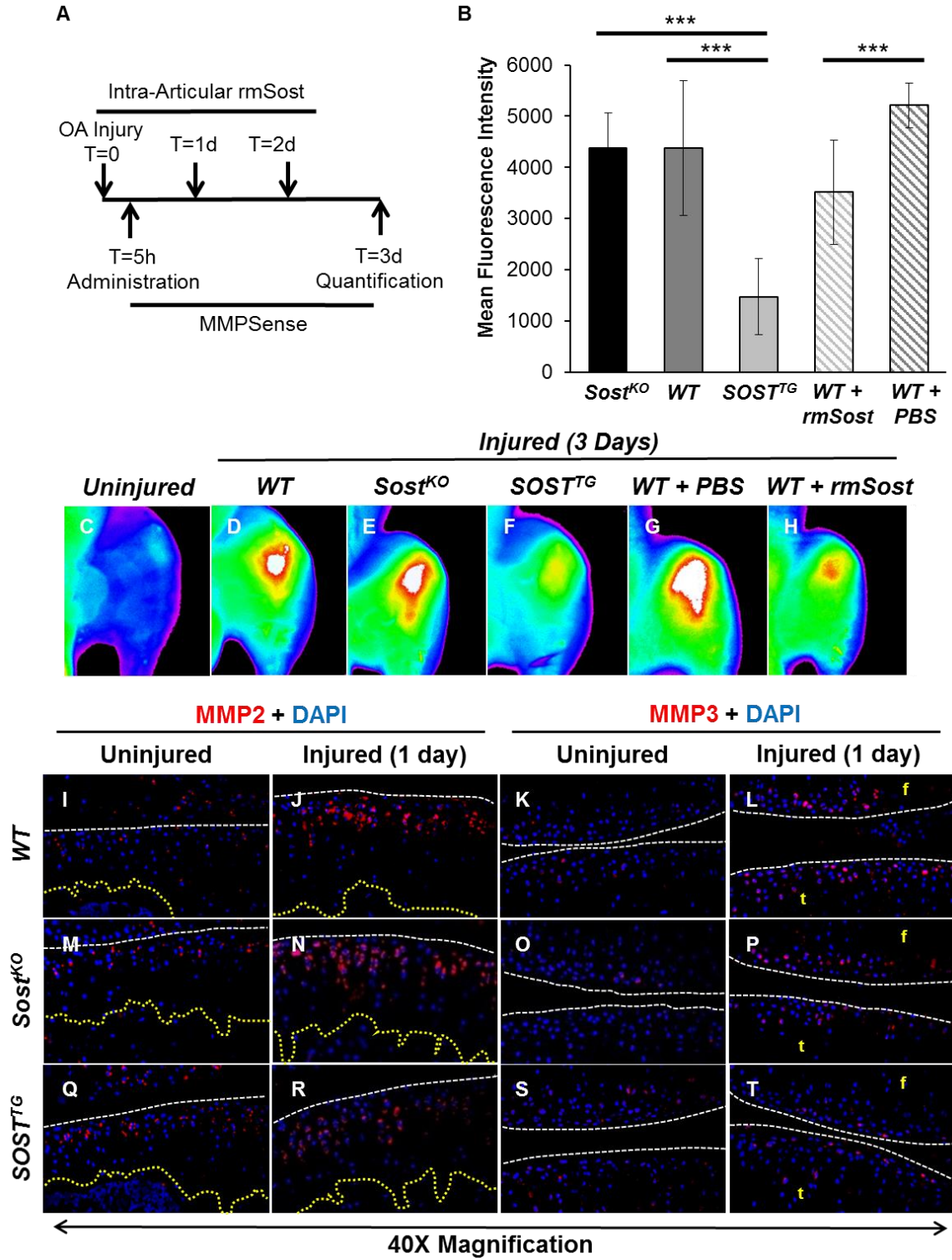
Figure 5. $SOST^{TG}$ **and WT injured joints treated with recombinant Sost protein have reduced levels of activated MMPs post injury.** MMPSense was administered 5 hours post injury; rmSost (intra-articular) injections were carried out on day 1 and 2, and mean fluorescence intensity was measured 3 days post injury as depicted in (A). $SOST^{TG}s$ as well as rmSost treated injured joints displayed significantly less fluorescence than $Sost^{KO}$ or *WT* control joints (*B*). Representative *ex vivo* images of *WT* uninjured (C) and injured *WT* (*D*), $Sost^{KO}$ (*E*), $SOST^{TG}$ (*F*) injured joints show reduced fluorescence in $SOST^{TG}s$. Similarly, rmSost treated injured joints (*H*) show less fluorescence than PBS controls (*G*). Immuno-localization of MMPs 2 (*I, J, M, N, Q, and R*) and 3 (*K, L, O, P, S, and T*) at 1 day post TC injury. Separation between joint space and articular cartilage surface (white dash line); separation between subchondral trabecular bone borders between calcified cartilages (yellow dash lines). "f" = Femur and "t" = tibia. ** $p < 0.01$ and *** $p < 0.001$

Name	gene Symbol	WT (1 Day Post Injury)				Sost^KO (1 Day Post Injury)			
		Injured	Uninjured	Fold Change	Adjusted P-Value	Injured	Uninjured	Fold Change	Adjusted P-Value
Aggrecan	**Acan**	7.442	3.792	0.973	0.00549	1.563	0.899	0.798	0.0251
Collagen, type X, alpha 1	**Col10a1**	7.000	2.574	1.443	0.02019	2.654	0.967	1.457	0.2715
Collagen, type II, alpha 1	**Col2a1**	19.202	5.560	1.788	0.00086	6.566	3.737	0.813	0.0137
Cartilage Oligomeric Matrix Protein	**COMP**	28.736	20.259	0.504	0.17340	17.588	13.089	0.426	0.1918
Tumor Necrosis Factor Receptor Superfamily, Member 1a	**Tnfrsf1a**	13.050	5.040	1.373	0.00086	23.996	7.786	1.624	0.0002
Tumor Necrosis Factor Receptor Superfamily, Member 1b	**Tnfrsf1b**	9.614	6.101	0.656	0.09228	10.034	2.052	2.290	0.0002
Cathepsin D	**Ctsd**	313.47	190.71	0.717	0.04985	692.59	159.52	2.118	0.0002
Cathepsin S	**Ctss**	243.93	144.81	0.752	0.02505	72.036	40.174	0.842	0.0045
Matrix Metallopeptidase 2	**Mmp2**	16.714	15.780	0.083	0.87063	14.204	8.251	0.784	0.0054
Matrix Metallopeptidase 3	**Mmp3**	9.470	1.405	2.753	0.00086	3.599	0.512	2.812	0.0007
Matrix Metallopeptidase 9	**Mmp9**	210.99	124.59	0.760	0.03556	203.11	35.752	2.506	0.0002
Matrix Metallopeptidase 13	**Mmp13**	45.510	54.705	-0.266	0.536	19.595	22.070	-0.172	0.6456
Matrix Metallopeptidase 14 (membrane-inserted)	**Mmp14**	19.903	15.436	0.367	0.35965	31.430	5.895	2.415	0.0002
A Disintegrin and Metallopeptidase Domain 8	**Adam8**	10.159	8.352	0.283	0.52093	8.252	1.772	2.219	0.0002
A Disintegrin-like and Metallopeptidase with Thrombospondin Type 1 Motif, 2	**Adamts2**	4.425	3.472	0.350	0.40744	3.204	1.423	1.171	0.0002

Table1: Comparing molecular changes between injured and uninjured whole joint RNA. RNASeq revealed a variety of matrix proteins, inflammatory receptors and cartilage degrading enzymes differentially up regulated in injured joints. Higher cartilage protein transcripts are upregulated in WT than KO injured joints. Conversely, many of the cartilage degrading enzymes are higher in KO than WT injured joints.

Both WT and KO presented similar upregulation pattern in injured joints

Both Injured are upregulated, however more differentially regulated in WT

Both Injured are upregulated, however more differentially regulated in KO

Significantly upregulation in KO only

Supplementary Figure 1. Standard Histological evaluation of Murine OA Joints

A

B

Score	Osteoarthritic Damage
0	Normal
0.5	Loss of Safranin-O stain only, no cartilage integrity compromise
1	Surface fibrillation without lost of cartilage
2	Minor clefts down below the superficial zone
3	Vertical cleft or erosion expanding to <25% of articular cartilage surface
4	Vertical cleft or erosion expanding to 25~50% of articular cartilage surface
5	Vertical cleft or erosion expanding to 50~75% of articular cartilage surface
6	Vertical cleft or erosion expanding to >75% of articular cartilage surface

Supplementary Figure 1. Histological atlas and mouse OA evaluation. Representative of articular cartilage phenotype in OA developing joints (A). Quantitative OA severity utilizing mouse joint atlas ranging from mild (0~2), moderate (3~4), and severe (5~6) (B).

Supplementary Figure 2. More Osteophyte Accumulates on the Medial Side of OA Joint
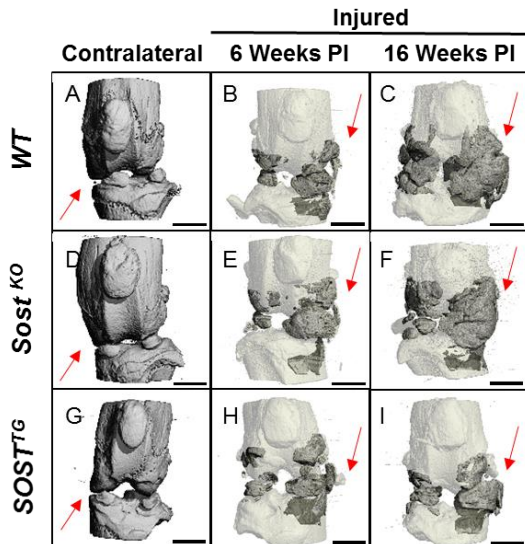
Supplementary Figure 2. A greater accumulation of osteophyte formation found on the medial compartment of injured joints. Frontal representation of μCT scans revealing *WT*, *Sost^{KO}*, and *SOST^{TG}* injured joints at 6- and 16- weeks post-injury. Darker regions in the injured scans represents ectopic bone nodules with arrows indicating the medial compartment. Scale bar = 1mm.

Supplementary Figure 3. Activated MMPs 9, 14, and Furin were unchanged immediately post injury
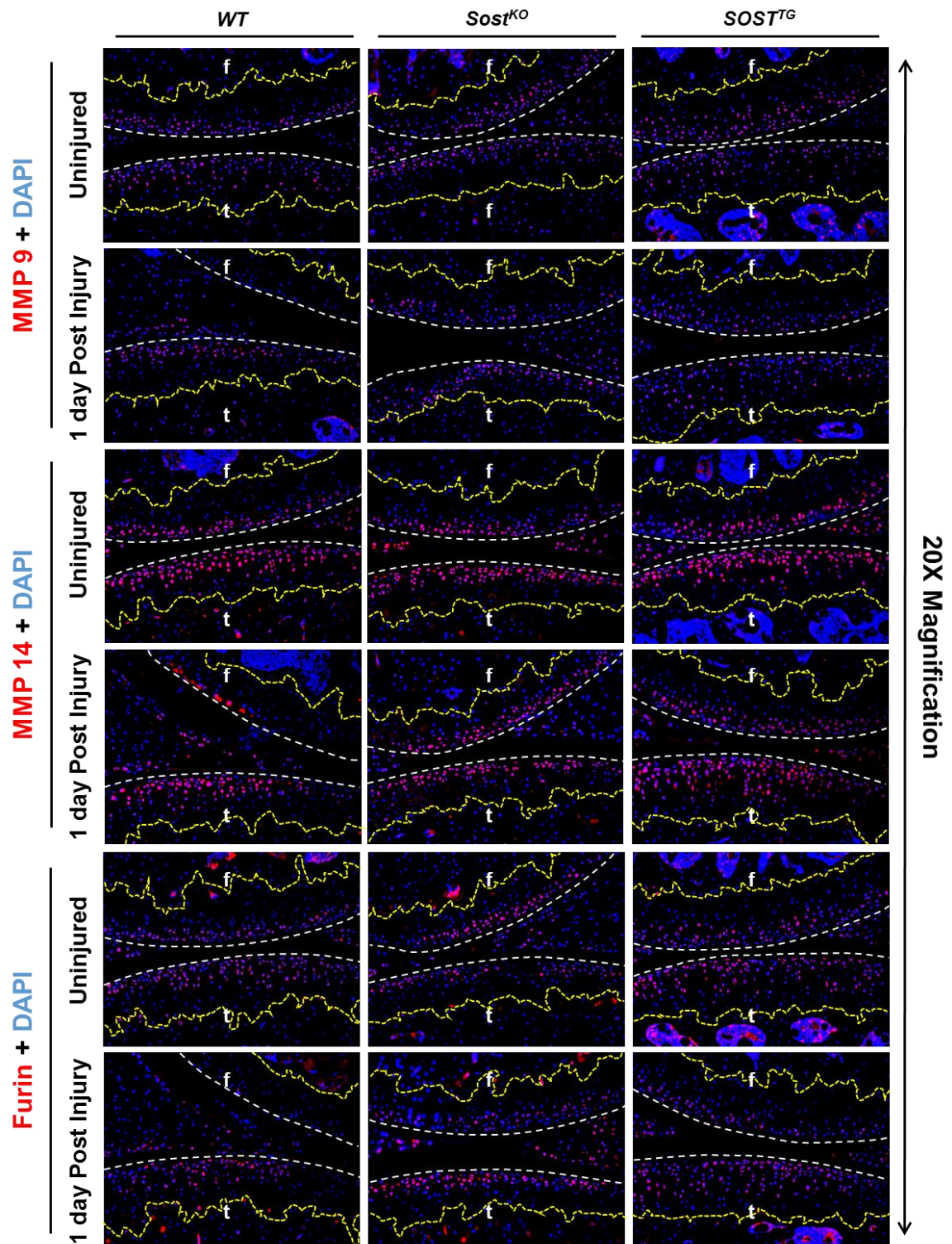
Supplementary Figure 3. Immunohistochemical localization of MMPs 9, 14, and Furin on 1 days post injured cartilage. No obvious difference were observed between the contralateral and the injured joints in all three genotypes. Separation between joint space and articular cartilage surface (white dash line); separation between subchondral trabecular bone borders between calcified cartilages (yellow dash lines). "f" = Femur and "t" = tibia. All images were taken at 20X magnification.

Chapter 3: Global Molecular Changes in a Tibial Compression Induced ACL Rupture Model of Post-Traumatic Osteoarthritis

Abstract

Joint injury causes post-traumatic osteoarthritis (PTOA). About ~50% of patients rupturing their anterior cruciate ligament (ACL) will develop PTOA within 1-2 decades of the injury, yet the mechanisms responsible for the development of PTOA after joint injury are not well understood. In this study, we examined whole joint gene expression by RNAseq at 1 day, 1-, 6- and 12-weeks post injury, in a non-invasive tibial compression (TC) overload mouse model of PTOA that mimics ACL rupture in humans. We identified 1446 genes differentially regulated between injured and contralateral joints. This includes known regulators of osteoarthritis such as *Mmp3*, *Fn1* and *Comp*, and several new genes including *Suco*, *Sorcs2* and *Medag*. We also identified 18 long noncoding RNAs that are differentially expressed in the injured joints. By comparing our data to gene expression data generated using the surgical destabilization of the medial meniscus (DMM) PTOA model, we identified several common genes and shared mechanisms including signaling pathways such as Wnt and Tgfβ signal transduction pathways. We also compared our gene expression data to candidate genes identified by transcriptional profiling of tissue samples from OA patients and genome wide association studies and identified several common genes. This study provides the

65

first account of gene expression changes associated with PTOA development and progression in a TC model.

Keywords: Osteoarthritis, RNA Sequencing, Tibial Compression, ACL

Introduction

Post-traumatic osteoarthritis (PTOA) is a painful and debilitating disease that is caused by mechanical destabilization of the joint and injury to the articular cartilage; however the molecular and cellular mechanisms leading to cartilage degeneration due to trauma are not well understood. It has been demonstrated that inflammation [51], abnormal subchondral bone properties [52] and loss of response to mechanical load [54] all contribute to the development of OA. Many individuals developing OA are asymptomatic until significant joint damage has occurred [55], at which point the only available long term treatment options are surgical replacement of the joint and or pain management [56]. Therefore, identifying and characterizing OA biomarkers for detecting and tracking the progression of the disease combined with developing new pharmacologic interventions aimed to minimize cartilage damage triggered by joint injury, are vital scientific endeavors.

In the past decade, using human biopsy and animal OA models, new insights about joint OA pathogenesis were uncovered. To date, several studies have evaluated molecular changes associated with human arthritic joint tissues including: synovium [137], meniscus [138], cartilage [139], osteophytes [140] and subchondral bone [141]. Several studies revealed molecular changes associated with late stages of OA but only a few examined earlier molecular events because of clinical limitations. It is difficult to discriminate asymptomatic OA tissues and compare it to age matched healthy controls. Instead, mouse models that mimic

67

human OA have been used with great success to study OA pathogenesis and to identify putative molecular and genetic factors driving the progression of the disease [142, 143].

Though OA is commonly diagnosed by visible damage to the articular cartilage, more recent assessments of OA have been migrating to evaluate the entire joint, and perceive the disease as a multi factorial, multi cell-type phenotype [144, 145]. In this study, we used a non-invasive tibial compression (TC) mouse model that closely mimics traumatic anterior cruciate ligament (ACL) rupture in humans to study molecular mechanisms driving PTOA development and progression [146]. Through RNA sequence analysis (RNAseq), we identified 1446 differentially regulated genes in injured joints. Furthermore, we compared our data with gene expression data generated from the surgical destabilization of the medial meniscus (DMM) [147, 148] model of PTOA, to highlight shared mechanisms.

Materials and Methods

Animals and Tibial Compression (TC) Joint Injury. Wildtype C57B/L6 mice underwent injury by applying a TC load (10~12N) to the right knee of 16 weeks old male mice, as previously described [146]. All animal experiments were conducted in accordance with institutional animal care and use committee guidelines at Lawrence Livermore National Laboratory and University of California, Davis.

Histology. Injured and uninjured (contralateral) joints were collected (N$\geq$5) at 1 day, 1-, 6- and 12- weeks post injury. Joints were dissected, fixed in 4% paraformaldehyde, decalcified using 0.5M EDTA, infiltrated in increasing concentrations of isopropanol, equilibrated into mineral oil, and embedded into paraffin wax. 6μm paraffin sections were stained on glass slides using 0.1% Safranin-O and 0.05% Fast Green using standard procedures (IHC world) and imaged using a Leica DM5000 microscope.

RNA Isolation and Sequencing (RNASeq). Injured and contralateral joints [1 day (n=5), 1week (n=5), 6 weeks (n=3), and 12 weeks (n=3)] were dissected and cut at the base edges of femoral and tibial joint regions with small traces of soft tissues to preserve the intact knee joint. Dissected joints (between 0.25~0.3g total weight) were then cut into small pieces and submerged in RNA Later (Qiagen) and stored at 4°C until processing. RNA Later solution was removed and dissected joints were homogenized in Qiazol lysis solution (Qiagen); RNA was isolated

utilizing RNeasy Qiagen kits according to manufacturer's instructions. Isolated RNA (between 1~2ug) was sequenced using an Illumina HiSeq 2000.

RNASeq Data Analysis. RNASeq data quality was checked using 'FastQC' (http://www.bioinformatics.bbsrc.ac.uk/projects/fastqc). Sequence reads were aligned to mouse genome (mm10) using 'TopHat' [129]. Differential gene expression analysis was conducted using an FPKM (fragments per kilobase of transcript per million mapped reads) based strategy and a count based strategy, to reduce the number of false positive discoveries. In the FPKM based strategy differentially expressed genes (DEGs) were identified using 'Cufflinks' and 'Cuffdiff' [130]. A gene was considered significantly differentially expressed when FDR corrected p-value was less than 0.05 and fold change was greater than 1.5. Subsequently, DEGs were filtered based on their expression values and low expressing genes with FPKM value < 2 were removed. In the count based strategy 'featureCounts' [149] was used to perform read summarization on reads mapped with 'TopHat'. Subsequently, the data was normalized using 'voom' [150] and DEGs with fold change > 1.5 and p-value < 0.05 were identified using 'limma' [151, 152]. Genes identified by both methods as significantly differentially expressed were used to generate a list of high-confidence DEGs. These high-confidence DEGs were used for further analyses. Venn diagrams were created using R package 'VennDiagram'.

Microarray Data Analysis. Previously published microarray data were downloaded from Gene Expression Omnibus (GEO) and the data analysis was conducted using Bioconductor [153]. Affymetrix data [138, 140, 154] preprocessing and normalization were performed using RMA method [155]. Agilent data [147] were background corrected with Normexp, normalized within arrays with loess and between arrays with Aquantile [151]. Differentially expressed genes were identified using 'limma' [151]. Genes with p-value less than 0.05, FDR corrected p-value less than 0.1 and fold change greater than 1.5 were considered significantly differentially expressed throughout the paper unless otherwise specified.

Functional annotation. Gene ontology analysis was performed using DAVID [131] and enriched gene ontology terms (p-value < 0.01) were identified. Gene Loci associated with osteoarthritis (OA), rheumatoid arthritis (RA), juvenile idiopathic arthritis (JIA) and ankylosing spondylitis (AS) were obtained from the GWAS website [http://www.ebi.ac.uk/gwas/] and compared to differentially expressed genes. Mouse phenotype data was obtained from MGI database (http://www.informatics.jax.org/). Long noncoding RNA (*lncRNA*) gene annotations were obtained from GENCODE [156]. ToppCluster was used to cluster differentially expressed genes from different time points based on functional enrichment [157] and Cytoscape was used for cluster visualization [158].

Results

Molecular Changes Associated with PTOA Development. Knee injury was induced by applying a single compressive load (10-12N) to the right knee (Fig. 1a), as previously described [146, 159]. Injured and contralateral joints were examined histologically and by RNASeq at 1 day, 1-, 6-, and 12- weeks post injury (Fig. 1b). Contralateral controls revealed no pathological changes at all times examined (Fig. 1c). Furthermore, no obvious morphological changes were observed histologically at 1 day post injury (Fig. 1d), suggesting that no articular fracture or damage was initially introduced by the compressive load and knee dislocation. As previously reported, we observed moderate and severe cartilage erosion (Fig. 1e, f) with osteophyte formation (Fig. 1g, h, i) at 6- and 12- weeks post injury, respectively [146, 159]. Subchondral bone loss was also observed, however, only at 12 weeks post injury the bone loss was significant (Fig. 1j).

The FPKM and the count based method (Fig. 2a) jointly identified a total of 1446 DEGs (Table S-1), where 599, 644, 511 and 201 DEGs were found at 1 day, 1-, 6- and 12- weeks post injury, respectively (Fig. 2b, c). The largest overlap among the DEGs was found between 1 day and 1 week post injury, where 272 up- and 23 down-regulated genes were in common (Fig. 2b and 2c). We also identified 15 genes that were up-regulated at all time points examined (Table 1). Interestingly, no genes were found to be down-regulated at all time points. Genes up-regulated at all time points included extracellular matrix (ECM) components [(*Fn1* [160, 161], collagens 3, 5 and 6 [162, 163], *Cthrc1*, *Thbs3*], collagen

metabolic enzymes [*Mmp3* [164]] and Wnt signaling proteins [*Sfrp2* and *Wisp2*]. In addition, it included ECM and cell adhesion proteins [*Srpx2* and *Tnn*] and a synovial fibroblast cell surface marker [165] [*Thy1*]. We also identified 18 *lncRNA* including *Dnm3os*, *Rian*, *H19* and *Snhg18* differentially regulated in injured knee joints compared to uninjured controls (Table 2).

Functional analysis of differentially regulated genes. For up-regulated genes, categories corresponding to *vasculature development*, *cell adhesion, extracellular matrix organization, extracellular structure organization* and *collagen fibril organization* were enriched at all time points examined (Table 3). Categories corresponding to *regulation of cell proliferation* and *chondroitin sulfate proteoglycan metabolic process* were enriched at all but the 12 week time point. *Angiogenesis* and *hypoxia* genes were enriched only at 1 day and 1 week post injury, while categories covering *bone* and *cartilage development* and collagen catabolism were enriched only at 1- and 6- weeks post injury correlating with the emergence of osteophyte formation and cartilage degradation as observed by histological analysis and micro-CT (Fig. 1e, f). *Wnt signaling* was enriched only at 1 week, while genes associated with *cell cycle* were enriched at 6 weeks post injury. Categories corresponding to *immune responses* were enriched at 1 day, 6- and 12- weeks post injury, while markers of *inflammation* were enriched at 1 day and 12 weeks post injury. Inflammation related genes up-regulated at 12 weeks post injury include several complement pathway components such as *C1qa*, *C1qc*, *Cfb* and *Cfp*. These data suggest significant cartilage remodeling occurs shortly

73

after injury, while immune responses oscillate, with an early phase at 1 day and a later phase initiating at 6 weeks post injury.

For down-regulated genes *monosaccharide metabolic process* and *alcohol catabolic process* were enriched at all but the 12 weeks post injury time point. Categories corresponding to *glycolysis*, *generation of precursor metabolites and energy,* and *striated muscle tissue development* were enriched at 1 week and 6 weeks post injury. Genes associated with *negative regulation of osteoblast differentiation*, and *carbohydrate* and *lipid biosynthetic process* were enriched at 1 day, while *muscle organ development*, *muscle system process* and *response to heat* were enriched at 1 week post injury. Categories corresponding to *ATP metabolic process*, *oxidative phosphorylation* and *electron transport chain* were enriched at 6 weeks post injury. We found several components of mitochondrial electron transport chain including *Ndufa1*, *Ndufa2*, *Ndufb3*, and *Uqcr10* to be down-regulated at 6 weeks post injury suggesting aberrant mitochondrial activity. The 12 week time point did not reveal enrichment for any ontology categories.

Next, we performed a comparative phenotype enrichment analysis using ToppCluster [157] and identified enriched mouse phenotypes associated with the DEGs. For up-regulated genes, *inflammatory/immune* response related phenotypes and *muscle* phenotypes were found to be enriched at 1 day post injury, whereas both 1- and 6- weeks data showed enrichment for *cartilage* and *bone* phenotypes. Three categories: *arthritis, abnormal cutaneous collagen fibril morphology* and *abnormal tendon morphology* were enriched at all time points,

74

except 12 weeks post injury. We identified 26 genes with *arthritis* phenotypes up-regulated at 1 day, 1-and/or 6 weeks (Fig. 3).

While 1 day, 1- and 6- weeks data shared a significant overlap, the 12 weeks post injury data did not have any overlap with any other time points, and showed enrichment for only 2 categories: *abnormal response to infection* and *increased susceptibility to infection*, suggesting that the severe cartilage damage observed histologically at this point (Fig. 1f) may render the organism susceptible to secondary health consequences due to viral or bacterial exposure (Fig. 3). Genes down regulated at 1- and 6- weeks showed enrichment for *muscle* phenotypes; by contrast, 1 day and 12 weeks genes did not show enrichment for any mouse phenotypes. Genes associated with *abnormal glycogen* and *triglyceride level*s were also found to be enriched at 1 week post injury. These data suggest that at early stages post injury, inflammation and vasculature are in play with the attempt to repair and remodel both cartilage and bone. However at later stages post injury, the enrichment in *abnormal bone and cartilage morphology* categories are consistent with a damaged joint that has accrued significant morphological changes in bone and cartilage such as articular cartilage erosion and osteophyte formation, which are consistent with the histological and micro-CT evaluations (Fig. 1e-j).

Comparison with gene expression changes induced by DMM surgery. DMM is a widely used and validated animal model for studying PTOA [143]. Gene expression profiling have been recently conducted on DMM injured mouse knee

joints, and significant transcriptional changes were reported at 2-, 4- and 16- week time points for whole-joint derived RNA [154] and at 1-, 2- and 6- week time points for micro-dissected articular cartilage derived RNA [147]. Here we sought to determine the overlapping genes and shared mechanisms contributing to PTOA from these distinct traumatic events. 485 [whole joint; 472 up- and 13 down-regulated] and 189 [micro-dissected cartilage; 168 up- and 21 down- regulated] of the DMM differentially expressed transcripts overlapped with our TC data, at least at one time point examined. A full list of these overlapping genes is provided in the Table S-1. For significantly up-regulated genes in whole joint RNA, 1 week post-TC and 4 weeks post-DMM injury had the largest overlap, with 382 shared [74.32% of TC genes] differentially expressed genes. By comparison, when micro-dissected DMM cartilage was paired to our data, 1 week post-TC and 2 weeks post DMM [cartilage] had the largest overlap, with 139 shared genes [27% of TC genes] (Table 4). Only 228 transcripts overlapped between the 1 week post-TC and 2-weeks post-DMM [whole joint]. The 6 weeks TC data shared only 32 genes with the 6 weeks cartilage data but had a 125 gene overlap with the 4 weeks DMM whole joint data. Very few genes were found to overlap among the differentially down-regulated transcripts or between our 12 weeks and the whole joint DMM 16 week data (Table 4).

TC model uniquely identified 582 up-, 295 down-, and 15-mixed [up or down at different time points] regulated genes (Table S-1). This includes several immune/inflammatory response related genes such as *Ccr2*, *C1qa*, *C1qb*, *C1qc* and *Cfb*; bone development related genes such as *Spp1*, *Ctgf*, *Dmp1*, *Gabbr1* and

Pth1r; cell adhesion genes such as *Emilin1*, *Gpnmb*, *Itga5* and *Stab1* and energy metabolism genes such as *Ndufa1*, *Ndufa2*, *Ndufb3*, *Uqcr10* and *Sdhb*. TC model also identified several novel genes including adipogenic gene *Medag* [166], *Suco* [167], and *Sorcs2* [168] as up-regulated in injured joints.

Next, we performed a comparative gene ontology enrichment analysis on the TC and DMM [whole joint] differentially expressed transcripts, and identified several enriched ontology terms common to both models. Ontology terms including *extracellular structure organization*, *collagen metabolic process*, *collagen fibril organization*, and *vasculature development* were identified as enriched at all TC and DMM time points examined. Genes associated with *muscle cell migration* and *response to TGFβ* were found to be enriched at 1 day and 1 week in TC and at 2- and 4- weeks in DMM. Genes associated with *chondrocyte differentiation* and *bone development* were enriched at 1- and 6-weeks in TC and at 2- and 4-weeks in DMM. We also identified several regulators of Wnt signaling including *Sfrp1*, *Sfrp2*, *Sfrp4*, *Dkk2* and *Dkk3* and TGFβ signaling including *Ltbp1*, *Fbn1* and *Fbn2* commonly changed in both the TC and DMM models (Figure 4).

Identification of commonly changed genes in human OA and TC induced OA, including genome association studies (GWAS). In an attempt to understand the contributions of individual tissue components of the joint to PTOA development and to evaluate the clinical relevance of our model, we compared our data to previously published expression data of different human OA tissues including synovium [137], osteophyte [140], tibial plateau [141], articular cartilage [139, 169]

and meniscus [138]. Gene list corresponding to the significantly differentially regulated genes were obtained from the publications whenever it was available. If the gene list was not available, we reanalyzed the raw data and identified genes with a fold change > 1.5 (p-value < 0.05; FDR corrected p-value < 0.1). For meniscus data, none of the genes passed our adjusted p-value cutoff so, all genes with p-value < 0.05 and fold change > 1.5 were selected for further analysis. We identified 374 genes commonly differentially regulated between both humans OA and TC induced mouse OA, the majority of which corresponding to osteophyte and subchondral bone changes (Figure 5; Table S-2), consistent with osteophyte formation being a major hallmark of PTOA in humans, and recapitulated in the TC mouse model examined herein (Fig. 1g, h). Next, we compared our data to GWAS loci associated with four major inflammatory joint diseases: OA, RA, JIA, and AS and identified 25 genes (Table 5) that map to these GWAS loci. In our data set, a few genes had been previously identified to have cartilage phenotype in mice including: *Comp*, *Haplln1*, and *Aldh1a2*. In addition, *Tnfrsf1a*, *Rel*, and *Ptgs2* have been demonstrated to develop a bone phenotype. Interestingly, *Runx1*, *Tlr4*, and *Il1r1* all demonstrate a susceptibility to OA in mice.

Discussion

The TC induced ACL rupture model of PTOA is a new animal model that has not yet been widely explored to study mechanisms of joint OA development. This study provides the first account of whole genome expression profiles to obtain new insights into the temporal progression of the disease in the TC PTOA model. Despite being a noninvasive procedure, and exhibiting no visible morphological or structural damages (Fig. 1c), we observed the largest transcriptional changes at these early time points, with 599 and 644 transcripts being differentially expressed. Also, most of the differentially expressed genes were up-regulated, with less than 30% of differentially expressed genes being significantly down-regulated, at any time point examined.

Consistent with reports by Gardiner *et al*. [160] where they examined transcriptional changes in micro-dissected cartilage derived from DMM injured joints, we also identified *Tnn* (*tenasin N*) and *Fn1* (*fibronectin 1*) as two molecules consistently up-regulated at all time points examined (Table 1). Also, similar to previous reports on DMM gene expression time-course experiments [154, 160], the TC model of PTOA also undergoes a decline in transcriptional changes with time, where by 12 weeks post injury, only 201 transcripts are differentially expressed, suggesting that the joint adapts to the injury, with time, to reach a new molecular homeostasis, despite the enormous articular cartilage loss evident at this time point (Fig. 1f).

In addition our model captures many of the transcriptional changes previously reported for DMM damaged cartilage, both reported for whole joints and

micro-dissected cartilage. Our 1 week data has the largest overlap with the 4 weeks post injury DMM [154] whole joint data, where 74% of our up-regulated transcripts were also found transcriptionally elevated in the DMM injured joints. We also found significant overlap between our 1 week post injury data and DMM injury pure cartilage data, where 67 genes (13%) overlapped with the 1 week and 139 genes (27%) overlapped with 2 weeks post DMM injury (Table 4). These data provides confirmation that the TC model recapitulates a large proportion of the gene expression reported for the DMM model, both at the whole joint and at the pure cartilage level. We also identified several genes including *Mmp3, Errfi1 and C1qtnf3* with known arthritis phenotype as differentially regulated in TC data and both DMM datasets. *C1qtnf3* has previously been implicated in autoimmune arthritis [170]; however further studies are required to understand its role in OA.

We also presented an analysis of the commonalities with transcriptional changes in OA patient derived samples. We found 374 transcripts (25%) of our data, to be changed in the same direction, as the transcriptional changes observed in human samples, highlighting the relevance of this model to modeling PTOA in humans. The majority of these genes corresponded to osteophyte derived transcriptional changes, suggesting that our model recapitulates a lot of the molecular changes associated with excessive ectopic ossification of joint tissues associated with PTOA, and visualized in the microCT images in Fig. 1.

Interestingly few genes upregulated in the TC PTOA time course are found to be significantly up-regulated in the patient-derived OA cartilage. In particular one gene, *Col6A2* is upregulated in TC joints, at all times points examined, but

significantly up-regulated in human OA articular cartilage only. Mutations in this protein are primarily associated with myopathies [171], but may also have an important role in ECM remodeling in PTOA. Serpines are peptidase inhibitors and Serpine2 has been shown to upregulated in cultured chondrocytes in response to IL1α to inhibit MMP13 expression. We find Serpine1 to be significantly up-regulated at 1 day and 1 week post injury, and similarly this molecule is upregulated in OA articular cartilage, suggesting that the upregulation of this peptidase may represent a regulatory mechanism for repressing the expression of cartilage catabolic enzymes.

Furthermore we mapped our differentially expressed genes onto GWAS determined putative susceptibility loci associated with OA, RA, JIA and AS and identified 25 genes that may potentially contribute to these phenotypes (Table 5). Of these 25 genes, 19 of them have available knockout out mouse strains, which we curated for detected cartilage, bone or immune phenotypes. Interestingly, we found 12/19 (63%) of these genes to bear various immune system deficiencies, most of which either impair the inflammatory response or affect the response to infectious agents, suggesting that PTOA may alter the immune system. Indeed, our analysis for enriched biological processes highlighted several 'immune response' categories, along the time course examination, suggesting that in addition to the initial inflammatory response, which is well documented to contribute to PTOA long term phenotypes, there may be additional immune system deficiencies that are triggered by joint injuries, and are worth exploring, both as a

means to prevent cartilage degeneration, as well as a means to obtain new insights into our response to infection.

Our Study also allowed us to examine transcriptional changes in several long non-coding RNA (*lncRNA*). We identified 18 *lncRNAs* differentially transcribed at least at one time point, 10 that were up- and 8 that were down-regulated (Table 2). Two of these *lncRNAs, Dnm3os* and *H19* have been previously described in the context of skeletal development [172] or OA [173], but all other *lncRNAs* identified herein have yet to be studied in the context of PTOA development. Furthermore, since we do not observe broad activation or repression across all time points examined, but rather see groups of *lncRNAs* transcriptionally changed at single time points, we speculated these noncoding RNAs may have unique functions to modulate the transcription of 'function specific' cohorts of genes. Also, it would be interesting to determine whether some of these *lncRNAs* modulate immune systems or are modulated by the immune system, since initial changes in inflammation may be able to trigger large cascades of gene expression by repressing or activating these regulatory RNAs.

A list of possible genes that remain to be explored as candidate biomarkers or local joint therapeutics includes *Ssc5d*, a gene primarily expressed in monocytes/macrophages and T-lymphocytes [174] and *Cemip* (*KIAA1199*), a gene involved in hyaluronan (HA) metabolism [175]. *Ssc5d*, a soluble scavenger protein, was previously identified to be elevated in synovial fluid of OA patients [176]. HA plays an important role in maintaining the integrity of articular cartilage by providing lubrication between the femoral and tibial surfaces. We identified

Cemip (KIAA1199), a gene that enhances HA catabolism in the synovium [175] and improves growth and angiogenesis of synovial tissue [177]. However its role in OA developing joints has not yet been explored and inhibitors of *Cemip* may potentially prevent cartilage degradation post injury.

Our study also identified several novel genes including *Suco, Sorcs2* and *Medag. Suco* (*Opt*) encodes a widely expressed rough endoplasmic reticulum-localized integral membrane protein. Mice lacking *Suco* develop acute onset of skeletal defects including impaired bone formation and spontaneous fractures [167]. *Suco* is >2 fold up-regulated at 6 weeks post injury suggesting a role in aberrant bone remodeling and/or osteophyte formation. *Sorcs2* is a member of vacuolar protein sorting 10 family proteins (*VPS10Ps*) with a potential role in protein trafficking and cell signaling [167]. Recent GWAS study identified *Sorcs2* as a candidate loci associated with cranial cruciate ligament rupture in Newfoundland dogs [168], however this gene has not been previously studied in the context of osteoarthritis. *Medag*, a gene we found up-regulated at 1 day, 1-and 6- weeks has been shown to play a role in adipose tissue development [166]; however its role in osteoarthritis has yet to be explored.

There are a few potential limitations to our study. First, we utilized the contralateral joint as controls instead of age matched sham injured joints. Because of this, it is difficult to distinguish between changes mediate by the injury that had systemic effects on both joints. In addition, there may also be changes occurring in the contralateral as a result of altered loading (more use of one joint) and changes in the injured joint/leg due to reduced mobility, disuse and pain. Second,

because we are sequencing whole joints instead of individual tissues of the joint, to tease out where the gene expressions are coming from presents a challenge. However, because OA is considered a "joint disease", comprehensive intact joint analysis may allow us to identified changes in tissues that may not normally be assumed to contribute to cartilage degradation or remodeling, such as muscle. Because of these caveats, we may lose some genes that are differentially expressed in a small area, or genes that are normally expressed broadly, but are affected regionally. These challenges may be overcome by examining candidate proteins for their tissue specific expression.

Our study uniquely introduces the gene expression changes associated with a new, noninvasive model of PTOA. It provides evidence that a significant number of changes correlate with both whole joint derived RNA and micro-dissected derived RNA from the widely studied surgical model of PTOA. Furthermore, it highlights many overlaps with molecular changes identified in human derived OA tissues including cartilage, osteophytes, subchondral bone, meniscus and synovium, and identifies several putative new genes associated with OA-derived GWAS data. The pathways and candidate genes presented herein represent additional opportunities for investigating new potential therapeutic targets and susceptibility loci for PTOA.

Figure 1. Histological Assessment of Tibial Compression (TC) OA injury

A

Unloaded → Tibial Compression → Loaded (Injured) → Joint Relaxation → Relaxed (Injured)

B

Uninjured Knee | Injured Knee

T_0 T_1 T_7 (1 Week) T_{42} (6 Weeks) T_{84} (12 Weeks)

Injured

| Uninjured | 1 Day | 6 Weeks | 12 Weeks |

C D E F

G 6 Weeks

H 12 Weeks

I Osteophyte

6 Weeks | 12 Weeks

Osteophyte Volume (mm^3)

J Subchondral Bone Volume

6 Weeks | 12 Weeks

ns | ***

Uninjured | Injured

Bone Volume/Total Volume

85
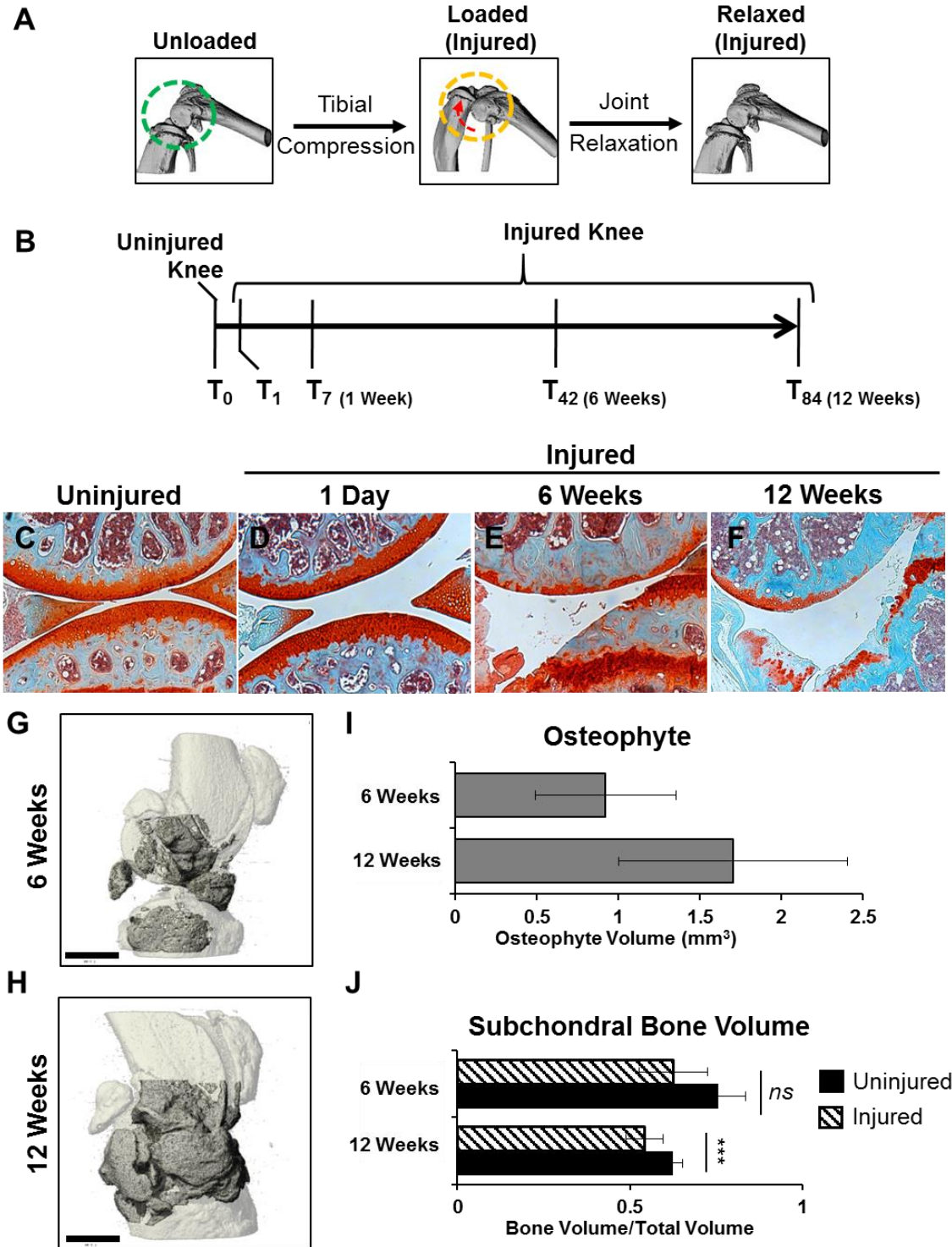
Figure 1. Histological evaluations of tibial compression (TC) OA injury. (A) TC overload leads to joint destabilization though ACL dislocation. The direction of joint displacement is indicated by the red arrow. (B) Time line where mice were injured and joints were collected at 1 day, 1-, 6-, and 12-weeks for either histology or RNA sequencing. Histological assessment of uninjured (C) and injured joints at various time points post injury (D-F) by Safranin-O and Fast Green staining. MicroCT highlight regions (dark gray) of osteophyte formation in 6- (G) and 12- (H) weeks injured joints. (I) Quantification of femoral subchondral trabecular bone formation between injured and uninjured joints. (J) MicroCT quantification of osteophyte formation in injured joints. All histological images were presents were taken at 10X magnification. Scale bar is 1mm; *** $p < 0.001$; and not significant (ns).

Figure 2. Various Differentiated Regulated Transcripts between Injured and Uninjured Joints in *WT*
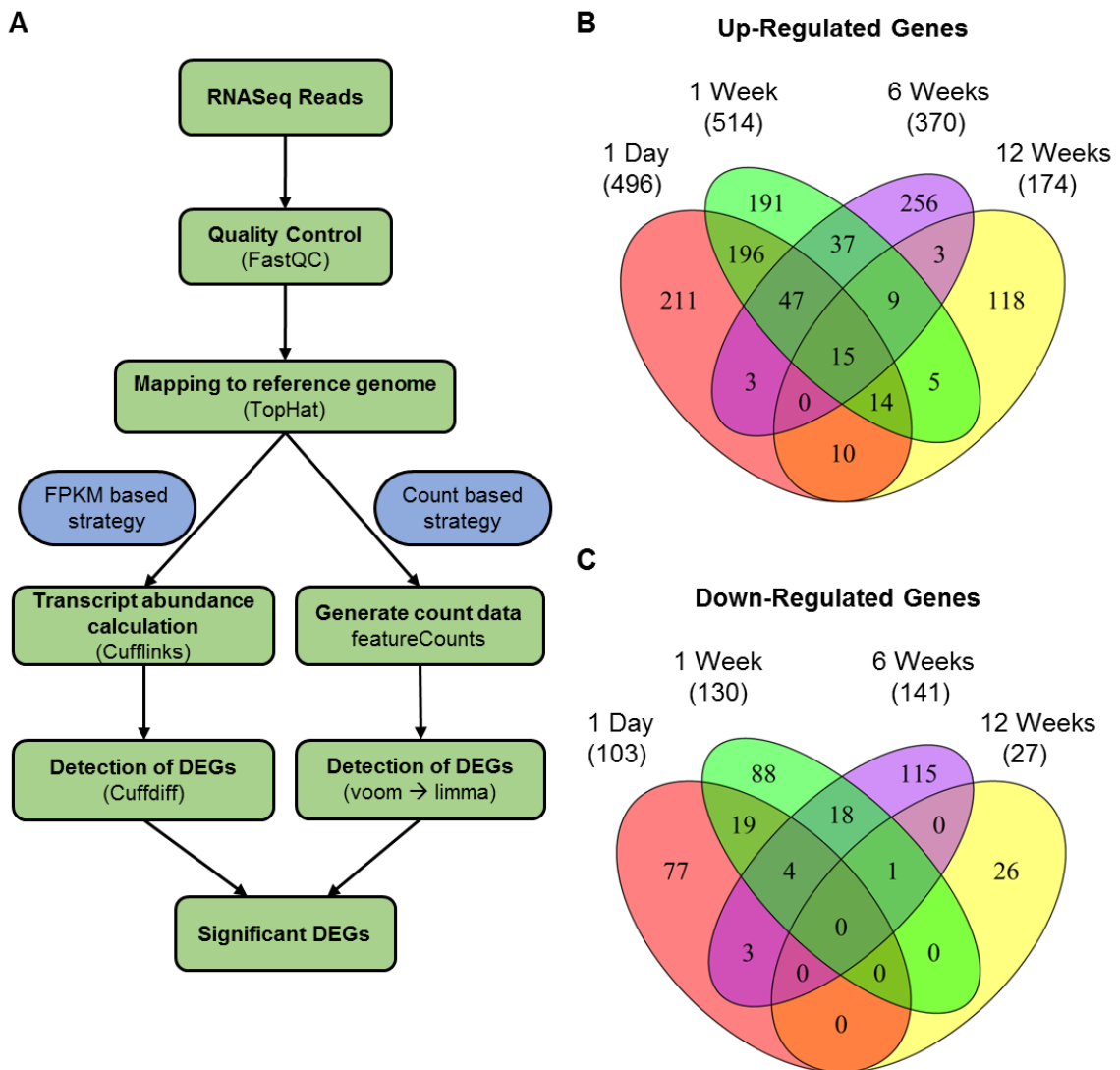
Figure 2. RNA sequencing analysis methodology and commonly expressed transcripts. (A) Flow chart of RNA sequencing after whole joint isolation. All of the differentially regulated genes presented was after final significant ($p < 0.05$) DEG reads. Common differentially up (B) and down (C) regulated genes between every time point post TC injury. The total number of genes per category is in brackets beneath each time point.
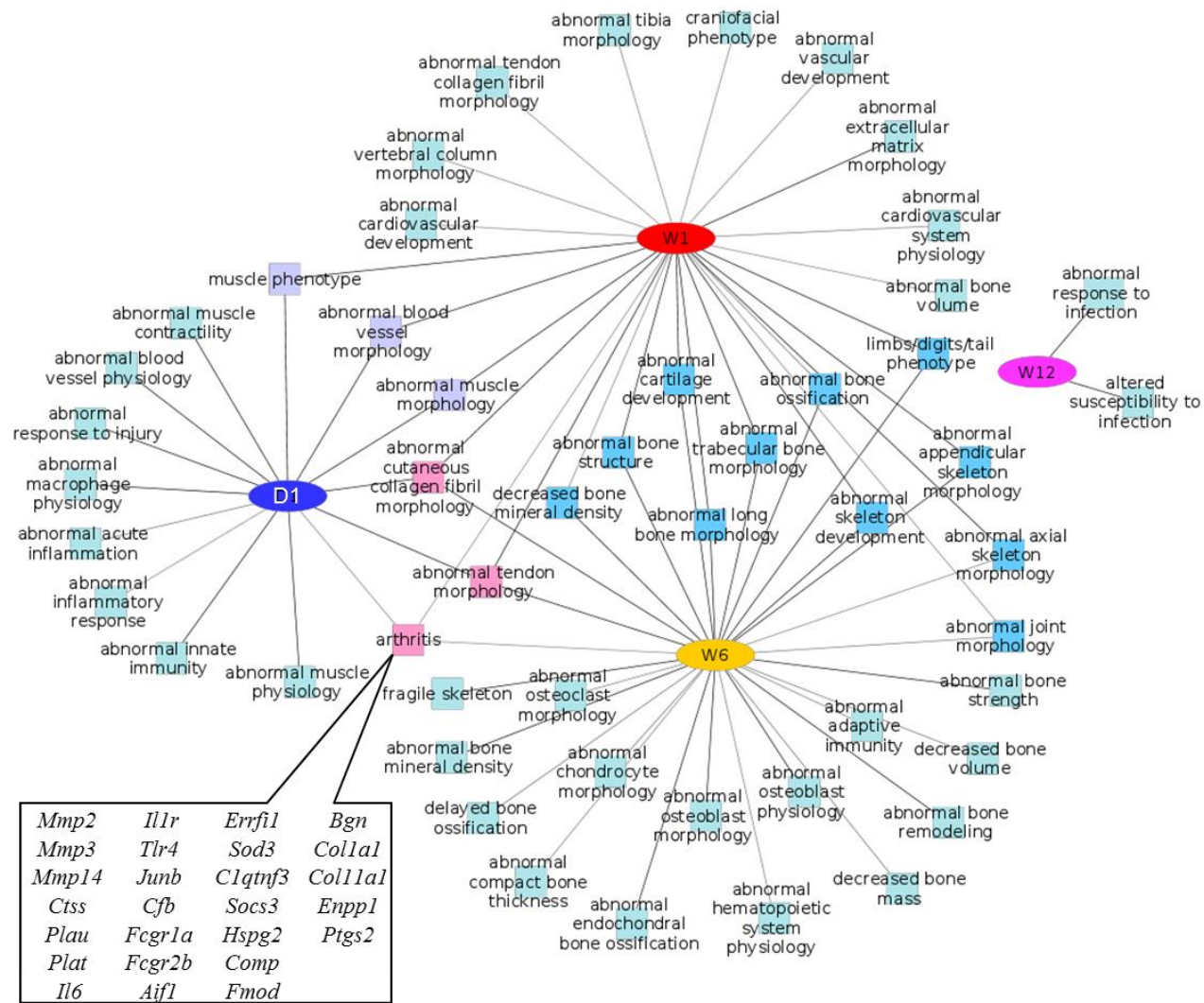
Figure 3. Gene clusters identified enriched phenotype by TC injury model. Up-regulated genes associated with Arthritis phenotypes (bottom left).
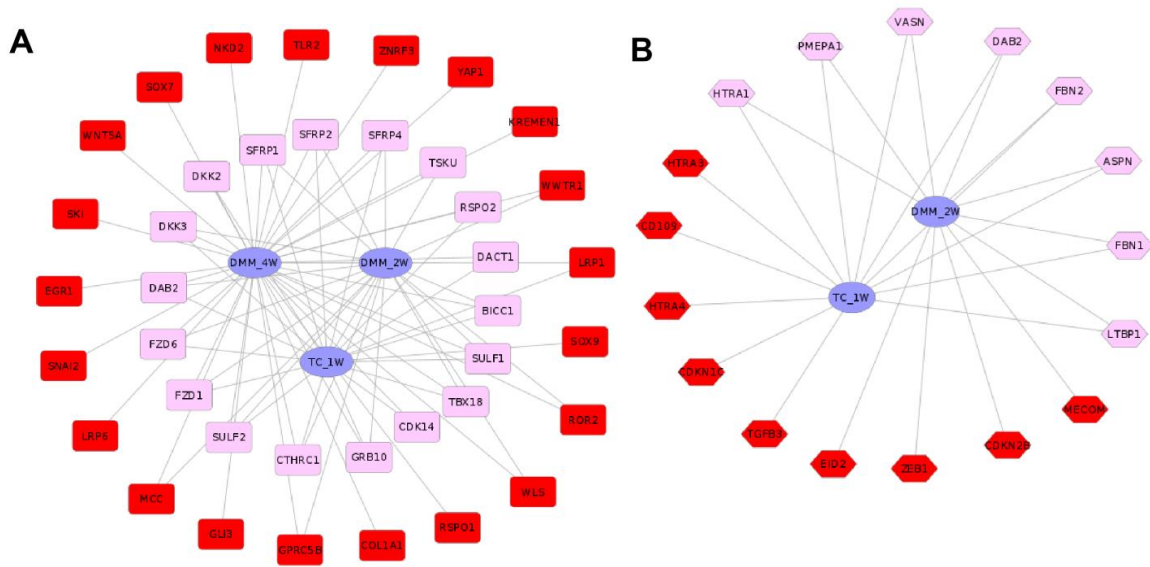
Figure 4. Distinct regulators of Wnt and TGFβ signaling pathways identified between DMM and TC injury model. (A) Clusters of common and distinct genes associated in Wnt signaling are identified between surgery and ACL tare methodology. (B) Clusters of common and distinct genes associated in TGFβ signaling are identified between surgery and ACL tare methodology. Genes shared between both methods are in pink, while genes specific to one methodology than the other is represented in green.
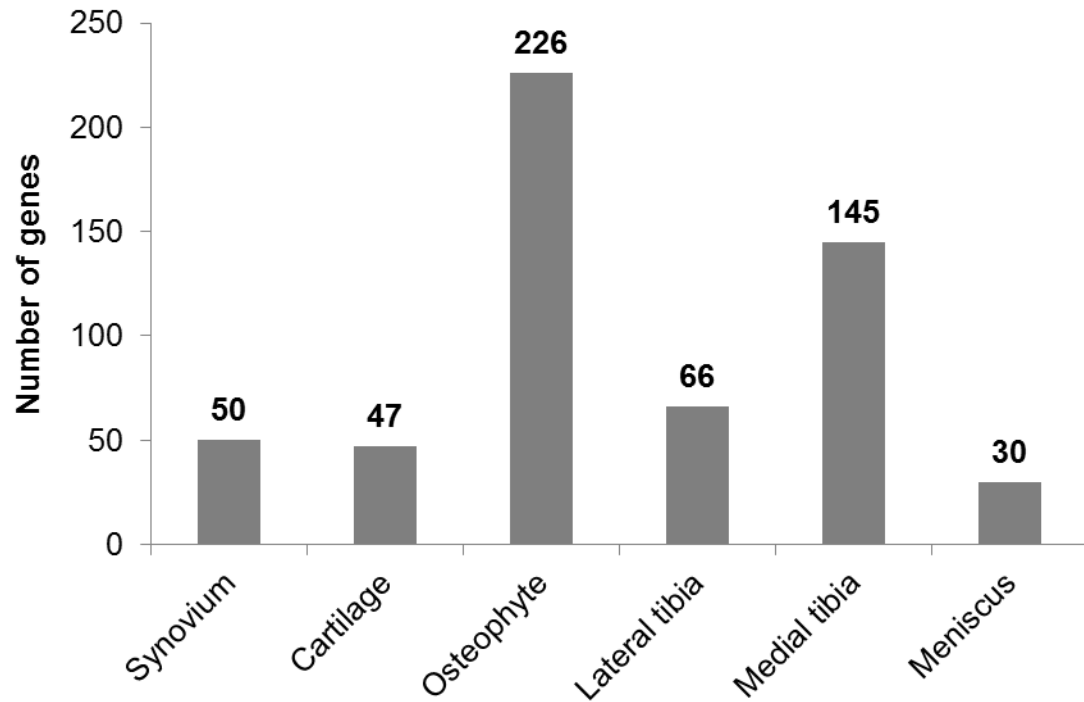
Figure 5. Numbers of genes overlapping between our TC expression data and genes found to be differentially expressed in OA derived clinical samples.

Table 1. Transcripts that were up-regulated in injured joints, at all time points examined. Values represent the log fold changes between injured and uninjured joints. ($p < 0.05$)

Gene Name	1 Day	1 Week	6 Weeks	12 Weeks
Mmp3	4.46	5.68	11.74	6.14
Col3a1	4.10	5.74	4.05	3.93
Cthrc1	3.83	5.05	1.86	2.92
Sfrp2	3.41	4.61	3.18	3.03
Wisp2	3.08	2.67	1.81	2.67
Tnn	2.69	4.22	3.17	3.02
Col5a1	2.52	3.80	2.43	2.17
Col6a3	2.24	4.39	3.14	2.39
Srpx2	2.21	2.94	2.53	2.48
Thy1	2.11	2.50	2.18	2.52
Col6a2	2.10	4.31	2.41	2.81
Col6a1	2.07	4.17	2.29	2.44
Col5a2	2.05	2.89	2.70	2.65
Thbs3	1.80	3.95	4.10	2.50
Fn1	1.58	3.02	4.46	2.93

Table 2. *LncRNAs* differentially expressed in injured joints.

LncRNA Name	1 Day	1 Week	6 Weeks	12 Weeks
Dnm3os*	0.672	1.324	ns	ns
Rian	0.942	2.002	ns	ns
2810433D01Rik	1.022	ns	ns	ns
H19#	ns	0.98	ns	ns
Snhg18	ns	0.777	ns	1.028
2610203C20Rik	ns	0.892	ns	ns
Gm11974	ns	ns	1.706	ns
E330020D12Rik	ns	ns	1.807	ns
AI504432	ns	ns	0.942	ns
Tmem134	ns	ns	ns	0.981
2310065F04Rik	-1.044	ns	ns	ns
C130080G10Rik	-2.921	ns	ns	ns
1810044D09Rik	ns	-1.007	ns	ns
Plet1os	ns	-0.988	ns	ns
2610306M01Rik	ns	ns	-0.616	ns
0610040B10Rik	ns	ns	-1.647	ns
BC018473	ns	ns	-1.04	ns
2610035D17Rik	ns	ns	-0.87	ns

*#*LncRNAs* previously shown to function during skeletal development* or be dysregulated in OA cartilage#.

Table 3. Gene Ontology Enriched Categories for Differentially Expressed Genes, at all time points examined.

	GO ID	GO category	1 Day		1 Week		6 Weeks		12 Weeks	
			No. Genes	*p*-value	No. Genes	*p*-value	No. Genes	*p*-value	No. Genes	*p*-value
Up - Regulated Genes	GO:0001944	vasculature development	29	5.08E-11	25	2.59E-08	14	6.20E-04	8	0.00671
	GO:0007155	cell adhesion	41	4.26E-09	63	3.16E-23	41	6.48E-14	17	3.33E-05
	GO:0030198	extracellular matrix organization	17	5.39E-09	25	4.35E-17	17	3.13E-11	8	3.04E-05
	GO:0030199	collagen fibril organization	7	1.06E-05	7	1.04E-05	9	1.66E-09	5	3.08E-05
	GO:0043062	extracellular structure organization	18	2.64E-07	29	7.22E-17	19	1.87E-10	8	3.50E-04
	GO:0042127	regulation of cell proliferation	25	0.00604	26	0.00291	23	2.98E-04	*ns*	*ns*
	GO:0050654	chondroitin sulfate proteoglycan metabolic process	4	0.00728	5	5.96E-04	5	1.58E-04	*ns*	*ns*
	GO:0009611	response to wounding	27	9.91E-07	18	0.00789	*ns*	*ns*	12	2.49E-04
	GO:0001525	angiogenesis	14	3.66E-05	12	6.04E-04	*ns*	*ns*	*ns*	*ns*
	GO:0001666	response to hypoxia	7	0.00581	8	0.00119	*ns*	*ns*	*ns*	*ns*
	GO:0006954	inflammatory response	23	7.64E-08	*ns*	*ns*	*ns*	*ns*	10	1.70E-04
	GO:0006955	immune response	33	4.93E-07	*ns*	*ns*	18	0.00523	16	1.68E-05
	GO:0060348	bone development	*ns*	*ns*	15	1.83E-06	14	2.01E-07	*ns*	*ns*
	GO:0051216	cartilage development	*ns*	*ns*	10	1.61E-04	11	1.30E-06	*ns*	*ns*
	GO:0001501	skeletal system development	*ns*	*ns*	30	2.19E-10	22	4.84E-08	*ns*	*ns*
	GO:0001503	ossification	*ns*	*ns*	14	2.94E-06	14	5.57E-08	*ns*	*ns*
	GO:0030574	collagen catabolic process	*ns*	*ns*	4	0.00860	5	2.04E-04	*ns*	*ns*
	GO:0001558	regulation of cell growth	*ns*	*ns*	13	3.69E-06	*ns*	*ns*	5	0.00890
	GO:0006508	proteolysis	*ns*	*ns*	*ns*	*ns*	*ns*	*ns*	19	0.00414
	GO:0006956	complement activation	*ns*	*ns*	*ns*	*ns*	*ns*	*ns*	4	0.00388
	GO:0016477	cell migration	*ns*	*ns*	18	1.47E-04	*ns*	*ns*	8	0.00540
	GO:0002062	chondrocyte differentiation	*ns*	*ns*	*ns*	*ns*	6	2.94E-05	*ns*	*ns*
	GO:0002063	chondrocyte development	*ns*	*ns*	*ns*	*ns*	3	0.00844	*ns*	*ns*
	GO:0002694	regulation of leukocyte activation	*ns*	*ns*	*ns*	*ns*	11	4.79E-04	*ns*	*ns*
	GO:0006029	proteoglycan metabolic process	*ns*	*ns*	6	0.00139	8	1.63E-06	*ns*	*ns*
	GO:0006260	DNA replication	*ns*	*ns*	*ns*	*ns*	10	0.00174	*ns*	*ns*
	GO:0006790	sulfur metabolic process	*ns*	*ns*	*ns*	*ns*	7	0.00703	*ns*	*ns*
	GO:0007017	microtubule-based process	*ns*	*ns*	*ns*	*ns*	12	0.00157	*ns*	*ns*
	GO:0007049	cell cycle	*ns*	*ns*	*ns*	*ns*	29	5.47E-06	*ns*	*ns*
	GO:0008630	DNA damage response, signal transduction resulting in induction of apoptosis	*ns*	*ns*	*ns*	*ns*	4	0.00785	*ns*	*ns*
	GO:0009100	glycoprotein metabolic process	*ns*	*ns*	*ns*	*ns*	11	3.31E-04	*ns*	*ns*
	GO:0030203	glycosaminoglycan metabolic process	*ns*	*ns*	*ns*	*ns*	6	7.19E-04	*ns*	*ns*
	GO:0031214	biomineral formation	*ns*	*ns*	*ns*	*ns*	7	3.38E-05	*ns*	*ns*
	GO:0006928	cell motion	*ns*	*ns*	22	4.97E-04	*ns*	*ns*	*ns*	*ns*
	GO:0016055	Wnt receptor signaling pathway	*ns*	*ns*	12	4.98E-04	*ns*	*ns*	*ns*	*ns*
	GO:0048870	cell motility	*ns*	*ns*	18	0.00103	*ns*	*ns*	*ns*	*ns*
	GO:0051674	localization of cell	*ns*	*ns*	18	0.00103	*ns*	*ns*	*ns*	*ns*
	GO:0000904	cell morphogenesis involved in differentiation	*ns*	*ns*	15	0.00111	*ns*	*ns*	*ns*	*ns*
	GO:0007169	transmembrane receptor protein tyrosine kinase signaling pathway	*ns*	*ns*	13	0.00386	*ns*	*ns*	*ns*	*ns*
	GO:0007167	enzyme linked receptor protein signaling pathway	*ns*	*ns*	16	0.00453	*ns*	*ns*	*ns*	*ns*
	GO:0001649	osteoblast differentiation	*ns*	*ns*	6	0.00672	*ns*	*ns*	*ns*	*ns*
	GO:0048771	tissue remodeling	*ns*	*ns*	6	0.00672	*ns*	*ns*	*ns*	*ns*
	GO:0006897	endocytosis	*ns*	*ns*	12	0.00911	*ns*	*ns*	*ns*	*ns*
	GO:0030036	actin cytoskeleton organization	*ns*	*ns*	11	0.00987	*ns*	*ns*	*ns*	*ns*
	GO:0006935	chemotaxis	11	4.81E-04	*ns*	*ns*	*ns*	*ns*	*ns*	*ns*
	GO:0010876	lipid localization	10	0.00565	*ns*	*ns*	*ns*	*ns*	*ns*	*ns*
	GO:0022604	regulation of cell morphogenesis	9	0.00341	*ns*	*ns*	*ns*	*ns*	*ns*	*ns*
	GO:0030029	actin filament-based process	13	0.00193	*ns*	*ns*	*ns*	*ns*	*ns*	*ns*
	GO:0045597	positive regulation of cell differentiation	13	0.00184	*ns*	*ns*	*ns*	*ns*	*ns*	*ns*
Down - Regulated Genes	GO:0005996	monosaccharide metabolic process	8	5.51E-05	9	2.11E-05	6	0.008343		
	GO:0046164	alcohol catabolic process	4	0.004552	4	0.007311	4	0.008855		
	GO:0006096	glycolysis	*ns*	*ns*	4	2.43E-03	4	2.96E-03		
	GO:0006091	generation of precursor metabolites and energy	*ns*	*ns*	10	2.95E-05	16	1.28E-10		
	GO:0014706	striated muscle tissue development	*ns*	*ns*	6	0.001069	5	0.009645		
	GO:0045668	negative regulation of osteoblast differentiation	3	0.00167	*ns*	*ns*	*ns*	*ns*		
	GO:0006071	glycerol metabolic process	3	6.17E-03	*ns*	*ns*	*ns*	*ns*		
	GO:0006094	gluconeogenesis	4	1.40E-04	*ns*	*ns*	*ns*	*ns*		
	GO:0006641	triglyceride metabolic process	4	8.28E-04	*ns*	*ns*	*ns*	*ns*		
	GO:0030278	regulation of ossification	4	0.002551	*ns*	*ns*	*ns*	*ns*		
	GO:0016051	carbohydrate biosynthetic process	4	8.97E-03	*ns*	*ns*	*ns*	*ns*		
	GO:0016052	carbohydrate catabolic process	5	7.97E-04	*ns*	*ns*	*ns*	*ns*		
	GO:0008610	lipid biosynthetic process	8	6.43E-04	*ns*	*ns*	*ns*	*ns*		
	GO:0007517	muscle organ development	*ns*	*ns*	9	1.17E-05	*ns*	*ns*		
	GO:0003012	muscle system process	*ns*	*ns*	6	5.40E-05	*ns*	*ns*		
	GO:0009408	response to heat	*ns*	*ns*	4	9.59E-04	*ns*	*ns*		
	GO:0046034	ATP metabolic process	*ns*	*ns*	*ns*	*ns*	8	1.96E-06		
	GO:0006119	oxidative phosphorylation	*ns*	*ns*	*ns*	*ns*	6	3.16E-05		
	GO:0022900	electron transport chain	*ns*	*ns*	*ns*	*ns*	7	9.14E-05		
	GO:0015992	proton transport	*ns*	*ns*	*ns*	*ns*	5	3.66E-04		

Table 4. Gene Expression similarities between TC (tibial compression) and DMM (destabilization of medial meniscus) at various time points post injury.

Number of overlapping genes are presented as the net number of genes up- (A) or down- (B) regulated in both the TC and DMM datasets, as well as percentage of the entire gene expression data set described for the TC time points.

A		TC							
		1 Day [496]		1 Week [514]		6 Weeks [370]		12 Weeks [174]	
	Time Point	No. Genes	% Genes	No. Genes	% Genes	No. Genes	% Genes	No. Genes	% Genes
DMM up-regulated transcripts	1 Week [C]	n/c		67	13.04%	n/c		n/c	
	2 Weeks [C]	n/c		139	27.04%	n/c		n/c	
	2 Weeks [WJ]	168	33.87%	228	44.36%	68	18.38%	26	14.94%
	4 Weeks [WJ]	262	52.82%	382	74.32%	125	33.78%	36	20.69%
	6 Weeks [C]	n/c		n/c		32	8.65%	n/c	
	16 Weeks [WJ]	21	4.23%	41	7.98%	28	7.57%	14	8.05%

B		1 Day [103]		1 Week [130]		6 Weeks [141]		12 Weeks [27]	
		No. Genes	% Genes	No. Genes	% Genes	No. Genes	% Genes	No. Genes	% Genes
DMM down-regulated transcripts	1 Week [C]	n/c		4	3.08%	n/c		n/c	
	2 Weeks [C]	n/c		17	13.08%	n/c		n/c	
	2 Weeks [WJ]	5	4.85%	6	4.62%	1	0.71%	0	0.00%
	4 Weeks [WJ]	9	8.74%	6	4.62%	1	0.71%	0	0.00%
	6 Weeks [C]	n/c		n/c		4	2.84%	n/c	
	16 Weeks [WJ]	0	0.00%	0	0.00%	0	0.00%	0	0.00%

[C] Cartilage (Bateman et al)   n/c comparison was not conducted
[WJ] Whole Joint (Loeser et al)

Table 5. Differentially expressed genes that overlap with genes identified by genome wide association studies (GWAS) as candidates associated with osteoarthritis (OA), rheumatoid arthritis (RA), juvenile idiopathic arthritis (JIA), and/or ankylosing spondylitis (AS). Known mouse phenotypes (cartilage, bone or immune) associated with these genes are also listed.

No.	Gene	Disease	TC-post injury				Mouse KO phenotye			Phenotype Description
			1 day	1 week	6 weeks	12 weeks	cartilage	bone	immune	
1	Comp	OA	ns	0.988	1.087	0.837	yes	yes	no	Null mutations are indistinguishable from controls. Mice homozygous for a knockin allele with two point mutations exhibit short limb dwarfism, osteoarthritis, abnormal chondrocytes, mild myopathy, and abnormal tendon morphology and stiffness
2	Fads3	RA	0.825	ns	ns	0.800	n/a	n/a	n/a	
3	Gch1	RA	ns	ns	ns	1.082	n/a	n/a	n/a	
4	Tnfrsf1a	AS	ns	ns	ns	1.024	yes	yes	yes	Null mutations exhibit disrupted splenic architecture, increased adult liver weights, reduced IgG immune response, deficits in some host defense and inflammatory responses, LPS resistance, and reduced graft-vs-host disease. Knockdown ameliorates collagen-induced arthritis; KO has high bone mass
5	Fndc1	RA	1.067	2.223	1.297	ns	n/a	n/a	n/a	
6	Edil3	AS	ns	1.038	1.202	ns	no	no	yes	abnormal hair growth; immune phenotype
7	Hapln1	AS	-0.594	ns	1.649	ns	yes	yes	no	Cartilage developmental defects, delayed bone formation, short limbs, craniofacial abnormalities, neonatal death
8	Stat4	RA	ns	ns	1.124	ns	no	no	yes	susceptibility to bacterial infection; immune
9	Mrc1	OA	ns	ns	0.893	ns	no	no	yes	decreased susceptibility to parasitic infection; immune; embryonic lethal
10	Casp8	RA	ns	ns	0.788	ns	no	no	yes	immune, cardiac
11	Runx1	RA	ns	ns	1.108	ns	yes	yes	yes	hematopoeitic defect, embryonic lethal at E12.5
12	Pla2g4a	OA	ns	ns	1.533	ns	no	no	yes	allergic and autoimmune reaction
13	Rel	RA	ns	ns	1.045	ns	no	no	yes	bone marrow hypoplasia; immune
14	Jmjd1c	JIA	ns	ns	1.426	ns	no	yes	no	Lumber vertebrae transformation; infertility
15	Ppil4	RA	ns	ns	1.317	ns	n/a	n/a	n/a	
16	Tlr4	OA	ns	ns	0.973	ns	yes	yes	yes	increased bone mass, decreased susceptibility to induced arthritis, hyporesponsive to bacterial infection
17	C1qtnf6	RA	0.593	1.483	ns	ns	no	no	no	
18	Il1r1	AS	1.109	0.733	ns	ns	yes	no	yes	decreased susceptibility to induced arthritis; immune
19	Ptgs2	OA	ns	2.010	ns	ns	yes	no	yes	decreased susceptibility to induced arthritis, neonatal death
20	Fam167a	RA	ns	0.788	ns	ns	n/a	n/a	n/a	
21	Sesn3	RA	ns	0.609	ns	ns	no	no	no	decreased response to stress induced hyperthermia
22	Aldh1a2	OA	1.608	ns	ns	ns	no	yes	no	embryonic lethal at E10.5, no limbs
23	Gatsl3	RA	0.640	ns	ns	ns	n/a	n/a	n/a	
24	Rcan1	RA	0.674	ns	ns	ns	no	no	yes	Slight reduction in heart size and an impaired T helper 1 response. Stress-induced cardiac hypertrophy, however, is attenuated in mutant mice.
25	Lsmem1	OA	-0.753	ns	ns	ns	n/a	n/a	n/a	

Supplementary Table S1. Differentially up- and down-regulated genes identified at 1 day, 1-, 6-, and 12-weeks post injury. Differentially expressed genes in the TC data that were also identified in DMM injured joints [Whole Joint RNA] and [micro-dissected cartilage RNA] are highlighted.

| | | TC genes present in whole joint DMM data | | | | TC genes present only in cartilage DMM data | | | | |

No.	Gene Name	TC-whole joint				DMM-whole joint			DMM-cartilage		
		1 Day	1 Week	6 Weeks	12 Weeks	2 Weeks	4 Weeks	16 Weeks	1 Week	2 Weeks	6 Weeks
1	Arg1	4.591	ns	ns	ns						
2	Ccl7	3.941	2.117	ns	ns		1.123				
3	Saa3	3.741	ns	ns	ns		3.351				
4	Ccl2	3.556	ns	ns	ns	1.258					
5	Chl1	3.03	ns	ns	ns		2.142				
6	Serpine1	3.03	1.955	ns	ns		1.234			1.377	
7	Ptx3	2.819	1.114	ns	ns	1.696	0.925				
8	Cxcl1	2.808	ns	ns	ns		2.357				
9	Cxcl5	2.723	ns	ns	ns		2.269				
10	Crlf1	2.668	2.306	ns	ns	1.395	1.143		3.683	2.762	
11	Il6	2.588	ns	ns	ns						
12	P4ha3	2.582	2.624	ns	ns	1.039	1.217				
13	C3ar1	2.506	1.414	ns	ns		0.620				
14	Fcrls	2.476	1.574	ns	ns		0.775				
15	Mt2	2.417	1.096	ns	ns	1.330	1.063			1.422	
16	Timp1	2.32	1.512	ns	ns	1.533	1.888		1.742	1.708	
17	Has2	2.31	1.563	ns	ns		0.901			0.952	
18	Sfrp1	2.301	1.988	ns	ns	1.314	1.036				
19	Tnfaip6	2.258	1.985	ns	ns		2.314			3.505	
20	Fbln2	2.251	1.431	ns	ns	1.129	0.880			0.901	
21	Trem2	2.229	0.996	ns	ns						
22	Serpina3n	2.208	1.233	1.301	ns		0.772		2.329	2.311	
23	Mmp3	2.156	2.506	3.554	2.618	2.714	3.514		3.165	4.401	2.650
24	Ankrd1	2.155	ns	ns							
25	Rrad	2.14	ns	ns	ns	0.748	1.006				
26	Crabp2	2.132	2.925	ns	ns	2.251	1.899				
27	Vgll3	2.125	1.482	ns	ns	1.484	1.469				
28	Pdpn	2.075	1.525	1.278	ns		1.366				
29	Chrna1	2.046	0.81	ns	ns						
30	Col3a1	2.037	2.522	2.017	1.976		1.825	2.192			
31	Eda2r	2.022	ns	ns	ns						
32	Tnnt2	2.012	ns	ns	ns						
33	Steap1	1.963	1.333	ns	ns		1.870		2.011	1.911	
34	Angptl4	1.959	0.833	ns	1.304	1.223	1.095				
35	Klrb1b	1.94	ns	ns	ns						
36	Prrx2	1.938	1.909	ns	ns	1.439	1.441	0.947			
37	Cthrc1	1.935	2.337	0.894	1.548	1.477	1.684				
38	Apln	1.906	ns	ns	ns						
39	Ltbp2	1.904	0.839	ns	ns		0.922		1.096	1.731	
40	Postn	1.856	1.925	1.167	ns		1.402				
41	Nxpe5	1.855	ns	ns	ns						
42	Csrp2	1.816	1.449	ns	ns	1.100	0.793				
43	Ms4a7	1.803	0.886	ns	ns						
44	Sod3	1.795	1.617	0.854	ns	0.865	1.091		0.692	0.964	
45	Dclk1	1.786	1.667	ns	ns	1.406	1.716				
46	Pcsk5	1.778	0.871	ns	ns		1.484			1.634	
47	Bmper	1.774	1.587	ns	ns		1.235				
48	Sfrp2	1.772	2.205	1.668	1.599	1.149	1.408	1.379			
49	Ms4a6d	1.771	0.751	ns	1.733						
50	Cxcl16	1.766	0.93	ns	ns						
51	Dpep2	1.747	ns	ns	ns						
52	Msr1	1.736	ns	ns	ns		0.765				
53	Cyp7b1	1.734	ns	ns	ns		1.022				
54	Has1	1.728	2.337	ns	ns		1.270			3.805	
55	Slc16a2	1.726	1.905	ns	ns	1.064	1.164				
56	Kcne4	1.722	1.287	ns	ns		0.818				
57	Akr1b8	1.721	1.486	ns	ns	0.901	1.029			1.171	
58	Prune2	1.718	ns	ns	ns		0.636				

96

		TC-whole joint				DMM-whole joint			DMM-cartilage		
No.	*Gene Name*	1 Day	1 Week	6 Weeks	12 Weeks	2 Weeks	4 Weeks	16 Weeks	1 Week	2 Weeks	6 Weeks
59	*Galnt16*	1.698	1.89	*ns*	*ns*						
60	*Ccr5*	1.667	*ns*	*ns*	*ns*						
61	*Mustn1*	1.665	*ns*	*ns*	*ns*						
62	*AW551984*	1.661	2.202	*ns*	*ns*	1.297	1.595				
63	*Fbn1*	1.639	1.566	*ns*	*ns*	0.914	1.466				
64	*Lrrc17*	1.637	0.971	*ns*	*ns*	1.068	1.246				
65	*Wisp2*	1.623	1.415	0.856	1.416	1.451	1.324				
66	*Aldh1a2*	1.608	*ns*	*ns*	*ns*						
67	*Ccl8*	1.605	1.85	*ns*	*ns*						
68	*Figf*	1.582	*ns*	*ns*	*ns*	0.654					
69	*Fam57a*	1.572	1.363	*ns*	*ns*	0.772	0.593				
70	*Il33*	1.566	1.111	*ns*	*ns*	1.602	1.497				
71	*C1qtnf3*	1.563	3.683	3.789	*ns*		3.686	3.306		0.703	
72	*Snai1*	1.559	1.491	*ns*	*ns*	0.714	0.792				
73	*Il4ra*	1.559	*ns*	*ns*	*ns*						
74	*Gm6377*	1.548	*ns*	*ns*	*ns*		0.707				
75	*Tubb2b*	1.52	1.132	*ns*	*ns*	1.075	0.964				
76	*Fstl1*	1.506	1.773	0.947	*ns*	0.941	1.294				
77	*Nox4*	1.497	1.284	*ns*	*ns*		1.222				
78	*Lox*	1.492	1.241	*ns*	*ns*		1.171				
79	*Fbxo32*	1.487	*ns*	*ns*	*ns*						
80	*Tubb6*	1.483	0.67	*ns*	*ns*		0.823			1.117	
81	*Mt1*	1.471	0.76	*ns*	*ns*	0.816				0.764	
82	*Gpx7*	1.462	1.312	*ns*	*ns*		0.955				
83	*Bcat1*	1.451	1.199	*ns*	*ns*						
84	*Scn7a*	1.437	0.786	*ns*	*ns*						
85	*Tnfrsf12a*	1.435	*ns*	*ns*	*ns*	0.987	0.892				
86	*Ccl12*	1.435	*ns*	*ns*	*ns*						
87	*Tnn*	1.429	2.076	1.666	1.595	1.973	1.926				
88	*P2ry6*	1.408	*ns*	*ns*	*ns*						
89	*Mmp19*	1.407	1.215	*ns*	*ns*	1.606	1.644				
90	*Gm765*	1.407	*ns*	*ns*	*ns*						
91	*Eln*	1.406	1.648	*ns*	*ns*		0.626				
92	*Ier5l*	1.405	*ns*	*ns*	*ns*	0.684	0.667				
93	*Vcan*	1.402	1.655	1.42	*ns*		1.078				
94	*Col14a1*	1.401	2.374	*ns*	*ns*	0.973	1.512			1.061	
95	*Kcnj15*	1.388	2.623	*ns*	*ns*	2.616	3.274				
96	*Lgmn*	1.387	*ns*	*ns*	*ns*						
97	*Stab1*	1.385	0.908	*ns*	*ns*						
98	*Arsi*	1.384	1.907	*ns*	*ns*	0.881	0.989				
99	*Anpep*	1.356	1.66	1.16	*ns*		0.819				
100	*Mfap5*	1.355	1.881	*ns*	*ns*		1.308				
101	*Ddah1*	1.349	1.977	*ns*	*ns*	1.312	1.327		1.504	0.840	
102	*Csgalnact1*	1.344	1.081	1.306	*ns*	1.230	1.007				
103	*Col5a1*	1.335	1.927	1.279	1.118	0.748	0.986			0.676	
104	*Tm4sf1*	1.329	1.193	*ns*	*ns*	0.984	1.132	0.776	2.062	2.419	
105	*Loxl1*	1.308	1.262	*ns*	*ns*	0.788	1.104				
106	*Ccbe1*	1.308	1.345	*ns*	*ns*		0.784				
107	*Fzd2*	1.297	*ns*	*ns*	*ns*	0.833	0.591				
108	*Socs3*	1.287	0.837	*ns*	*ns*	0.939	1.057		1.205	1.496	
109	*Il13ra1*	1.286	0.762	*ns*	*ns*	1.200	1.166		2.079	1.105	
110	*Clec4n*	1.283	0.765	*ns*	1.214		0.892				
111	*Scx*	1.279	1.535	*ns*	*ns*		0.771				
112	*Slc39a14*	1.276	0.992	*ns*	*ns*	1.085	1.165			1.497	
113	*Loxl3*	1.276	1.349	*ns*	*ns*	0.870	1.007		1.376	1.095	
114	*Vim*	1.264	0.89	1.065	*ns*						
115	*Slc1a4*	1.258	2.025	*ns*	*ns*	0.991	0.944	0.893		0.714	
116	*AF251705*	1.248	*ns*	*ns*	*ns*						
117	*Ccdc109b*	1.246	0.618	0.732	*ns*					1.315	
118	*A4galt*	1.245	1.431	*ns*	*ns*	0.760	0.897				
119	*Slc27a3*	1.24	1.699	*ns*	*ns*	0.908	0.653				
120	*Map6*	1.238	*ns*	*ns*	*ns*						
121	*Tnfrsf23*	1.227	1.037	*ns*	*ns*						
122	*Trim63*	1.223	-0.616	*ns*	*ns*						

No.	Gene Name	TC-whole joint				DMM-whole joint			DMM-cartilage		
		1 Day	1 Week	6 Weeks	12 Weeks	2 Weeks	4 Weeks	16 Weeks	1 Week	2 Weeks	6 Weeks
123	5430435G22Rik	1.222	ns	ns	ns						
124	S100a4	1.215	0.655	ns	1.145						
125	Adamtsl3	1.212	ns	ns	ns						
126	Dab2	1.21	1.368	1.271	ns	0.829	1.222				
127	Asap3	1.208	ns	ns	ns						
128	Pxdn	1.206	1.627	ns	ns	1.053	1.268			1.131	
129	Itga7	1.205	ns	ns	ns						
130	Thbs2	1.204	1.893	1.006	ns	1.505	1.427				
131	Sorcs2	1.202	1.212	ns	ns						
132	Col18a1	1.197	1.696	ns	ns	0.870	0.963				
133	Tacc2	1.197	ns	ns	ns						
134	Sulf1	1.194	1.561	1.051	ns	1.122	1.369		1.575	1.562	1.026
135	Hspb7	1.193	-0.97	ns	ns						
136	Angptl1	1.19	2.48	1.591	ns	1.512	2.180				
137	Junb	1.178	ns	ns	ns		0.684				
138	Tgfbi	1.169	0.866	ns	1.146	0.689			2.237	3.077	
139	Col6a3	1.165	2.133	1.652	1.256	0.876	1.349	1.115	2.518	1.633	
140	Bex1	1.156	ns	ns	ns						
141	Aspn	1.156	2.012	1.904	ns	1.315	1.350				
142	Praf2	1.155	1.004	ns	ns	0.696	0.873			0.709	
143	Srpx2	1.145	1.555	1.337	1.312	1.038	1.091		1.472	0.850	
144	Arl4c	1.141	0.652	ns	ns		0.622				
145	nsg1	1.141	0.875	ns	ns	0.766	0.799				
146	Enpp1	1.14	1.698	1.629	ns	1.231	0.963				
147	Prkcdbp	1.13	1.025	ns	1.683	0.736	0.748				
148	Itga5	1.129	0.912	ns	1.124						
149	Il1rl1	1.129	ns	ns	ns	1.548					
150	Lmna	1.121	0.743	ns	ns	0.773	0.598				
151	Lrrn1	1.12	ns	ns	ns						
152	Cfb	1.111	1.013	ns	1.088						
153	Il1r1	1.109	0.733	ns	ns		0.670				
154	Osr1	1.106	0.991	ns	ns		0.895				
155	Fcgr1	1.105	ns	ns	ns						
156	Layn	1.103	0.803	1.238	ns	0.627					
157	Plat	1.092	1.039	1.101	ns		0.915			1.733	
158	Fkbp11	1.092	1.095	ns	ns						
159	Aldh1l2	1.09	0.781	ns	ns		0.912		1.243		
160	Ctss	1.084	ns	ns	ns						
161	Mfap4	1.083	1.861	ns	ns		1.367				
162	Apoc2	1.08	ns	ns	ns						
163	Hs6st2	1.08	ns	ns	-1.152						
164	Myof	1.077	1.296	1.06	ns	0.691	0.667				
165	Klhl38	1.076	ns	ns	ns						
166	Thy1	1.076	1.321	1.121	1.335	1.173	1.343				
167	Thbs4	1.074	1.174	ns	ns	0.957	1.153	1.122			
168	Col6a2	1.071	2.108	1.266	1.489	1.074	1.617		1.567	1.465	
169	Fndc1	1.067	2.223	1.297	ns	1.437	1.597	1.385			
170	Fscn1	1.064	0.982	ns	ns		1.205				
171	Nol3	1.061	ns	ns	ns						
172	Cd14	1.058	0.74	ns	ns				1.904	2.228	
173	Pdia4	1.058	ns	ns	ns						
174	Cxcl14	1.057	ns	ns	1.255		0.998				
175	Cnksr1	1.056	-0.722	ns	ns						
176	Lamb1	1.056	1.354	ns	ns	1.141	1.623				
177	Medag	1.053	1.907	1.091	ns						
178	Col6a1	1.05	2.06	1.196	1.284	1.157	1.520	1.322	1.503	0.795	
179	Ppp1r27	1.048	-1.04	ns	ns						
180	Nnmt	1.048	0.744	ns	ns		0.761				
181	Efemp2	1.044	1.054	ns	ns	0.639	0.905				
182	Prg4	1.044	1.46	3.006	ns						
183	Nfatc4	1.044	1.484	ns	ns	1.068	1.143				
184	Col5a3	1.043	1.457	1.122	ns	1.029	1.397				
185	Cx3cr1	1.039	ns	ns	ns						
186	Nek6	1.039	ns	ns	ns						

No.	Gene Name	TC-whole joint				DMM-whole joint			DMM-cartilage		
		1 Day	1 Week	6 Weeks	12 Weeks	2 Weeks	4 Weeks	16 Weeks	1 Week	2 Weeks	6 Weeks
187	Col5a2	1.038	1.53	1.435	1.408		1.102	0.917		0.697	
188	Igsf10	1.037	1.848	ns	ns						
189	Adh1*	1.033	ns	ns	ns		-0.718				
190	Hif1a	1.028	0.976	ns	ns	0.884	1.139		1.920	1.194	
191	Wfdc17	1.024	ns	ns	ns						
192	Adam12	1.023	1.141	ns	ns		0.640				
193	Pdia5	1.022	0.921	ns	ns						
194	2810433D01Rik	1.022	ns	ns	ns	0.606					
195	Gpr153	1.019	1.216	ns	ns		1.166				
196	Emp1	1.017	1.212	0.903	ns	0.630	0.773		2.545	3.440	2.337
197	Bok	1.015	ns	ns	ns						
198	Osmr	1.013	0.818	0.926	ns	0.853	1.080		1.186		
199	Mss51	1.012	ns	ns	ns						
200	Art5	1.01	ns	ns	ns						
201	Atp8b1	1.006	0.901	ns	ns		1.102				
202	Ildr2	0.997	ns	ns	ns						
203	Ablim2	0.996	ns	ns	ns						
204	Lgals1	0.992	0.758	ns	ns						
205	Ifi205	0.991	ns	ns	ns						
206	Socs1	0.99	ns	ns	ns						
207	Ptgfrn	0.986	1.437	ns	ns	0.990	1.389			1.433	
208	Cysltr1	0.984	ns	ns	ns						
209	Fzd1	0.978	0.786	ns	ns	0.921	1.234				
210	Slc41a2	0.978	1.143	ns	ns	0.829	1.097			1.100	
211	Numbl	0.977	ns	ns	ns						
212	Akap5	0.97	ns	ns	ns						
213	Cbr2	0.97	ns	ns	ns						
214	Apoe	0.963	ns	ns	ns						
215	Plau	0.963	ns	ns	ns						
216	B3galnt1	0.95	0.95	ns	ns	0.730					
217	Igf1	0.946	1.636	1.135	ns	0.991	1.078			1.223	
218	Cttnbp2nl	0.945	ns	ns	ns		0.682				
219	Phldb2	0.942	ns	ns	ns		0.808				
220	Rian	0.942	2.002	ns	ns	1.294	1.103				
221	Aebp1	0.939	1.41	ns	ns	0.999	1.331		1.496		
222	AU023762	0.938	ns	ns	ns						
223	Sulf2	0.937	1.71	1.082	ns	0.877	0.948				
224	Podn	0.937	0.743	ns	ns						
225	Serpinh1	0.937	0.834	ns	1.64		1.043				
226	Cdc42ep5	0.936	ns	ns	ns						
227	Mecom	0.933	ns	ns	ns	0.951	0.919				
228	Morc4	0.933	1.132	ns	ns	0.882	1.076				
229	Lpxn	0.929	ns	ns	ns						
230	Pdk4	0.929	ns	ns	ns						
231	Tmem198b	0.924	0.78	ns	ns		0.702				
232	Mest	0.924	2.6	ns	ns	0.988	0.843		2.256		
233	B4galt2	0.923	0.928	ns	ns						
234	H2-Eb1	0.922	ns	ns	1.269						
235	Inhba	0.922	0.857	1.451	ns		0.768		3.426	3.743	2.329
236	C1qb	0.921	ns	ns	ns						
237	Fam129b	0.916	0.644	ns	1.177	0.630					
238	Adamts12	0.915	1.638	ns	ns		1.353			0.603	
239	Ccdc102a	0.915	1.086	ns	ns	0.966	0.697				
240	Dbn1	0.914	1.295	ns	ns						
241	Gpnmb	0.914	0.865	ns	ns						
242	Tmem106a	0.911	ns	ns	ns						
243	Ly6a	0.909	0.903	ns	ns		0.834				
244	Bend6	0.909	0.598	ns	ns	0.948	0.634				
245	Gatsl2	0.903	ns	ns	ns		0.599				
246	Gm13889	0.901	ns	ns	ns						
247	Svep1	0.9	1.248	ns	ns	0.734	0.873				
248	Epb4.1l3	0.897	1.05	ns	ns	0.755					
249	Nrn1	0.893	1.525	ns	ns	0.804			1.509		
250	Pmepa1	0.892	1.1	ns	ns	0.742	1.078				

No.	Gene Name	TC-whole joint				DMM-whole joint			DMM-cartilage		
		1 Day	1 Week	6 Weeks	12 Weeks	2 Weeks	4 Weeks	16 Weeks	1 Week	2 Weeks	6 Weeks
251	Cd248	0.884	1.61	ns	ns		0.707				
252	Mmp23	0.883	1.131	ns	ns		0.678				
253	Sh3rf2	0.876	ns	ns	ns						
254	Hspb1	0.876	ns	-1.162	ns						
255	Adam9	0.873	ns	ns	ns	0.808	0.801				
256	Dse	0.872	0.621	ns	ns	0.834	0.800				
257	Tmem37	0.872	ns	ns	1.252						
258	Col8a1	0.871	1.106	0.772	ns	0.793	0.767			2.698	2.642
259	Calu	0.869	0.877	ns	ns		0.857		1.618	1.776	
260	Pltp	0.868	ns	ns	ns		0.655				
261	Ppap2c	0.867	ns	ns	ns						
262	Myh1	0.864	ns	ns	ns						
263	Ndn	0.863	1.05	ns	ns						
264	Ahr	0.859	ns	ns	ns	0.758	0.688				
265	Basp1	0.856	ns	ns	ns						
266	Ttc9	0.856	ns	ns	ns						
267	Rab23	0.855	0.689	ns	ns		0.666				
268	Rasgef1b	0.855	ns	ns	ns						
269	Ier3	0.854	0.63	ns	ns		0.662			2.552	
270	Amotl2	0.852	0.674	ns	ns				1.830	1.579	
271	Lrrc15	0.852	1.961	ns	ns	1.871	2.022	2.389			
272	Cryab	0.851	-0.635	ns	ns						
273	Tlr1	0.85	ns	ns	ns						
274	Mnda	0.849	ns	1.307	ns						
275	Pvr	0.849	0.666	ns	ns		0.949		1.053	0.773	
276	Plod1	0.849	0.728	ns	ns	0.623	0.714				
277	Gpr34	0.848	ns	ns	ns						
278	Abcc3	0.847	ns	ns	ns						
279	Thbs3	0.847	1.981	2.037	1.32	1.023	1.437	1.362		1.108	
280	Fgf7	0.847	ns	ns	ns		0.808553				
281	Fgf2	0.845	ns	ns	ns						
282	Tbx18	0.845	1.208	ns	ns	0.985	1.081				
283	Grb10	0.844	1.259	ns	ns	0.830	1.229				
284	Pex13	0.834	ns	ns	ns						
285	Smpdl3b	0.833	ns	ns	ns						
286	Ctsc	0.832	ns	ns	ns		1.472				
287	Pdlim4	0.832	0.788	ns	ns	0.841	0.871			1.297	
288	Fcgr2b	0.83	ns	0.991	ns						
289	Abcb1b	0.827	ns	ns	ns						
290	Fads3	0.825	ns	ns	0.8						
291	Ms4a6b	0.825	ns	ns	ns						
292	Fos	0.825	0.735	ns	ns		1.268		3.321	4.118	
293	Flnc	0.822	-0.67	ns	ns						
294	Bgn	0.821	1.421	1.433	ns	0.851	1.603			0.945	
295	Fam171a2	0.821	1.019	ns	ns	1.124	1.071				
296	Ccdc80	0.817	0.929	1.476	ns		0.646	0.804			
297	Adamts1	0.816	ns	ns	ns		0.857				
298	Nt5dc2	0.812	0.603	ns	ns		0.770				
299	Nmrk1	0.812	ns	ns	ns						
300	Slamf9	0.812	ns	ns	ns						
301	Atp9a	0.812	ns	-0.685	ns						
302	P4ha2	0.81	1.071	ns	ns		1.172				
303	Emilin1	0.808	0.807	ns	ns						
304	Maged1	0.807	0.862	ns	ns		0.675				
305	C1qc	0.803	ns	ns	1.345						
306	Txndc5	0.803	0.763	ns	ns					0.662	
307	Maged2	0.802	0.955	ns	ns		0.754				
308	Smoc1	0.794	1.656	ns	ns	1.442	1.035			1.216	
309	Cyb561	0.793	ns	ns	ns		0.850				
310	Obsl1	0.791	ns	ns	ns						
311	Ubtd1	0.789	ns	ns	ns						
312	Tbx1	0.789	ns	ns	ns						
313	Rhoc	0.788	0.673	ns	ns		0.722				
314	Lama4	0.787	1.099	ns	ns	0.819	1.004		0.602	0.781	

No.	Gene Name	TC-whole joint				DMM-whole joint			DMM-cartilage		
		1 Day	1 Week	6 Weeks	12 Weeks	2 Weeks	4 Weeks	16 Weeks	1 Week	2 Weeks	6 Weeks
315	Igfn1	0.786	ns	ns	ns						
316	Cdk14	0.786	0.77	ns	ns		0.872				
317	C1qtnf2	0.786	1.441	ns	ns		1.205				
318	Myh14	0.785	ns	ns	ns						
319	Plce1	0.785	ns	ns	ns	0.802	0.826				
320	Gpr183	0.785	ns	ns	ns						
321	Col16a1	0.784	1.293	1.097	ns	0.903	1.023				
322	Angptl2	0.783	1.748	ns	ns	1.255	1.069	1.204			
323	Olfml3	0.783	ns	ns	ns		0.781				
324	Tmem45a	0.78	1.498	ns	ns	0.715	0.940				
325	Rgs1	0.779	ns	ns	ns						
326	Cav1	0.779	ns	ns	ns						
327	Pid1	0.778	ns	ns	ns						
328	Chrnb1	0.778	ns	ns	ns						
329	H2-Ab1	0.776	ns	ns	ns						
330	Bcl3	0.775	ns	ns	ns		0.789				
331	Cyb5r3	0.774	0.669	ns	ns		1.215				
332	Armcx2	0.772	0.661	ns	ns		0.603				
333	Gprc5b	0.772	ns	ns	ns	0.653	0.694				
334	Synj2	0.767	ns	ns	ns						
335	Chst14	0.766	0.658	ns	ns						
336	Tubb2a	0.764	0.66	ns	0.826	0.650					
337	C1qa	0.764	ns	ns	0.771						
338	Ttc12	0.76	ns	ns	ns						
339	Nt5e	0.76	1.06	1.029	ns	1.341	1.206	1.082	3.797	2.382	2.492
340	Lmod2	0.76	-0.946	ns	ns						
341	Ccr2	0.76	ns	ns	ns						
342	Tnfrsf11a	0.759	ns	ns	ns						
343	Epb4.1l1	0.759	0.739	ns	ns				1.665	1.506	
344	Ecscr	0.757	ns	ns	ns	0.816	0.913				
345	Igdcc4	0.755	ns	ns	ns	0.727	0.881				
346	Aplnr	0.752	0.699	ns	ns		0.932				
347	Pros1	0.752	ns	ns	ns						
348	Map1b	0.751	ns	ns	ns						
349	Frk	0.749	0.796	ns	ns		0.977				
350	P4hb	0.748	ns	ns	ns						
351	Mxra7	0.747	0.904	ns	ns	0.878	1.350				
352	Dsel	0.746	1.402	ns	ns	1.046	1.228				
353	Lyplal1	0.743	ns	ns	ns						
354	Itgb5	0.742	ns	ns	ns		0.596				
355	Ankrd29	0.742	1.046	ns	ns		0.836				
356	Chpf	0.741	1.356	ns	ns						
357	Fabp5	0.74	ns	ns	ns						
358	Aif1	0.735	ns	ns	ns						
359	Bicc1	0.735	0.908	ns	ns	0.715	0.984				
360	Tpbg	0.733	ns	ns	ns						
361	Atf3	0.731	ns	ns	ns						
362	H2-Aa	0.73	ns	ns	0.9						
363	Ptn	0.729	1.634	ns	ns	1.188	1.177				
364	Zfp503	0.728	ns	ns	ns						
365	Fkbp10	0.727	1.014	ns	ns		0.887				
366	Tmtc4	0.727	ns	ns	ns						
367	Kdelr2	0.727	ns	ns	ns						
368	Erf	0.726	ns	ns	ns						
369	Slfn9	0.725	ns	ns	ns						
370	Eps8	0.725	ns	ns	ns	0.673	0.593				
371	Gadd45g	0.724	ns	ns	ns						
372	Folr2	0.724	0.707	ns	ns				2.485	2.791	
373	Zfp449	0.724	ns	ns	ns		1.140				
374	Sigmar1	0.723	ns	ns	ns						
375	Cttn	0.721	0.643	ns	ns						
376	Tspan4	0.718	ns	ns	ns						
377	Pdlim3	0.716	ns	ns	ns						
378	Cul7	0.716	0.823	ns	ns						

No.	Gene Name	TC-whole joint				DMM-whole joint			DMM-cartilage		
		1 Day	1 Week	6 Weeks	12 Weeks	2 Weeks	4 Weeks	16 Weeks	1 Week	2 Weeks	6 Weeks
379	Rcn1	0.716	0.687	ns	ns	1.036	0.773				
380	Lgi2	0.716	ns	ns	ns						
381	Igfbp7	0.715	0.908	ns	ns					0.913	
382	Ndrg4	0.713	1.419	ns	ns	1.009	1.208			1.369	
383	Meox2	0.713	0.779	ns	ns	0.788	1.043				
384	Sertad4	0.711	1.563	0.962	ns	1.031	1.367	1.139			
385	Trabd2b	0.71	ns	ns	ns						
386	Plod3	0.71	ns	ns	ns						
387	Ebpl	0.709	ns	ns	ns						
388	Dpysl3	0.709	0.706	0.709	ns	0.760	1.000			2.294	1.227
389	Pcolce	0.709	1.094	ns	0.906		1.182				
390	Lrp1	0.709	0.888	ns	ns		0.871				
391	Casp12	0.709	ns	ns	ns	0.706	0.807				
392	Slc2a1	0.707	ns	ns	ns						
393	Myod1	0.707	ns	ns	ns						
394	Serpinb8	0.706	1.043	ns	ns		0.820			0.761	
395	Kcnc4	0.702	ns	ns	ns						
396	Cnn3	0.702	0.737	ns	ns	0.804	0.868				
397	Gulp1	0.701	0.91	ns	ns	0.899	1.156				
398	Lrrc2	0.7	-0.772	ns	ns						
399	Plxnb2	0.698	ns	ns	ns						
400	Phf11d	0.698	ns	1.112	ns						
401	Anxa2	0.697	ns	ns	1.016						
402	Stmn2	0.697	ns	ns	ns	0.972	0.824				
403	Kctd17	0.695	0.743	ns	0.936		0.790				
404	Tmem97	0.695	ns	ns	1.509						
405	Dpt	0.695	1.856	1.339	ns	0.985	1.361	1.127			
406	Snx7	0.692	1.057	1.347	ns	0.722	0.851		1.383	1.725	1.044
407	Rcn3	0.691	0.736	ns	ns						
408	Tgfb3	0.691	0.846	ns	ns		0.838				
409	Clmp	0.691	0.757	ns	ns						
410	3632451O06Rik	0.689	1.424	ns	ns	0.810	1.031				
411	Lrrc59	0.689	ns	ns	ns						
412	Fam13c	0.688	ns	ns	ns	0.824	0.825				
413	Capn6	0.688	1.773	ns	ns	1.022	0.766				
414	Lima1	0.686	0.795	0.892	ns	0.667	0.686			1.859	1.268
415	2610034B18Rik	0.685	0.635	ns	ns		0.747				
416	Avpi1	0.684	ns	ns	ns						
417	Depdc7	0.681	ns	ns	ns						
418	AI607873	0.68	ns	ns	ns						
419	B4galt5	0.679	ns	ns	ns						
420	Rrbp1	0.677	0.591	0.895	ns		0.661		1.263	1.317	
421	Gmds	0.677	ns	ns	ns						
422	Gas8	0.675	ns	ns	ns						
423	Pea15a	0.674	ns	ns	ns						
424	Siglec1	0.674	ns	ns	ns						
425	Ctsl	0.674	ns	ns	ns		0.621				
426	Rcan1	0.674	ns	ns	ns		0.935				
427	Ppfibp1	0.674	0.689	ns	ns					1.248	
428	Dnm3os	0.672	1.324	ns	ns		0.706				
429	Fxyd6	0.671	0.863	-0.616	ns	0.864	0.855	0.696		1.422	
430	Srxn1	0.671	ns	ns	ns						
431	Fam114a1	0.671	0.992	1.438	ns	0.585	1.047				
432	Prrx1	0.671	0.726	ns	ns		0.630				
433	Kdelc2	0.67	0.768	0.899	ns		0.913				
434	Phf11a	0.669	ns	ns	ns						
435	Ccdc36	0.665	ns	ns	ns						
436	Lrrc32	0.664	ns	ns	ns						
437	Adck4	0.664	ns	ns	ns						
438	Fn1	0.664	1.597	2.158	1.55		0.686	0.785	3.183	2.543	
439	Ltbp1	0.663	0.877	ns	ns	0.741	0.680		1.895	1.826	
440	Fmn1	0.663	1.217	ns	ns	0.770	1.126				
441	Clec11a	0.662	0.851	1.865	ns	0.635	0.776				
442	Gjc1	0.657	ns	ns	ns	0.843	1.067				

No.	Gene Name	TC-whole joint				DMM-whole joint			DMM-cartilage		
		1 Day	1 Week	6 Weeks	12 Weeks	2 Weeks	4 Weeks	16 Weeks	1 Week	2 Weeks	6 Weeks
443	Pdia6	0.657	ns	ns	ns						
444	Prss23	0.656	ns	ns	ns		0.941				
445	10-Sep	0.654	ns	ns	ns						
446	Vsig4	0.653	0.683	2.94	ns						
447	Clip3	0.652	1.077	ns	ns						
448	Glis2	0.651	1.038	ns	ns	0.613	0.727				
449	Ms4a4d	0.649	ns	ns	ns						
450	Dkk3	0.648	1.848	ns	ns	1.373	1.360	1.165			
451	Tspan6	0.646	1.222	ns	ns	0.775	0.871		1.544	1.232	
452	Dnajc25	0.644					0.660				
453	Npdc1	0.644	0.974	ns	1.233	0.592	0.745				
454	Enc1	0.643	ns	ns	ns						
455	Kctd11	0.643	0.795	ns	ns						
456	Gfra1	0.643	ns	ns	ns						
457	Lrig3	0.641	1.025	ns	ns	0.812	0.680				
458	Gatsl3	0.64	ns	ns	ns						
459	Coro6	0.637	ns	ns	ns						
460	Plk2	0.634	ns	ns	ns						
461	Ednrb	0.634	ns	ns	ns						
462	Loxl2	0.634	1.631	1.127	ns		2.041			1.275	
463	Cyr61	0.633	0.805	ns	ns		0.813		2.700	2.367	
464	Gas6	0.633	ns	ns	ns						
465	Cmklr1	0.633	ns	ns	ns						
466	Npl	0.63	ns	ns	0.973						
467	Mvp	0.63	ns	ns	ns						
468	Trim47	0.627	1.008	ns	ns		0.655				
469	A630033H20Rik	0.625	0.728	ns	ns	0.974	0.841				
470	Pofut2	0.624	0.816	ns	ns	0.722	0.670				
471	Mxra8	0.624	1.015	0.823	ns	0.658	0.856				
472	Itgbl1	0.624	1.408	ns	ns	1.369	1.528				
473	Pvrl3	0.623	0.971	ns	ns	1.019	1.136		1.476	0.713	
474	Arl6	0.621	ns	ns	ns						
475	Ikbip	0.619	0.892	0.928	ns	0.806	0.996				
476	Serpinb6a	0.619	ns	ns	ns						
477	Adap2	0.617	ns	ns	ns						
478	Magee1	0.617	ns	ns	ns		0.674				
479	Fkbp1b	0.616	ns	ns	ns						
480	Nr2f6	0.613	ns	ns	ns						
481	Sec24d	0.606	0.862	ns	ns		0.694			1.720	
482	Ecm1	0.603	1.183	ns	ns	0.680	0.786		1.210	1.823	
483	Baiap2	0.6	1.038	ns	ns					1.814	
484	Selm	0.597	ns	ns	ns						
485	Eva1b	0.594	ns	ns	ns						
486	C1qtnf6	0.593	1.483	ns	ns	0.597	0.707				
487	Cd68	0.591	ns	ns	ns						
488	Mybl1	0.59	ns	ns	ns						
489	Rab34	0.589	0.77	ns	ns		0.658				
490	Hpgds	0.588	ns	ns	ns						
491	Ggt5	0.586	ns	ns	ns						
492	Prrg1	0.585	ns	ns	ns		0.637				
493	Man2a1	0.583	ns	ns	ns						
494	Adcy2	0.583	ns	ns	ns	0.647					
495	Mamstr	0.582	ns	ns	ns						
496	Gpm6b	0.582	1.023	ns	ns	1.209	1.840				
497	Gm6307	-0.583	-0.897	ns	ns						
498	Pvalb	-0.587	ns	ns	ns						
499	Col9a1	-0.587	ns	ns	ns						
500	Acaca	-0.588	ns	ns	ns						
501	Pygm	-0.592	ns	ns	ns						
502	Cilp2	-0.593	ns	ns	ns						
503	Hapln1	-0.594	ns	1.649	ns						
504	Dgat2	-0.595	ns	ns	ns						
505	Ky	-0.596	ns	ns	ns						
506	Mylk4	-0.598	ns	ns	ns						

No.	Gene Name	TC-whole joint				DMM-whole joint			DMM-cartilage		
		1 Day	1 Week	6 Weeks	12 Weeks	2 Weeks	4 Weeks	16 Weeks	1 Week	2 Weeks	6 Weeks
507	1300017J02Rik	-0.599	ns	ns	ns						
508	Zfp773	-0.602	ns	ns	ns						
509	Orm1	-0.607	ns	ns	ns						
510	Bex4	-0.615	ns	ns	ns						
511	Btnl10	-0.616	ns	ns	ns						
512	Gp6	-0.618	ns	ns	ns						
513	Sema3e	-0.619	ns	ns	ns						
514	Frat2	-0.621	ns	ns	ns						
515	Pcx	-0.623	ns	ns	ns						
516	Synpo2	-0.628	ns	ns	ns						
517	Gm9895	-0.631	ns	ns	ns						
518	Tpi1	-0.635	ns	-0.969	ns						
519	Vpreb1	-0.641	ns	ns	ns						
520	Fcer2a	-0.649	ns	ns	ns						
521	Prg3	-0.656	ns	ns	ns						
522	Map3k7cl	-0.661	ns	ns	ns						
523	Pgam2	-0.662	ns	ns	ns						
524	Fsd2	-0.663	ns	ns	ns						
525	Tob1	-0.663	ns	ns	ns						
526	Acss2	-0.664	ns	ns	ns						
527	Ostn	-0.666	ns	ns	ns						
528	Mgl2	-0.668	ns	ns	ns						
529	Lect1	-0.672	ns	0.982	ns						
530	Myh2	-0.676	-1.524	ns	ns						
531	Tnxb	-0.677	ns	ns	ns						
532	Klhl33	-0.687	ns	ns	ns						
533	Plcd4	-0.688	ns	ns	ns						
534	Tac2	-0.696	ns	ns	ns						
535	Ampd1	-0.698	ns	ns	ns						
536	Aldh1a7	-0.7	ns	ns	ns						
537	Casq1	-0.705	ns	ns	ns						
538	Ppl	-0.705	ns	ns	ns						
539	Kcng4	-0.706	ns	ns	ns						
540	Col10a1	-0.712	-0.602	2.296	ns						
541	Abra	-0.712	-0.799	ns	ns						
542	Gsn	-0.737	ns	ns	ns						
543	Nrep	-0.742	ns	ns	ns						
544	6430571L13Rik	-0.746	ns	ns	ns						
545	Lsmem1	-0.753	ns	ns	ns						
546	Gpd1	-0.771	ns	ns	ns						
547	Apobec2	-0.792	-0.675	ns	ns						
548	Itgb1bp2	-0.807	ns	ns	ns						
549	Pamr1	-0.812	1.945	1.265	1.27	1.257	1.200				
550	Olfr420	-0.825	ns	2.071	ns						
551	Mlf1	-0.838	-0.593	ns	ns						
552	Eno3	-0.848	-0.717	-0.891	ns					-2.028	-1.408
553	Dupd1	-0.858	ns	-0.609	ns						
554	Pfkfb1	-0.872	-0.617	ns	ns					-0.900	
555	Cdo1	-0.885	ns	ns	ns						
556	Myoc	-0.9	ns	ns	ns	-1.225	-0.880				
557	Ccl24	-0.905	ns	ns	ns						
558	Tceal7	-0.907	ns	ns	ns						
559	Nnat	-0.91	ns	ns	ns		-1.425				
560	G630055G22Rik	-0.91	ns	ns	ns						
561	Matn3	-0.922	ns	ns	ns						
562	Yipf7	-0.923	-0.816	ns	ns						
563	Slc47a1	-0.923	-0.962	ns	ns						
564	Dhrs7c	-0.928	ns	ns	ns						
565	Clec3b	-0.958	0.952	ns	ns		0.647				
566	Amd1	-0.959	ns	ns	ns						
567	Timp4	-0.961	-0.747	ns	ns		-0.822			-2.063	
568	Smco1	-0.967	ns	ns	ns						
569	Sbk2	-0.972	-1.127	-1.221	ns						
570	Scd1	-0.974	ns	ns	ns						

No.	Gene Name	TC-whole joint				DMM-whole joint			DMM-cartilage		
		1 Day	1 Week	6 Weeks	12 Weeks	2 Weeks	4 Weeks	16 Weeks	1 Week	2 Weeks	6 Weeks
571	Gdap1	-0.976	ns	ns	ns						
572	Adig	-1.016	ns	-1.732	ns		-0.653				
573	2310065F04Rik	-1.044	ns	ns	ns						
574	Kcnc1	-1.088	ns	ns	ns						
575	Ucma	-1.102	ns	ns	ns						
576	Smox	-1.126	ns	ns	ns						
577	Myl2	-1.144	-2.132	-2.417	ns						
578	Pon1	-1.151	ns	ns	ns						
579	Aqp4	-1.158	ns	ns	ns						
580	Perm1	-1.16	-1.044	ns	ns						
581	Htra4	-1.208	0.711	1.302	ns		0.857				
582	Csrp3	-1.229	-1.433	-0.815	ns						
583	Slurp1	-1.244	ns	ns	ns						
584	Fasn	-1.247	ns	ns	ns						
585	Tmem45b	-1.266	-0.75	ns	ns	-1.079	-1.007				
586	Pck1	-1.273	-0.866	ns	ns	-1.354					
587	C7	-1.275	ns	ns	ns						
588	Ces1d	-1.282	ns	ns	ns	-0.962	-1.326				
589	Retn	-1.3	-1.471	ns	ns		-0.784				
590	Cyp2e1	-1.323	-1.103	ns	ns						
591	Pla1a	-1.384	ns	ns	ns						
592	Thrsp	-1.394	-0.782	ns	ns		-0.892				
593	Cytl1	-1.407	-1.502	ns	ns	-1.430	-1.295				
594	Pnpla3	-1.58	ns	ns	ns						
595	Mybph	-1.652	ns	ns	ns						
596	Mettl21c	-1.746	ns	ns	ns						
597	Actc1	-1.944	-1.715	ns	ns						
598	Retnla	-2.169	-0.598	ns	ns						
599	C130080G10Rik	-2.921	ns	ns	ns						
600	Klhl34	ns	-1.562	-0.996	-0.764						
601	Comp	ns	0.988	1.087	0.837			0.764			
602	Antxr1	ns	1.752	1.888	1.086	1.107	1.640	1.248			1.567
603	Htra1	ns	1.341	0.855	1.197	1.007	1.283	1.516		1.907	
604	Hbegf	ns	0.691	1.052	1.284		0.896		2.235	3.030	
605	Fbln7	ns	1.536	1.932	1.305		1.197				
606	Mmp2	ns	1.715	1.752	1.46	1.113	1.700	1.323			
607	Scara3	ns	0.706	1.746	1.686		0.872	0.801			
608	Anxa8	ns	1.654	2.452	2.056	0.751	0.765	1.016		0.706	
609	Ccdc3	ns	ns	0.798	0.919		1.342				
610	Ctgf	ns	ns	1.177	1.023						
611	Lbp	ns	ns	1.01	1.201		0.857				
612	Crip1	ns	0.934	ns	0.978					0.995	
613	Sdc1	ns	0.933	ns	0.997	0.708	1.141				
614	Snhg18	ns	0.777	ns	1.028						
615	Olfml2b	ns	0.711	ns	1.304		0.658				
616	Nbl1	ns	1.421	ns	1.642	0.875	1.209	1.079	1.821	2.268	
617	Tigd4	ns	ns	ns	-1.933						
618	Pgpep1l	ns	ns	ns	-1.334						
619	Ovol1	ns	ns	ns	-1.262						
620	Car8	ns	ns	ns	-1.223						
621	Cpeb2	ns	ns	ns	-1.157						
622	C1galt1	ns	ns	ns	-1.055						
623	Nudt12	ns	ns	ns	-1.046						
624	Trim24	ns	ns	ns	-1.02						
625	Nexn	ns	ns	ns	-0.98						
626	Slc12a2*	ns	ns	ns	-0.932	0.669					
627	Dyrk2	ns	ns	ns	-0.905						
628	Akap6	ns	ns	ns	-0.878						
629	Esco1	ns	ns	ns	-0.86						
630	Cdkl2	ns	ns	ns	-0.854						
631	Impad1	ns	ns	ns	-0.838						
632	Qk	ns	ns	ns	-0.813						
633	Mib1	ns	ns	ns	-0.802						
634	Arrdc3	ns	ns	ns	-0.789						

No.	Gene Name	TC-whole joint				DMM-whole joint			DMM-cartilage		
		1 Day	1 Week	6 Weeks	12 Weeks	2 Weeks	4 Weeks	16 Weeks	1 Week	2 Weeks	6 Weeks
635	Rmnd5a	ns	ns	ns	-0.773						
636	Gm9159	ns	ns	ns	-0.736						
637	Rhobtb3	ns	ns	ns	-0.731						
638	Klhl31	ns	ns	ns	-0.718						
639	Arhgap20	ns	ns	ns	-0.704						
640	Atxn7	ns	ns	ns	-0.693						
641	Taf13	ns	ns	ns	-0.681						
642	Rabac1	ns	ns	ns	0.714						
643	Ctsg	ns	ns	ns	0.736						
644	Selplg	ns	ns	ns	0.746						
645	Prelid1	ns	ns	ns	0.752						
646	Prkab1	ns	ns	ns	0.759						
647	Pfn1	ns	ns	ns	0.777						
648	Prss34	ns	ns	ns	0.789						
649	Rbm38	ns	ns	ns	0.805						
650	Cenpa	ns	ns	ns	0.813						
651	Gipc1	ns	ns	ns	0.814						
652	Mrto4	ns	ns	ns	0.82						
653	Napsa	ns	ns	ns	0.828						
654	Tmem106c	ns	ns	ns	0.844						
655	Dnajb1	ns	ns	ns	0.848						
656	Cdk2ap2	ns	ns	ns	0.857						
657	Pdcd6	ns	ns	ns	0.866						
658	Hes6	ns	ns	ns	0.871						
659	Nr1h2	ns	ns	ns	0.872						
660	Slc29a1	ns	ns	ns	0.876						
661	Med28	ns	ns	ns	0.876						
662	Slc9a3r1	ns	ns	ns	0.879						
663	Ube2m	ns	ns	ns	0.881						
664	Eif4ebp1	ns	ns	ns	0.893						
665	Ltb*	ns	ns	ns	0.895	-0.61369					
666	Rbm42	ns	ns	ns	0.895						
667	Fzr1	ns	ns	ns	0.904						
668	Idnk	ns	ns	ns	0.905						
669	Ap2s1	ns	ns	ns	0.918						
670	Coa6	ns	ns	ns	0.927						
671	Fcho1	ns	ns	ns	0.937						
672	Pdk3	ns	ns	ns	0.939						
673	Rps18	ns	ns	ns	0.944						
674	Ftl1	ns	ns	ns	0.944						
675	Nmral1	ns	ns	ns	0.945						
676	Nhp2	ns	ns	ns	0.951						
677	Chst12	ns	ns	ns	0.952						
678	Eefsec	ns	ns	ns	0.954						
679	Tor2a	ns	ns	ns	0.961						
680	Capg	ns	ns	ns	0.965						
681	Pglyrp1	ns	ns	ns	0.967						
682	Creld2	ns	ns	ns	0.969						
683	Cd52	ns	ns	ns	0.97						
684	Cdca5*	ns	ns	ns	0.974	-0.61209					
685	Rpl28	ns	ns	ns	0.977						
686	Tmem134	ns	ns	ns	0.981						
687	Ccnd3	ns	ns	ns	0.981						
688	Tpst1	ns	ns	ns	0.995						
689	Cdc20	ns	ns	ns	0.999						
690	Rps2	ns	ns	ns	1.004						
691	Crlf2	ns	ns	ns	1.007						
692	2700094K13Rik	ns	ns	ns	1.008						
693	Ube2s	ns	ns	ns	1.011						
694	Lrg1	ns	ns	ns	1.014						
695	Tpst2	ns	ns	ns	1.017						
696	Cebpe	ns	ns	ns	1.017						
697	Def6	ns	ns	ns	1.018						
698	Tnfrsf1a	ns	ns	ns	1.024						

No.	Gene Name	TC-whole joint				DMM-whole joint			DMM-cartilage		
		1 Day	1 Week	6 Weeks	12 Weeks	2 Weeks	4 Weeks	16 Weeks	1 Week	2 Weeks	6 Weeks
699	Limd2	ns	ns	ns	1.025						
700	Faim3	ns	ns	ns	1.034						
701	Tamm41	ns	ns	ns	1.036						
702	Fam212a	ns	ns	ns	1.043						
703	Nfe2	ns	ns	ns	1.057						
704	Fam173a	ns	ns	ns	1.063						
705	Rab3il1	ns	ns	ns	1.082						
706	Gch1	ns	ns	ns	1.082						
707	Rsph3a	ns	ns	ns	1.083						
708	Map3k11	ns	ns	ns	1.085						
709	Dok2	ns	ns	ns	1.098						
710	Itprip	ns	ns	ns	1.099						
711	Ssbp4	ns	ns	ns	1.099						
712	E2f4	ns	ns	ns	1.101						
713	Arl11	ns	ns	ns	1.104						
714	Marcksl1	ns	ns	ns	1.105						
715	Rdm1	ns	ns	ns	1.115						
716	Ppp4c	ns	ns	ns	1.123						
717	Efhd2	ns	ns	ns	1.126						
718	2210016F16Rik	ns	ns	ns	1.129						
719	Rnh1	ns	ns	ns	1.147						
720	Asb6	ns	ns	ns	1.161						
721	Slc19a1	ns	ns	ns	1.162						
722	Sdf2l1	ns	ns	ns	1.165						
723	Hist1h2ab	ns	ns	ns	1.167						
724	S100a6	ns	ns	ns	1.172						
725	Coro1a*	ns	ns	ns	1.176	-0.60832					
726	Fam132a	ns	ns	ns	1.181						
727	H2afj	ns	ns	ns	1.19						
728	Cfp	ns	ns	ns	1.201						
729	Pla2g15	ns	ns	ns	1.201						
730	Ptpn18	ns	ns	ns	1.202						
731	Rpl18	ns	ns	ns	1.203						
732	Nenf	ns	ns	ns	1.205						
733	Plvap	ns	ns	ns	1.208						
734	Dok3	ns	ns	ns	1.215						
735	Emilin2	ns	ns	ns	1.217						
736	Cnpy3	ns	ns	ns	1.217						
737	Rhbdl1	ns	ns	ns	1.234						
738	Acot7	ns	ns	ns	1.255						
739	Ly6c2	ns	ns	ns	1.265						
740	Alg1	ns	ns	ns	1.274						
741	H2afx	ns	ns	ns	1.274						
742	Ptprcap	ns	ns	ns	1.286						
743	Kng1	ns	ns	ns	1.303						
744	Emc10	ns	ns	ns	1.31						
745	Ifitm3	ns	ns	ns	1.312						
746	Tgfb1	ns	ns	ns	1.324						
747	Ddost	ns	ns	ns	1.333						
748	Adam8	ns	ns	ns	1.333						
749	Ifitm2	ns	ns	ns	1.334						
750	Phgdh	ns	ns	ns	1.354						
751	Tssc1	ns	ns	ns	1.408						
752	Id1	ns	ns	ns	1.422						
753	Pycard	ns	ns	ns	1.489						
754	Clec10a*	ns	ns	ns	1.498	-0.665					
755	Lgals3	ns	ns	ns	1.545						
756	Sertad1	ns	ns	ns	1.634						
757	Tspo	ns	ns	ns	1.787						
758	Dapl1	ns	ns	ns	2.358						
759	H2-DMb2	ns	ns	ns	2.622						
760	Myl3	ns	-1.605	-1.436	ns						
761	Vwa1	ns	0.863	-1.368	ns					1.322	
762	Bdh1	ns	-1.298	-1.359	ns						

		TC-whole joint				DMM-whole joint			DMM-cartilage		
No.	Gene Name	1 Day	1 Week	6 Weeks	12 Weeks	2 Weeks	4 Weeks	16 Weeks	1 Week	2 Weeks	6 Weeks
763	Tnnt1	ns	-1.254	-1.032	ns						
764	Tnnc1	ns	-1.574	-1.031	ns						
765	Tnni1	ns	-1.742	-1.01	ns						
766	Fndc5	ns	-0.892	-1.009	ns						
767	Egln3	ns	-0.8	-0.934	ns						
768	Adprhl1	ns	-0.586	-0.904	ns					-0.689	
769	Myh7	ns	-1.674	-0.899	ns						
770	Coq10a	ns	-0.956	-0.897	ns						
771	Mreg	ns	-0.913	-0.865	ns						
772	Ankrd2	ns	-1.579	-0.856	ns						
773	Myoz2	ns	-1.711	-0.804	ns						
774	Ldhb	ns	-0.959	-0.783	ns	-0.617				-0.895	
775	Cox7a1	ns	-0.809	-0.778	ns						
776	Vgll2	ns	-1.229	-0.7	ns						
777	Atp5g1	ns	-0.669	-0.653	ns						
778	Fabp3	ns	-0.89	-0.648	ns						
779	Pkd2	ns	1.222	0.644	ns	0.922	1.139			0.681	
780	Bmp1	ns	0.763	0.67	ns		0.732				
781	Nov	ns	1.09	0.733	ns		0.996		1.886	2.742	2.587
782	Fibin	ns	0.804	0.761	ns		1.021				
783	C1s1	ns	0.839	0.809	ns						
784	Islr	ns	0.699	0.825	ns	0.701	1.045				
785	Sh3d19	ns	0.82	0.839	ns	0.603	0.836			1.215	
786	Gfpt2	ns	0.77	0.866	ns		0.735			1.107	
787	Plxdc2	ns	0.782	0.925	ns		0.626				
788	Col15a1	ns	1.182	0.942	ns	1.006	1.174				
789	Mrc2	ns	0.999	0.959	ns		0.887				
790	Trps1	ns	0.957	0.966	ns	0.943	0.813				
791	Pls3	ns	0.651	0.976	ns		0.713				
792	Dcn	ns	0.676	1.023	ns		1.018			4.799	1.347
793	Mmp14	ns	1.287	1.026	ns	0.727	1.110				
794	Lrrn4cl	ns	1.029	1.027	ns		1.098				
795	Pdgfra	ns	1.641	1.057	ns	0.722	0.758			0.854	2.095
796	Col12a1	ns	1.428	1.059	ns	1.287	1.501	1.160			
797	Cdon	ns	1.317	1.125	ns		0.935	0.790			
798	Gem	ns	1.4	1.139	ns	1.102	1.306				
799	Edil3	ns	1.038	1.202	ns	1.225	1.368	1.073			
800	Ssc5d	ns	2.256	1.229	ns						
801	Egfr	ns	1.253	1.237	ns	0.711	0.973			0.859	
802	Sbsn	ns	1.725	1.331	ns		0.975	1.124		1.317	
803	Plod2	ns	1.305	1.34	ns	0.873	1.133			1.316	
804	Sfrp4	ns	0.692	1.342	ns	0.707	0.802	0.657			0.934
805	Tmem119	ns	0.628	1.351	ns		0.713				
806	Fkbp7	ns	0.912	1.353	ns		1.067			1.532	
807	Cd109	ns	0.732	1.363	ns		0.601			0.858	
808	Spon1	ns	0.829	1.407	ns	0.921	1.050				
809	Prelp	ns	1.106	1.44	ns		0.829	1.160		1.143	
810	Matn2	ns	1.998	1.489	ns	1.613	1.802	1.550			
811	Acan	ns	1.306	1.505	ns						
812	Sdc2	ns	0.812	1.755	ns		0.621			0.869	
813	Lum	ns	1.428	2.203	ns	0.872	1.389	1.509		2.566	2.861
814	Abi3bp	ns	1.264	2.207	ns	0.966	1.202	0.995			
815	Prelid2	ns	ns	-3.671	ns						
816	Tmem203	ns	ns	-2.117	ns						
817	Zdhhc23	ns	ns	-2.033	ns						
818	Ctf1	ns	ns	-1.838	ns						
819	Tmem160	ns	ns	-1.787	ns						
820	Cebpb	ns	ns	-1.761	ns						
821	0610040B10Rik	ns	ns	-1.647	ns						
822	Mir690	ns	ns	-1.613	ns						
823	Atp2a2	ns	ns	-1.604	ns						
824	Hsbp1l1	ns	ns	-1.509	ns						
825	Hist2h4	ns	ns	-1.478	ns						
826	Rpl22l1	ns	ns	-1.442	ns						

No.	Gene Name	TC-whole joint				DMM-whole joint			DMM-cartilage		
		1 Day	1 Week	6 Weeks	12 Weeks	2 Weeks	4 Weeks	16 Weeks	1 Week	2 Weeks	6 Weeks
827	Clec2d	ns	ns	-1.44	ns						
828	Mylpf	ns	ns	-1.435	ns						
829	Cox7c	ns	ns	-1.376	ns						
830	Timm8b	ns	ns	-1.364	ns						
831	Mocs3	ns	ns	-1.35	ns						
832	Gm7120	ns	ns	-1.329	ns						
833	Tmem223	ns	ns	-1.272	ns						
834	Malsu1	ns	ns	-1.263	ns						
835	Chchd2	ns	ns	-1.26	ns						
836	Mcat	ns	ns	-1.234	ns						
837	Klhl21	ns	ns	-1.191	ns						
838	Cpeb1	ns	ns	-1.183	ns						
839	Mettl23	ns	ns	-1.162	ns						
840	Snrpg	ns	ns	-1.15	ns						
841	Eif3f	ns	ns	-1.137	ns						
842	Fxyd1	ns	ns	-1.132	ns						
843	Atp5g2	ns	ns	-1.132	ns						
844	Pfn2	ns	ns	-1.128	ns						
845	Tcap	ns	ns	-1.117	ns						
846	Scand1	ns	ns	-1.114	ns						
847	Mtg2	ns	ns	-1.106	ns						
848	Cacng7	ns	ns	-1.064	ns						
849	Fopnl	ns	ns	-1.058	ns						
850	BC018473	ns	ns	-1.04	ns						
851	Sobp	ns	ns	-1.04	ns						
852	Cox5a	ns	ns	-1.033	ns						
853	Sdhb	ns	ns	-1.028	ns						
854	Cln6	ns	ns	-1.007	ns						
855	Dexi	ns	ns	-1.004	ns						
856	Atp5e	ns	ns	-0.999	ns						-1.062
857	Bri3	ns	ns	-0.981	ns						
858	Lars2	ns	ns	-0.976	ns						
859	Uqcr10	ns	ns	-0.973	ns						
860	Klhl30	ns	ns	-0.957	ns						
861	Mcts1	ns	ns	-0.955	ns						
862	Sema6c	ns	ns	-0.943	ns						
863	Ppif	ns	ns	-0.936	ns						
864	Pla2g12a	ns	ns	-0.934	ns						
865	Gyg	ns	ns	-0.93	ns						
866	Gm4980	ns	ns	-0.924	ns						
867	Plekhb1	ns	ns	-0.922	ns						
868	Mgst3	ns	ns	-0.917	ns						
869	Sepw1	ns	ns	-0.895	ns						
870	Otud1	ns	ns	-0.895	ns						
871	Hs3st5	ns	ns	-0.894	ns						
872	Cox6b1	ns	ns	-0.885	ns						
873	Fdx1	ns	ns	-0.884	ns						
874	Mettl20	ns	ns	-0.873	ns						
875	2610035D17Rik	ns	ns	-0.87	ns						
876	Mrpl44	ns	ns	-0.839	ns						
877	Cfl2	ns	ns	-0.837	ns						
878	N6amt2	ns	ns	-0.835	ns						
879	Bcat2	ns	ns	-0.834	ns						-0.986
880	Eif1b	ns	ns	-0.825	ns						
881	Tst	ns	ns	-0.823	ns						
882	Ndufb8	ns	ns	-0.82	ns						
883	Atp5g3	ns	ns	-0.814	ns						
884	Saysd1	ns	ns	-0.811	ns						
885	Plekhb2	ns	ns	-0.809	ns						
886	Thnsl2	ns	ns	-0.799	ns						
887	Siah1a	ns	ns	-0.796	ns						
888	Cox8b	ns	ns	-0.788	ns						
889	Fzd9	ns	ns	-0.785	ns						
890	Map1lc3a	ns	ns	-0.783	ns						

No.	Gene Name	TC-whole joint				DMM-whole joint			DMM-cartilage		
		1 Day	1 Week	6 Weeks	12 Weeks	2 Weeks	4 Weeks	16 Weeks	1 Week	2 Weeks	6 Weeks
891	2810428I15Rik	ns	ns	-0.782	ns						
892	Samm50	ns	ns	-0.782	ns						
893	Dusp18*	ns	ns	-0.774	ns	0.967	1.140				
894	Gpt	ns	ns	-0.768	ns						
895	Yars2	ns	ns	-0.727	ns						
896	Ldha	ns	ns	-0.726	ns						
897	Ndufa1	ns	ns	-0.718	ns						
898	Atp5j2	ns	ns	-0.716	ns						
899	Metrn	ns	ns	-0.698	ns						
900	Tmem126a	ns	ns	-0.698	ns						
901	Bcam	ns	ns	-0.695	ns						
902	Hspb8	ns	ns	-0.692	ns						
903	Pdgfa*	ns	ns	-0.69	ns		0.642				
904	Ech1	ns	ns	-0.686	ns						
905	Ppara	ns	ns	-0.685	ns						
906	Rangrf	ns	ns	-0.68	ns						
907	Mcee	ns	ns	-0.68	ns						
908	Rapsn	ns	ns	-0.677	ns						
909	Twf2	ns	ns	-0.67	ns						
910	Phpt1	ns	ns	-0.66	ns						
911	Neurl1a	ns	ns	-0.657	ns						
912	St3gal3	ns	ns	-0.655	ns						
913	Fam131b	ns	ns	-0.649	ns						
914	Ndufb3	ns	ns	-0.64	ns						
915	Coq3	ns	ns	-0.638	ns						
916	Casq2	ns	ns	-0.633	ns						
917	Dusp13	ns	ns	-0.624	ns						
918	Ndufa2	ns	ns	-0.617	ns						
919	2610306M01Rik	ns	ns	-0.616	ns						
920	Acadvl	ns	ns	-0.604	ns						
921	Clip4*	ns	ns	-0.597	ns	1.005	0.991	1.040			
922	Popdc2	ns	ns	-0.595	ns						
923	Npepl1	ns	ns	-0.592	ns						-1.328
924	Mrpl4	ns	ns	-0.591	ns						
925	Bckdha	ns	ns	-0.581	ns						
926	Col1a2	ns	ns	0.599	ns		1.040				
927	Wdr76	ns	ns	0.601	ns						
928	Hnrnpa1	ns	ns	0.602	ns						
929	Pth1r	ns	ns	0.619	ns						
930	Slc37a2	ns	ns	0.627	ns						
931	Tbc1d23	ns	ns	0.649	ns						
932	Gpr65	ns	ns	0.652	ns						
933	Rnase6	ns	ns	0.679	ns						
934	Acpp	ns	ns	0.694	ns						
935	Alpl	ns	ns	0.701	ns						
936	Strn	ns	ns	0.714	ns						1.081
937	Zwilch	ns	ns	0.72	ns						
938	Mepe	ns	ns	0.725	ns						
939	Atp11b	ns	ns	0.726	ns						
940	Cp	ns	ns	0.731	ns						
941	Cdc40	ns	ns	0.737	ns						
942	Tnfrsf13c	ns	ns	0.738	ns						
943	Fbxo11	ns	ns	0.738	ns						
944	Adamts2	ns	ns	0.745	ns		0.941				
945	Vangl1	ns	ns	0.761	ns						
946	Col11a2	ns	ns	0.764	ns						
947	Brip1	ns	ns	0.764	ns						
948	Serpinf1	ns	ns	0.771	ns		0.771				
949	Cyp1b1	ns	ns	0.775	ns						
950	Brca2	ns	ns	0.777	ns						
951	Usp32	ns	ns	0.779	ns						
952	Ctsk	ns	ns	0.781	ns						
953	Lin9	ns	ns	0.785	ns						
954	Mb21d1	ns	ns	0.787	ns						

No.	Gene Name	TC-whole joint				DMM-whole joint			DMM-cartilage		
		1 Day	1 Week	6 Weeks	12 Weeks	2 Weeks	4 Weeks	16 Weeks	1 Week	2 Weeks	6 Weeks
955	Casp8	ns	ns	0.788	ns						
956	Supt16	ns	ns	0.79	ns						
957	Col1a1	ns	ns	0.814	ns		0.778				
958	Ddr2	ns	ns	0.816	ns		0.625				0.994
959	Creb3l1	ns	ns	0.817	ns		0.637				
960	Ypel4	ns	ns	0.858	ns						
961	Tmem154	ns	ns	0.859	ns						
962	Cdh2	ns	ns	0.869	ns						
963	Mbd4	ns	ns	0.871	ns						
964	Zfp189	ns	ns	0.879	ns						
965	Dapp1	ns	ns	0.886	ns						
966	BC027231	ns	ns	0.89	ns						
967	Zfp780b	ns	ns	0.892	ns						
968	Mrc1	ns	ns	0.894	ns						
969	Snx22	ns	ns	0.899	ns						
970	Zfp451	ns	ns	0.9	ns						1.060
971	Bbx	ns	ns	0.901	ns						
972	Rbmx2	ns	ns	0.901	ns						
973	Zdhhc20	ns	ns	0.904	ns		0.594				
974	Sgms2	ns	ns	0.905	ns						
975	Smpd3	ns	ns	0.921	ns						
976	Kif4	ns	ns	0.924	ns						
977	Col9a2	ns	ns	0.924	ns						
978	Gabbr1	ns	ns	0.925	ns						
979	Chd1	ns	ns	0.928	ns						
980	Far1	ns	ns	0.932	ns						
981	Siglecg	ns	ns	0.932	ns						
982	Epb4.1l5	ns	ns	0.933	ns						
983	AI504432	ns	ns	0.942	ns						
984	Diap3	ns	ns	0.944	ns						
985	Phf3	ns	ns	0.944	ns						
986	Adam10	ns	ns	0.948	ns						
987	Btla	ns	ns	0.96	ns						
988	Fgl2	ns	ns	0.962	ns						
989	Nipbl	ns	ns	0.969	ns						
990	Calhm2	ns	ns	0.972	ns						
991	Pkhd1l1	ns	ns	0.972	ns						
992	Tlr4	ns	ns	0.973	ns						0.836
993	Ptprd*	ns	ns	0.973	ns		-0.932				
994	Itih5	ns	ns	0.976	ns						
995	Nin	ns	ns	0.981	ns						
996	Hsp90b1	ns	ns	0.982	ns						
997	Sec62	ns	ns	0.988	ns						
998	Dmkn	ns	ns	0.988	ns						
999	Bglap	ns	ns	0.989	ns						
1000	Polq	ns	ns	0.994	ns						
1001	Pls1	ns	ns	0.995	ns						
1002	Cnpy4	ns	ns	1.003	ns						
1003	Fam76b	ns	ns	1.007	ns						
1004	Mdm4	ns	ns	1.014	ns						
1005	Rab44	ns	ns	1.016	ns						
1006	Vipas39	ns	ns	1.018	ns						
1007	Cstf3	ns	ns	1.022	ns						
1008	Smchd1	ns	ns	1.024	ns						
1009	Atad5	ns	ns	1.038	ns						
1010	Rel	ns	ns	1.045	ns						
1011	Suco	ns	ns	1.046	ns						
1012	Col9a3	ns	ns	1.05	ns						
1013	Fam45a	ns	ns	1.052	ns						
1014	Twf1	ns	ns	1.053	ns		0.590				
1015	Zfp65	ns	ns	1.056	ns						
1016	Sema3a	ns	ns	1.058	ns		0.635				
1017	Zc3hav1	ns	ns	1.061	ns						
1018	Arhgap11a	ns	ns	1.062	ns						

111

No.	Gene Name	TC-whole joint				DMM-whole joint			DMM-cartilage		
		1 Day	1 Week	6 Weeks	12 Weeks	2 Weeks	4 Weeks	16 Weeks	1 Week	2 Weeks	6 Weeks
1019	Ccnt2	ns	ns	1.062	ns						
1020	Mettl14	ns	ns	1.062	ns						
1021	Dock11	ns	ns	1.063	ns						
1022	Nucb2	ns	ns	1.073	ns						
1023	Mamdc2	ns	ns	1.081	ns		1.014				
1024	Atad2	ns	ns	1.081	ns						
1025	Fyb	ns	ns	1.088	ns						
1026	Galnt7	ns	ns	1.093	ns						0.797
1027	Mmrn1	ns	ns	1.099	ns						
1028	Crispld1	ns	ns	1.103	ns						
1029	Smek2	ns	ns	1.104	ns						
1030	Rnasel	ns	ns	1.105	ns						
1031	Runx1	ns	ns	1.108	ns	0.767	0.917				
1032	Lyve1	ns	ns	1.111	ns						
1033	Fam46a	ns	ns	1.111	ns						
1034	Zgrf1	ns	ns	1.113	ns						
1035	Shox2	ns	ns	1.115	ns		0.599				
1036	Il18r1	ns	ns	1.116	ns						
1037	Kif11	ns	ns	1.119	ns						
1038	Gja1	ns	ns	1.12	ns		0.790				1.765
1039	Stat4	ns	ns	1.124	ns						
1040	Gp49a	ns	ns	1.127	ns						
1041	Dtl	ns	ns	1.135	ns						
1042	Brca1	ns	ns	1.138	ns						
1043	B3gnt5	ns	ns	1.145	ns						
1044	F13a1	ns	ns	1.146	ns						1.531
1045	Phc3	ns	ns	1.148	ns						
1046	Arid4a	ns	ns	1.151	ns						
1047	Rbm27	ns	ns	1.154	ns						
1048	Cdh11	ns	ns	1.155	ns						
1049	Pola1	ns	ns	1.156	ns						
1050	Tpx2	ns	ns	1.157	ns						
1051	Myo5a	ns	ns	1.157	ns		0.586				
1052	Nupr1	ns	ns	1.16	ns		1.172				
1053	Ptprc	ns	ns	1.162	ns						
1054	Ranbp2	ns	ns	1.163	ns						
1055	Exo1	ns	ns	1.168	ns						
1056	Cd84	ns	ns	1.169	ns						
1057	Mpp7	ns	ns	1.175	ns						
1058	Stk3	ns	ns	1.18	ns						0.741
1059	Ccdc174	ns	ns	1.188	ns						
1060	Lair1	ns	ns	1.192	ns						
1061	Ckap2l	ns	ns	1.195	ns						
1062	Fmr1	ns	ns	1.196	ns						
1063	Hmmr	ns	ns	1.203	ns						
1064	Dzip3	ns	ns	1.205	ns						
1065	Rapgef6	ns	ns	1.206	ns						
1066	Lyst	ns	ns	1.212	ns						
1067	Sparc	ns	ns	1.222	ns						
1068	Zcchc6	ns	ns	1.222	ns						
1069	Ankrd12	ns	ns	1.223	ns						1.026
1070	Arap2	ns	ns	1.225	ns						
1071	Aim2	ns	ns	1.238	ns						
1072	Cd33	ns	ns	1.242	ns						
1073	Setd2	ns	ns	1.248	ns						0.713
1074	Dock7	ns	ns	1.251	ns						
1075	Trim58	ns	ns	1.252	ns						
1076	Skil	ns	ns	1.253	ns						
1077	Zscan26	ns	ns	1.259	ns						
1078	Angpt2	ns	ns	1.264	ns						
1079	Gbp7	ns	ns	1.264	ns						
1080	C1ra	ns	ns	1.266	ns		0.899				
1081	Suv39h2	ns	ns	1.268	ns						
1082	Gal3st4	ns	ns	1.276	ns						

No.	Gene Name	TC-whole joint				DMM-whole joint			DMM-cartilage		
		1 Day	1 Week	6 Weeks	12 Weeks	2 Weeks	4 Weeks	16 Weeks	1 Week	2 Weeks	6 Weeks
1083	Nusap1	ns	ns	1.276	ns						
1084	Cep152	ns	ns	1.277	ns						
1085	Zfp608	ns	ns	1.282	ns						
1086	Cep170	ns	ns	1.289	ns						
1087	F5	ns	ns	1.291	ns						0.767
1088	Dennd4a	ns	ns	1.293	ns						
1089	Tnfrsf11b	ns	ns	1.298	ns						
1090	Safb2	ns	ns	1.3	ns						
1091	Emp3	ns	ns	1.301	ns						
1092	Tmem184c	ns	ns	1.302	ns						
1093	Col11a1	ns	ns	1.303	ns						
1094	Top2a	ns	ns	1.305	ns						
1095	Ccdc55	ns	ns	1.307	ns						0.694
1096	Thoc2	ns	ns	1.308	ns						
1097	Cybb	ns	ns	1.31	ns						
1098	Ppil4	ns	ns	1.317	ns						
1099	Zfp263	ns	ns	1.321	ns						
1100	Casc5	ns	ns	1.323	ns						
1101	Akna*	ns	ns	1.323	ns	-0.595					
1102	Cep192	ns	ns	1.323	ns						
1103	Ncapd3	ns	ns	1.332	ns						
1104	Apol11a	ns	ns	1.338	ns						
1105	Map3k8	ns	ns	1.344	ns						
1106	Parp14	ns	ns	1.345	ns						
1107	Col22a1	ns	ns	1.352	ns		0.846				
1108	Ceacam1	ns	ns	1.354	ns						
1109	Cep162	ns	ns	1.357	ns						
1110	Golim4	ns	ns	1.36	ns						
1111	Dock10	ns	ns	1.366	ns						
1112	Gimap3	ns	ns	1.372	ns						
1113	Wrn	ns	ns	1.374	ns						
1114	Gcc2	ns	ns	1.38	ns						
1115	Clec3a	ns	ns	1.387	ns						
1116	Iqgap2	ns	ns	1.388	ns						
1117	Susd5	ns	ns	1.392	ns						
1118	Cep70	ns	ns	1.394	ns						
1119	Cntrl	ns	ns	1.405	ns						
1120	Ddx60	ns	ns	1.411	ns						
1121	Smc4	ns	ns	1.423	ns						
1122	Taf1	ns	ns	1.424	ns						
1123	Ndc80	ns	ns	1.424	ns						
1124	Jmjd1c	ns	ns	1.426	ns						
1125	Primpol	ns	ns	1.432	ns						
1126	Hmgn3	ns	ns	1.432	ns						1.097
1127	Ccdc88a	ns	ns	1.433	ns						
1128	Hemgn	ns	ns	1.441	ns						
1129	Igsf6	ns	ns	1.446	ns						
1130	Treml2	ns	ns	1.447	ns						
1131	Aspm	ns	ns	1.454	ns						
1132	Hirip3	ns	ns	1.456	ns						
1133	nsun6	ns	ns	1.458	ns						
1134	Mis18bp1	ns	ns	1.465	ns						
1135	Gm1966	ns	ns	1.472	ns						
1136	Spp1	ns	ns	1.481	ns						
1137	Cd300lf	ns	ns	1.494	ns						
1138	Cpne3	ns	ns	1.507	ns						1.529
1139	Il7r	ns	ns	1.51	ns						
1140	Eif2ak2	ns	ns	1.521	ns		0.687				
1141	Pla2g4a	ns	ns	1.533	ns						0.884
1142	Ccar1	ns	ns	1.536	ns						
1143	Apobr	ns	ns	1.545	ns						
1144	Cenpf	ns	ns	1.558	ns						
1145	Cep55	ns	ns	1.565	ns						
1146	Cfh	ns	ns	1.573	ns						

No.	Gene Name	TC-whole joint				DMM-whole joint			DMM-cartilage		
		1 Day	1 Week	6 Weeks	12 Weeks	2 Weeks	4 Weeks	16 Weeks	1 Week	2 Weeks	6 Weeks
1147	Mmp13	ns	ns	1.573	ns		0.851				
1148	Kif20b	ns	ns	1.576	ns						
1149	Stfa2l1	ns	ns	1.579	ns						
1150	Cd300ld	ns	ns	1.586	ns						
1151	Ccp110	ns	ns	1.595	ns						
1152	Mastl	ns	ns	1.6	ns						
1153	Chml	ns	ns	1.602	ns						
1154	Col2a1	ns	ns	1.607	ns						
1155	Gramd1c	ns	ns	1.616	ns						
1156	Cep135	ns	ns	1.629	ns						
1157	Lilrb4	ns	ns	1.658	ns						
1158	Dmp1	ns	ns	1.668	ns						
1159	1700112E06Rik	ns	ns	1.676	ns						
1160	Cenpj	ns	ns	1.691	ns						
1161	Bex6	ns	ns	1.697	ns						
1162	Gm11974	ns	ns	1.706	ns						
1163	Colec12	ns	ns	1.722	ns		0.833				
1164	Fap	ns	ns	1.734	ns		0.889				
1165	Spta1	ns	ns	1.781	ns						
1166	Snai2	ns	ns	1.802	ns		0.785				
1167	Blm	ns	ns	1.802	ns						3.125
1168	E330020D12Rik	ns	ns	1.807	ns						
1169	Mki67	ns	ns	1.822	ns						
1170	Ibsp	ns	ns	1.863	ns		0.758				
1171	Atp6v0d2	ns	ns	1.881	ns						
1172	Serpini1	ns	ns	1.921	ns						1.212
1173	Dio2	ns	ns	1.947	ns		0.686				
1174	Kif15	ns	ns	1.983	ns						
1175	Cenpe	ns	ns	2.241	ns						
1176	Gm9079	ns	ns	2.81	ns						
1177	Sned1	ns	ns	10.904	ns	0.771	1.448				
1178	Esrrg	ns	-1.526	ns	ns						
1179	Ckmt2	ns	-1.3	ns	ns						
1180	Smtnl1	ns	-1.255	ns	ns						
1181	Nos1	ns	-1.082	ns	ns						
1182	Actn2	ns	-1.056	ns	ns						
1183	Xirp1	ns	-1.034	ns	ns						
1184	Hspa1l	ns	-1.01	ns	ns						
1185	1810044D09Rik	ns	-1.007	ns	ns						
1186	Plet1os	ns	-0.988	ns	ns						
1187	Mb	ns	-0.977	ns	ns					-1.820	
1188	Dusp26	ns	-0.971	ns	ns						
1189	Asb5	ns	-0.887	ns	ns						
1190	Cidec	ns	-0.862	ns	ns	-1.271	-1.009				
1191	B330016D10Rik	ns	-0.85	ns	ns						
1192	Lmcd1	ns	-0.845	ns	ns						
1193	Kcna7	ns	-0.839	ns	ns						
1194	Hspb6	ns	-0.832	ns	ns						
1195	Alpk3	ns	-0.831	ns	ns						
1196	Fhl1	ns	-0.812	ns	ns						
1197	Lmod3	ns	-0.799	ns	ns						
1198	Nrap	ns	-0.797	ns	ns						
1199	Mapt	ns	-0.77	ns	ns						
1200	Ppargc1a	ns	-0.766	ns	ns						
1201	A930003A15Rik	ns	-0.752	ns	ns						
1202	Asb12	ns	-0.745	ns	ns						
1203	3425401B19Rik	ns	-0.735	ns	ns						
1204	Angptl7	ns	-0.722	ns	ns				-1.695		
1205	Myot	ns	-0.704	ns	ns						
1206	Usp13	ns	-0.704	ns	ns						
1207	Fam13a	ns	-0.701	ns	ns						
1208	Ugp2	ns	-0.697	ns	ns						
1209	Asb11	ns	-0.694	ns	ns						
1210	Rbm20	ns	-0.692	ns	ns						

No.	Gene Name	TC-whole joint				DMM-whole joint			DMM-cartilage		
		1 Day	1 Week	6 Weeks	12 Weeks	2 Weeks	4 Weeks	16 Weeks	1 Week	2 Weeks	6 Weeks
1211	Kbtbd13	ns	-0.687	ns	ns						
1212	Cox6a2	ns	-0.68	ns	ns					-2.204	
1213	Adssl1	ns	-0.674	ns	ns						
1214	Pm20d2	ns	-0.671	ns	ns						
1215	Adck3	ns	-0.67	ns	ns						
1216	Mlxipl	ns	-0.669	ns	ns						
1217	Ifitm5	ns	-0.669	ns	ns						
1218	Atp1a2	ns	-0.666	ns	ns					-1.075	
1219	Lrrc14b	ns	-0.662	ns	ns						
1220	Padi2	ns	-0.658	ns	ns				-2.928	-3.742	
1221	Ppp1r1a	ns	-0.657	ns	ns						
1222	Homer2	ns	-0.655	ns	ns						
1223	Asb2	ns	-0.65	ns	ns						
1224	Mgmt	ns	-0.644	ns	ns						
1225	Slc2a4	ns	-0.642	ns	ns					-2.034	
1226	Got1	ns	-0.641	ns	ns						
1227	Unc45b	ns	-0.636	ns	ns						
1228	Tdrp	ns	-0.636	ns	ns						
1229	Vegfb	ns	-0.634	ns	ns					-0.745	
1230	Slc9a2	ns	-0.63	ns	ns						
1231	Ppp1r3c	ns	-0.629	ns	ns					-3.235	
1232	Tpm2	ns	-0.627	ns	ns					-0.687	
1233	E2f6	ns	-0.625	ns	ns						
1234	Slc38a3	ns	-0.625	ns	ns					-1.094	
1235	Myom3	ns	-0.618	ns	ns						
1236	Srl	ns	-0.611	ns	ns						
1237	Prob1	ns	-0.61	ns	ns						
1238	Mtfp1	ns	-0.609	ns	ns						
1239	Magix	ns	-0.607	ns	ns						
1240	Lynx1	ns	-0.604	ns	ns				-0.671	-1.230	
1241	Myl1	ns	-0.604	ns	ns						
1242	Eci1	ns	-0.603	ns	ns						
1243	Tpd52l1	ns	-0.602	ns	ns						
1244	Mdh1	ns	-0.601	ns	ns						
1245	Fam57b	ns	-0.599	ns	ns						
1246	Lipc	ns	-0.596	ns	ns	-0.640					
1247	Zswim7	ns	-0.593	ns	ns						
1248	St8sia5	ns	-0.592	ns	ns						
1249	Pfkm	ns	-0.592	ns	ns					-0.846	
1250	Mylk2	ns	-0.591	ns	ns						
1251	Txlnb	ns	-0.589	ns	ns						
1252	Fam134b	ns	-0.587	ns	ns						
1253	Lpl	ns	-0.586	ns	ns						
1254	Bglap2	ns	-0.585	ns	ns						
1255	Fbp2	ns	-0.585	ns	ns						
1256	Clic5	ns	-0.583	ns	ns						
1257	Acacb	ns	-0.582	ns	ns				-0.981	-1.572	
1258	Ephb4	ns	0.592	ns	ns					0.619	
1259	Trim2	ns	0.594	ns	ns		0.647				
1260	Rbfox2	ns	0.597	ns	ns		0.717				
1261	Crip2	ns	0.597	ns	ns						
1262	Pik3r3	ns	0.6	ns	ns		0.615				
1263	Zfp9	ns	0.607	ns	ns		0.754			0.710	
1264	Gale	ns	0.607	ns	ns						
1265	Ddah2	ns	0.608	ns	ns						
1266	Sesn3	ns	0.609	ns	ns		0.610				
1267	Sfxn3	ns	0.609	ns	ns	0.642	0.687				
1268	Twist1	ns	0.61	ns	ns				1.056	1.537	
1269	Cdkn1c	ns	0.611	ns	ns						
1270	Ppapdc1b	ns	0.621	ns	ns						
1271	Slc39a13	ns	0.623	ns	ns						
1272	Lhfp	ns	0.625	ns	ns		0.705			1.435	
1273	Fam102b	ns	0.625	ns	ns						
1274	Tmem158	ns	0.625	ns	ns						

No.	Gene Name	TC-whole joint				DMM-whole joint			DMM-cartilage		
		1 Day	1 Week	6 Weeks	12 Weeks	2 Weeks	4 Weeks	16 Weeks	1 Week	2 Weeks	6 Weeks
1275	Gstm2	ns	0.626	ns	ns						
1276	Tmem263	ns	0.627	ns	ns						
1277	Pam	ns	0.63	ns	ns						
1278	Mex3b	ns	0.63	ns	ns	0.826	0.938				
1279	Sash1	ns	0.633	ns	ns		0.733				
1280	Vkorc1	ns	0.633	ns	ns		0.688				
1281	Ehd2	ns	0.635	ns	ns		0.632				
1282	Emp2	ns	0.642	ns	ns	0.591	0.630				
1283	Ccdc122	ns	0.648	ns	ns						
1284	Tram2	ns	0.649	ns	ns						
1285	Col4a1	ns	0.653	ns	ns		1.091		1.233		
1286	Col4a2	ns	0.653	ns	ns		1.129			0.690	
1287	1500015O10Rik	ns	0.654	ns	ns					1.160	
1288	Plekhg5	ns	0.654	ns	ns						
1289	Ralgds	ns	0.654	ns	ns	0.590				0.982	
1290	Cgnl1	ns	0.656	ns	ns					1.078	
1291	Dkk2	ns	0.657	ns	ns		0.857		1.013		
1292	Fkbp9	ns	0.66	ns	ns		0.766				
1293	Smo	ns	0.661	ns	ns		0.962				
1294	Ldlrad4	ns	0.662	ns	ns						
1295	Igfbp5	ns	0.663	ns	ns						
1296	Phldb1	ns	0.665	ns	ns						
1297	Rhoj	ns	0.672	ns	ns		0.715				
1298	Mcam	ns	0.675	ns	ns				1.599	2.199	
1299	Rbp4	ns	0.682	ns	ns						
1300	Mageh1	ns	0.683	ns	ns						
1301	Mgp	ns	0.684	ns	ns					3.777	
1302	Kirrel	ns	0.686	ns	ns		0.652				
1303	Tlr3	ns	0.687	ns	ns				0.687		
1304	Soga1	ns	0.688	ns	ns						
1305	Rgs4	ns	0.69	ns	ns		0.819				
1306	Prdm5	ns	0.69	ns	ns		1.061				
1307	Flrt2	ns	0.691	ns	ns		0.874				
1308	Plekhf1	ns	0.691	ns	ns						
1309	Mras	ns	0.692	ns	ns				0.948	0.612	
1310	Slitrk6	ns	0.692	ns	ns		0.733		2.011	1.776	
1311	Ubtd2	ns	0.692	ns	ns	0.731	0.999				
1312	Crtap	ns	0.694	ns	ns						
1313	Fam198b	ns	0.695	ns	ns		0.682				
1314	Spats2l	ns	0.696	ns	ns	1.100	0.812				
1315	Armcx1	ns	0.697	ns	ns		0.653				
1316	Copz2	ns	0.698	ns	ns		0.823				
1317	Crispld2	ns	0.699	ns	ns	0.975	1.057			1.294	
1318	Lamc1	ns	0.701	ns	ns	0.770	0.700				
1319	Igfbp6	ns	0.703	ns	ns		0.666				
1320	Rftn2	ns	0.703	ns	ns		0.883				
1321	Ston1	ns	0.704	ns	ns		0.617				
1322	Dact1	ns	0.705	ns	ns		0.646				
1323	Ism1	ns	0.707	ns	ns		0.817				
1324	Slco2a1	ns	0.71	ns	ns					1.216	
1325	Pkn3	ns	0.711	ns	ns						
1326	Tspan2	ns	0.73	ns	ns	0.701	0.823			2.268	
1327	Creb3l2	ns	0.731	ns	ns	0.615	0.734				
1328	Anxa5	ns	0.734	ns	ns		0.651		0.861	0.752	
1329	Cercam	ns	0.739	ns	ns						
1330	Nova1	ns	0.74	ns	ns						
1331	Igfbp4	ns	0.748	ns	ns						
1332	Ntn1	ns	0.749	ns	ns					1.352	
1333	Arhgef40	ns	0.751	ns	ns						
1334	Triqk	ns	0.752	ns	ns						
1335	Ooep	ns	0.755	ns	ns						
1336	nsmf	ns	0.758	ns	ns						
1337	Adamtsl4	ns	0.759	ns	ns	0.658	0.609				
1338	Hebp2	ns	0.762	ns	ns					1.509	

No.	Gene Name	TC-whole joint				DMM-whole joint			DMM-cartilage		
		1 Day	1 Week	6 Weeks	12 Weeks	2 Weeks	4 Weeks	16 Weeks	1 Week	2 Weeks	6 Weeks
1339	Tmem47	ns	0.774	ns	ns	0.673	0.894				
1340	Srpx	ns	0.775	ns	ns		0.758				
1341	Gstt3	ns	0.777	ns	ns		0.596				
1342	Ednra	ns	0.777	ns	ns	0.762	1.364				
1343	Gxylt2	ns	0.78	ns	ns		0.947				
1344	Vasn	ns	0.78	ns	ns	0.613	0.871		0.834	0.885	
1345	Gpx8	ns	0.788	ns	ns		0.725				
1346	Fam167a	ns	0.788	ns	ns		0.905				
1347	Errfi1	ns	0.789	ns	ns		1.020		2.585	2.418	
1348	Myadm	ns	0.789	ns	ns	0.626	0.629			0.795	
1349	Hspg2	ns	0.791	ns	ns	0.774	0.889				
1350	Fndc3b	ns	0.792	ns	ns		0.732			1.058	
1351	Lhfpl2	ns	0.794	ns	ns		0.592				
1352	Igfbp3	ns	0.795	ns	ns	0.955	1.279				
1353	Nid1	ns	0.804	ns	ns		0.593			1.044	
1354	S1pr2	ns	0.805	ns	ns						
1355	Serf1	ns	0.808	ns	ns		0.635				
1356	Mdk	ns	0.817	ns	ns	0.589	0.668				
1357	Lrrc49	ns	0.822	ns	ns		0.625				
1358	Rtkn	ns	0.823	ns	ns						
1359	Atp8b2	ns	0.826	ns	ns		0.695				
1360	Lix1l	ns	0.827	ns	ns	0.756	0.844				
1361	Tnc	ns	0.829	ns	ns		0.618				
1362	Dlg4	ns	0.84	ns	ns	0.598					
1363	Slc7a2	ns	0.851	ns	ns	1.133	1.203			1.910	
1364	Rbms3	ns	0.853	ns	ns		0.597				
1365	Nid2	ns	0.854	ns	ns		0.952		0.883		
1366	Parva	ns	0.856	ns	ns	0.759	0.663		0.682	0.877	
1367	Rhbdf1	ns	0.86	ns	ns						
1368	Spats2	ns	0.861	ns	ns	0.616					
1369	Klhl13	ns	0.869	ns	ns		1.311				
1370	B3gnt9	ns	0.875	ns	ns						
1371	Lpar1	ns	0.877	ns	ns	0.665	0.865				
1372	Cemip	ns	0.882	ns	ns						
1373	Tsku	ns	0.885	ns	ns		0.705				
1374	2610203C20Rik	ns	0.892	ns	ns	0.681	0.834				
1375	Sema3c	ns	0.899	ns	ns		0.616			0.909	
1376	Sh3pxd2b	ns	0.9	ns	ns		0.769				
1377	Pdgfc	ns	0.903	ns	ns	0.590	0.632		1.419	1.770	
1378	Rin2	ns	0.906	ns	ns					1.835	
1379	Farp1	ns	0.914	ns	ns		0.678				
1380	Cdr2l	ns	0.915	ns	ns		0.588				
1381	Gpc6	ns	0.919	ns	ns						
1382	Boc	ns	0.923	ns	ns						
1383	Slc2a13	ns	0.929	ns	ns		0.896				
1384	Arhgef25	ns	0.93	ns	ns						
1385	Cspg4	ns	0.936	ns	ns			0.643			
1386	Fzd6	ns	0.941	ns	ns	0.875	0.904				
1387	Procr	ns	0.942	ns	ns		0.708			1.038	
1388	Arhgap42	ns	0.944	ns	ns	0.630	0.791				
1389	Spaca6	ns	0.953	ns	ns						
1390	9230110C19Rik	ns	0.964	ns	ns						
1391	Fzd8	ns	0.971	ns	ns	0.969	0.623				
1392	Ackr3	ns	0.972	ns	ns						
1393	Cys1	ns	0.973	ns	ns						
1394	H19	ns	0.98	ns	ns	1.425	1.679				
1395	L3hypdh	ns	0.996	ns	ns						
1396	Fkbp14	ns	0.997	ns	ns	0.711	1.098		0.675	0.621	
1397	Peg3	ns	1.001	ns	ns		0.868				
1398	Ltbp3	ns	1.006	ns	ns	0.921	0.837		1.275	0.973	
1399	Mtmr11	ns	1.014	ns	ns	1.087	1.119				
1400	Ndufa4l2	ns	1.016	ns	ns						
1401	Scarf2	ns	1.024	ns	ns	0.652	0.786				
1402	Fmod	ns	1.025	ns	ns	1.060	1.445	1.562			

No.	Gene Name	TC-whole joint				DMM-whole joint			DMM-cartilage		
		1 Day	1 Week	6 Weeks	12 Weeks	2 Weeks	4 Weeks	16 Weeks	1 Week	2 Weeks	6 Weeks
1403	Nlgn2	ns	1.03	ns	ns						
1404	Zfp521	ns	1.035	ns	ns	0.914	1.137				
1405	Ppic	ns	1.035	ns	ns	0.718	0.899				
1406	Zfp354c	ns	1.043	ns	ns	0.887	1.110				
1407	Spsb1	ns	1.062	ns	ns	0.736	0.948		1.303	1.226	
1408	Sec16b	ns	1.079	ns	ns		0.943				
1409	Timp2	ns	1.082	ns	ns	0.868	0.841				
1410	Tfpi2	ns	1.083	ns	ns		1.099				
1411	Lpar4	ns	1.084	ns	ns		0.899				
1412	Slc2a10	ns	1.092	ns	ns	0.599	0.846			1.502	
1413	Sox9	ns	1.099	ns	ns					0.979	
1414	Pdgfrl	ns	1.125	ns	ns	0.961	1.290			0.791	
1415	Htra3	ns	1.127	ns	ns		0.995		1.603	1.367	
1416	Ogn	ns	1.129	ns	ns						
1417	Cd276	ns	1.133	ns	ns		0.679				
1418	Pkd1	ns	1.147	ns	ns	0.731	0.747				
1419	Fgf14	ns	1.162	ns	ns						
1420	Igf2	ns	1.184	ns	ns	0.708					
1421	Pitx1	ns	1.185	ns	ns						
1422	Olfml1	ns	1.198	ns	ns		0.754				
1423	Gas1	ns	1.257	ns	ns						
1424	Plagl1	ns	1.272	ns	ns						
1425	Nr4a2	ns	1.283	ns	ns	1.529	2.246			1.997	
1426	Robo1	ns	1.293	ns	ns		1.227				
1427	Itga11	ns	1.311	ns	ns						
1428	Kera	ns	1.327	ns	ns		1.886				
1429	Cpxm2	ns	1.336	ns	ns	1.160	1.355				
1430	Dnm1	ns	1.39	ns	ns	0.595	0.667				
1431	C1qtnf1	ns	1.437	ns	ns	0.941	1.216				
1432	Col8a2	ns	1.449	ns	ns	1.313	1.738				
1433	Chsy3	ns	1.465	ns	ns	1.117	0.869				
1434	Matn4	ns	1.469	ns	ns		0.987				
1435	Spon2	ns	1.481	ns	ns	0.862	0.789		0.984	1.073	
1436	Cpxm1	ns	1.502	ns	ns	0.756	1.012				
1437	Mfap2	ns	1.56	ns	ns		0.921				
1438	Rspo2	ns	1.562	ns	ns		0.924				
1439	Itm2a	ns	1.607	ns	ns	1.133	1.239				
1440	Tnmd	ns	1.832	ns	ns	1.873	2.136	1.916			
1441	Piezo2	ns	2.01	ns	ns						
1442	Ptgs2	ns	2.01	ns	ns		1.724		3.632	3.770	
1443	Fam180a	ns	2.072	ns	ns						
1444	Fbn2	ns	2.503	ns	ns	1.591	1.555				
1445	Moxd1	ns	2.79	ns	ns	1.780	1.420		1.926	1.277	
1446	Agtr2	ns	3.75	ns	ns		1.048		0.801		

Supplementary Table S2. Transcriptional expression overlap between our TC data and published data derived from human OA biopsies including: articular cartilage, osteophyte (calcified cartilage), synovium, meniscus and subchondral bone. Values represented are log2 fold changes.

Up - Regulated   Down - Regulated   *ns* = nonsignificant

No.	Gene Name	TC (mouse) 1 Day	1 Week	6 Weeks	12 Weeks	OA (human) Synovium	Osteophyte	Tibia Lateral	Medial	Cartilage	Meniscus
1	*Fyb*	*ns*	*ns*	1.088	*ns*		*ns*	*ns*	*ns*	*ns*	*ns*
2	*Cd68*	0.591	*ns*	*ns*	*ns*		*ns*	*ns*	*ns*	*ns*	*ns*
3	*Pla2g4a*	*ns*	*ns*	1.533	*ns*		*ns*	*ns*	*ns*	*ns*	*ns*
4	*Lilrb4*	*ns*	*ns*	1.658	*ns*		*ns*	*ns*	*ns*	*ns*	*ns*
5	*Fcgr2b*	0.83	*ns*	0.991	*ns*		*ns*	*ns*	*ns*	*ns*	*ns*
6	*Tsku*	*ns*	0.885	*ns*	*ns*		*ns*	*ns*	*ns*	*ns*	*ns*
7	*Gfpt2*	*ns*	0.77	0.866	*ns*		*ns*	*ns*	*ns*	*ns*	*ns*
8	*C1qtnf1*	*ns*	1.437	*ns*	*ns*		*ns*	*ns*	*ns*	*ns*	*ns*
9	*Pmepa1*	0.892	1.1	*ns*	*ns*		*ns*	*ns*	*ns*	*ns*	*ns*
10	*Pdk4*	0.929	*ns*	*ns*	*ns*		*ns*	*ns*	*ns*	*ns*	*ns*
11	*Klhl13*	*ns*	0.869	*ns*	*ns*		*ns*	*ns*	*ns*	*ns*	*ns*
12	*Cxcl1*	2.808	*ns*	*ns*	*ns*		*ns*	*ns*	*ns*	*ns*	*ns*
13	*Cxcl16*	1.766	0.93	*ns*	*ns*		*ns*	*ns*	*ns*	*ns*	*ns*
14	*Cd14*	1.058	0.74	*ns*	*ns*		*ns*	*ns*	*ns*	*ns*	*ns*
15	*Tfpi2*	*ns*	1.083	*ns*	*ns*		*ns*	*ns*	*ns*	*ns*	*ns*
16	*C1qc*	0.803	*ns*	*ns*	1.345		*ns*	*ns*	*ns*	*ns*	*ns*
17	*Cxcl5*	2.723	*ns*	*ns*	*ns*		*ns*	*ns*	*ns*	*ns*	*ns*
18	*Lbp*	*ns*	*ns*	1.01	1.201		*ns*	*ns*	*ns*	*ns*	*ns*
19	*Fhl1*	*ns*	-0.812	*ns*	*ns*		*ns*	*ns*	*ns*	*ns*	*ns*
20	*Hapln1*	-0.594	*ns*	1.649	*ns*		*ns*	*ns*	*ns*	*ns*	*ns*
21	*Ednrb*	0.634	*ns*	*ns*	*ns*			*ns*	*ns*	*ns*	*ns*
22	*Adap2*	0.617	*ns*	*ns*	*ns*			*ns*	*ns*	*ns*	*ns*
23	*C3ar1*	2.506	1.414	*ns*	*ns*			*ns*	*ns*	*ns*	*ns*
24	*Folr2*	0.724	0.707	*ns*	*ns*			*ns*	*ns*	*ns*	*ns*
25	*Npl*	0.63	*ns*	*ns*	0.973			*ns*	*ns*	*ns*	*ns*
26	*Hbegf*	*ns*	0.691	1.052	1.284			*ns*	*ns*	*ns*	*ns*
27	*C1qa*	0.764	*ns*	*ns*	0.771			*ns*	*ns*	*ns*	*ns*
28	*Apoe*	0.963	*ns*	*ns*	*ns*			*ns*	*ns*	*ns*	*ns*
29	*C1qb*	0.921	*ns*	*ns*	*ns*			*ns*	*ns*	*ns*	*ns*
30	*Has1*	1.728	2.337	*ns*	*ns*			*ns*	*ns*	*ns*	*ns*
31	*Gpr34*	0.848	*ns*	*ns*	*ns*			*ns*	*ns*	*ns*	*ns*
32	*Rnase6*	*ns*	*ns*	0.679	*ns*			*ns*	*ns*	*ns*	*ns*
33	*Ms4a7*	1.803	0.886	*ns*	*ns*			*ns*	*ns*	*ns*	*ns*
34	*Ubtd2*	*ns*	0.692	*ns*	*ns*	*ns*		*ns*	*ns*	*ns*	*ns*
35	*Rin2*	*ns*	0.906	*ns*	*ns*	*ns*		*ns*	*ns*	*ns*	*ns*
36	*Zc3hav1*	*ns*	*ns*	1.061	*ns*	*ns*		*ns*	*ns*	*ns*	*ns*
37	*Casp8*	*ns*	*ns*	0.788	*ns*	*ns*		*ns*	*ns*	*ns*	*ns*
38	*Antxr1*	*ns*	1.752	1.888	1.086	*ns*		*ns*	*ns*	*ns*	*ns*
39	*Atad2*	*ns*	*ns*	1.081	*ns*	*ns*		*ns*	*ns*	*ns*	*ns*
40	*Smc4*	*ns*	*ns*	1.423	*ns*	*ns*		*ns*	*ns*	*ns*	*ns*
41	*Med28*	*ns*	*ns*	*ns*	0.876	*ns*		*ns*	*ns*	*ns*	*ns*
42	*Itprip*	*ns*	*ns*	*ns*	1.099	*ns*		*ns*	*ns*	*ns*	*ns*
43	*Pth1r*	*ns*	*ns*	0.619	*ns*	*ns*		*ns*	*ns*	*ns*	*ns*
44	*Cd33*	*ns*	*ns*	1.242	*ns*	*ns*		*ns*	*ns*	*ns*	*ns*
45	*Cep135*	*ns*	*ns*	1.629	*ns*	*ns*		*ns*	*ns*	*ns*	*ns*
46	*Adam10*	*ns*	*ns*	0.948	*ns*	*ns*		*ns*	*ns*	*ns*	*ns*
47	*Cybb*	*ns*	*ns*	1.31	*ns*	*ns*		*ns*	*ns*	*ns*	*ns*
48	*Lrrc32*	0.664	*ns*	*ns*	*ns*	*ns*		*ns*	*ns*	*ns*	*ns*
49	*Mecom*	0.933	*ns*	*ns*	*ns*	*ns*		*ns*	*ns*	*ns*	*ns*
50	*Pcsk5*	1.778	0.871	*ns*	*ns*	*ns*		*ns*	*ns*	*ns*	*ns*
51	*Socs3*	1.287	0.837	*ns*	*ns*	*ns*		*ns*	*ns*	*ns*	*ns*
52	*Cttnbp2nl*	0.945	*ns*	*ns*	*ns*	*ns*		*ns*	*ns*	*ns*	*ns*
53	*Ikbip*	0.619	0.892	0.928	*ns*	*ns*		*ns*	*ns*	*ns*	*ns*
54	*Lgals1*	0.992	0.758	*ns*	*ns*	*ns*		*ns*	*ns*	*ns*	*ns*

#	Gene									
55	Twf1	ns	ns	1.053	ns	ns	ns	ns	ns	ns
56	Myof	1.077	1.296	1.06	ns	ns	ns	ns	ns	ns
57	Clec11a	0.662	0.851	1.865	ns	ns	ns	ns	ns	ns
58	Lhfpl2	ns	0.794	ns	ns	ns	ns	ns	ns	ns
59	Cep152	ns	ns	1.277	ns	ns	ns	ns	ns	ns
60	Fbxo32	1.487	ns	ns	ns	ns	ns	ns	ns	ns
61	Man2a1	0.583	ns	ns	ns	ns	ns	ns	ns	ns
62	Top2a	ns	ns	1.305	ns	ns	ns	ns	ns	ns
63	Snx7	0.692	1.057	1.347	ns	ns	ns	ns	ns	ns
64	Cmklr1	0.633	ns	ns	ns	ns	ns	ns	ns	ns
65	Fkbp14	ns	0.997	ns	ns	ns	ns	ns	ns	ns
66	Lamc1	ns	0.701	ns	ns	ns	ns	ns	ns	ns
67	Clec10a	ns	ns	ns	1.498	ns	ns	ns	ns	ns
68	Nfatc4	1.044	1.484	ns	ns	ns	ns	ns	ns	ns
69	Selplg	ns	ns	ns	0.746	ns	ns	ns	ns	ns
70	Rapgef6	ns	ns	1.206	ns	ns	ns	ns	ns	ns
71	Fbln2	2.251	1.431	ns	ns	ns	ns	ns	ns	ns
72	Far1	ns	ns	0.932	ns	ns	ns	ns	ns	ns
73	Depdc7	0.681	ns	ns	ns	ns	ns	ns	ns	ns
74	Prrg1	0.585	ns	ns	ns	ns	ns	ns	ns	ns
75	Ctsg	ns	ns	ns	0.736	ns	ns	ns	ns	ns
76	Slc41a2	0.978	1.143	ns	ns	ns	ns	ns	ns	ns
77	Nox4	1.497	1.284	ns	ns	ns	ns	ns	ns	ns
78	Pik3r3	ns	0.6	ns	ns	ns	ns	ns	ns	ns
79	Grb10	0.844	1.259	ns	ns	ns	ns	ns	ns	ns
80	Smchd1	ns	ns	1.024	ns	ns	ns	ns	ns	ns
81	Fstl1	1.506	1.773	0.947	ns	ns	ns	ns	ns	ns
82	Tnn	1.429	2.076	1.666	1.595	ns	ns	ns	ns	ns
83	Tnfrsf11a	0.759	ns	ns	ns	ns	ns	ns	ns	ns
84	Dbn1	0.914	1.295	ns	ns	ns	ns	ns	ns	ns
85	Efhd2	ns	ns	ns	1.126	ns	ns	ns	ns	ns
86	Adam9	0.873	ns	ns	ns	ns	ns	ns	ns	ns
87	Fzd1	0.978	0.786	ns	ns	ns	ns	ns	ns	ns
88	Chml	ns	ns	1.602	ns	ns	ns	ns	ns	ns
89	Myo5a	ns	ns	1.157	ns	ns	ns	ns	ns	ns
90	Ggt5	0.586	ns	ns	ns	ns	ns	ns	ns	ns
91	Il7r	ns	ns	1.51	ns	ns	ns	ns	ns	ns
92	Coro1a	ns	ns	ns	1.176	ns	ns	ns	ns	ns
93	Igsf10	1.037	1.848	ns	ns	ns	ns	ns	ns	ns
94	Tpst2	ns	ns	ns	1.017	ns	ns	ns	ns	ns
95	Sema3c	ns	0.899	ns	ns	ns	ns	ns	ns	ns
96	Sfrp2	1.772	2.205	1.668	1.599	ns	ns	ns	ns	ns
97	B4galt5	0.679	ns	ns	ns	ns	ns	ns	ns	ns
98	Msr1	1.736	ns	ns	ns	ns	ns	ns	ns	ns
99	Plvap	ns	ns	ns	1.208	ns	ns	ns	ns	ns
100	Fam198b	ns	0.695	ns	ns	ns	ns	ns	ns	ns
101	Marcksl1	ns	ns	ns	1.105	ns	ns	ns	ns	ns
102	Olfml1	ns	1.198	ns	ns	ns	ns	ns	ns	ns
103	Hpgds	0.588	ns	ns	ns	ns	ns	ns	ns	ns
104	Ctsk	ns	ns	0.781	ns	ns	ns	ns	ns	ns
105	Fam102b	ns	0.625	ns	ns	ns	ns	ns	ns	ns
106	Adamts2	ns	ns	0.745	ns	ns	ns	ns	ns	ns
107	Stmn2	0.697	ns	ns	ns	ns	ns	ns	ns	ns
108	Dclk1	1.786	1.667	ns	ns	ns	ns	ns	ns	ns
109	Slco2a1	ns	0.71	ns	ns	ns	ns	ns	ns	ns
110	Cd84	ns	ns	1.169	ns	ns	ns	ns	ns	ns
111	Ptprc	ns	ns	1.162	ns	ns	ns	ns	ns	ns
112	Arl4c	1.141	0.652	ns	ns	ns	ns	ns	ns	ns
113	Igsf6	ns	ns	1.446	ns	ns	ns	ns	ns	ns
114	Dock10	ns	ns	1.366	ns	ns	ns	ns	ns	ns
115	Ecscr	0.757	ns	ns	ns	ns	ns	ns	ns	ns
116	Iqgap2	ns	ns	1.388	ns	ns	ns	ns	ns	ns
117	Lyst	ns	ns	1.212	ns	ns	ns	ns	ns	ns
118	Aplnr	0.752	0.699	ns	ns	ns	ns	ns	ns	ns
119	Tnc	ns	0.829	ns	ns	ns	ns	ns	ns	ns
120	Gpr183	0.785	ns	ns	ns	ns	ns	ns	ns	ns
121	Map1b	0.751	ns	ns	ns	ns	ns	ns	ns	ns
122	Atp8b1	1.006	0.901	ns	ns	ns	ns	ns	ns	ns
123	Mnda	0.849	ns	1.307	ns	ns	ns	ns	ns	ns

#	Gene	1	2	3	4	5	6	7	8	9	10
124	*Rgs1*	0.779	ns	ns	ns	ns		ns	ns	ns	ns
125	*Fam13c*	0.688	ns	ns	ns	ns		ns	ns	ns	ns
126	*Nid1*	ns	0.804	ns	ns	ns		ns	ns	ns	ns
127	*Mrc1*	ns	ns	0.894	ns	ns		ns	ns	ns	ns
128	*Plk2*	0.634	ns	ns	ns	ns		ns	ns	ns	ns
129	*Gjc1*	0.657	ns	ns	ns	ns		ns	ns	ns	ns
130	*Vgll3*	2.125	1.482	ns	ns	ns		ns	ns	ns	ns
131	*Col4a1*	ns	0.653	ns	ns	ns		ns	ns	ns	ns
132	*Phldb2*	0.942	ns	ns	ns	ns		ns	ns	ns	ns
133	*Col8a1*	0.871	1.106	0.772	ns	ns		ns	ns	ns	ns
134	*Srpx*	ns	0.775	ns	ns	ns					ns
135	*Mmp13*	ns	ns	1.573	ns	ns					ns
136	*Gpnmb*	0.914	0.865	ns	ns	ns					ns
137	*Plau*	0.963	ns	ns	ns	ns					ns
138	*Vcan*	1.402	1.655	1.42	ns	ns				ns	ns
139	*Tgfbi*	1.169	0.866	ns	1.146	ns				ns	ns
140	*Nbl1*	ns	1.421	ns	1.642	ns	ns	ns	ns		ns
141	*Abi3bp*	ns	1.264	2.207	ns	ns	ns	ns	ns		ns
142	*Gas1*	ns	1.257	ns	ns	ns	ns	ns	ns		ns
143	*Igfbp4*	ns	0.748	ns	ns	ns	ns	ns	ns		ns
144	*Col6a2*	1.071	2.108	1.266	1.489	ns	ns	ns	ns		ns
145	*Igfbp6*	ns	0.703	ns	ns	ns	ns	ns	ns		ns
146	*Igfbp3*	ns	0.795	ns	ns	ns	ns	ns	ns		ns
147	*Col15a1*	ns	1.182	0.942	ns	ns	ns	ns	ns		ns
148	*Slc39a14*	1.276	0.992	ns	ns	ns	ns	ns	ns		ns
149	*Ntn1*	ns	0.749	ns	ns	ns	ns	ns	ns		ns
150	*Tspan2*	ns	0.73	ns	ns	ns	ns	ns	ns		ns
151	*Serpine1*	3.03	1.955	ns	ns	ns	ns	ns	ns		ns
152	*Atp8b2*	ns	0.826	ns	ns	ns	ns	ns	ns		ns
153	*Nt5e*	0.76	1.06	1.029	ns	ns	ns	ns	ns		ns
154	*Loxl3*	1.276	1.349	ns	ns	ns	ns	ns	ns		ns
155	*Anxa8*	ns	1.654	2.452	2.056	ns	ns	ns	ns		ns
156	*Atp9a*	0.812	ns	-0.685	ns	ns				ns	ns
157	*Timp1*	2.32	1.512	ns	ns	ns				ns	ns
158	*Sec24d*	0.606	0.862	ns	ns	ns				ns	ns
159	*Pdia5*	1.022	0.921	ns	ns	ns				ns	ns
160	*Mapt*	ns	-0.77	ns	ns	ns				ns	ns
161	*Kdelr2*	0.727	ns	ns	ns	ns				ns	ns
162	*Mfap4*	1.083	1.861	ns	ns	ns				ns	ns
163	*Cep55*	ns	ns	1.565	ns	ns				ns	ns
164	*Klhl30*	ns	ns	-0.957	ns	ns				ns	ns
165	*Fam57a*	1.572	1.363	ns	ns	ns				ns	ns
166	*Gpx7*	1.462	1.312	ns	ns	ns				ns	ns
167	*Plekhg5*	ns	0.654	ns	ns	ns				ns	ns
168	*Plcd4*	-0.688	ns	ns	ns	ns				ns	ns
169	*Cpxm1*	ns	1.502	ns	ns	ns				ns	ns
170	*Bmp1*	ns	0.763	0.67	ns	ns				ns	ns
171	*Capn6*	0.688	1.773	ns	ns	ns				ns	ns
172	*Fkbp7*	ns	0.912	1.353	ns	ns				ns	ns
173	*Cilp2*	-0.593	ns	ns	ns	ns				ns	ns
174	*Tpst1*	ns	ns	ns	0.995	ns				ns	ns
175	*Tceal7*	-0.907	ns	ns	ns	ns				ns	ns
176	*Igdcc4*	0.755	ns	ns	ns	ns				ns	ns
177	*Mmp14*	ns	1.287	1.026	ns	ns				ns	ns
178	*Trem2*	2.229	0.996	ns	ns	ns				ns	ns
179	*Tmem45a*	0.78	1.498	ns	ns	ns				ns	ns
180	*Ptgfrn*	0.986	1.437	ns	ns	ns				ns	ns
181	*Serpinh1*	0.937	0.834	ns	1.64	ns				ns	ns
182	*Slamf9*	0.812	ns	ns	ns	ns				ns	ns
183	*P4ha2*	0.81	1.071	ns	ns	ns				ns	ns
184	*Cd276*	ns	1.133	ns	ns	ns				ns	ns
185	*Aebp1*	0.939	1.41	ns	ns	ns				ns	ns
186	*Prrx2*	1.938	1.909	ns	ns	ns				ns	ns
187	*Dapl1*	ns	ns	ns	2.358	ns				ns	ns
188	*Col18a1*	1.197	1.696	ns	ns	ns				ns	ns
189	*Copz2*	ns	0.698	ns	ns	ns				ns	ns
190	*Edil3*	ns	1.038	1.202	ns	ns				ns	ns
191	*Matn3*	-0.922	ns	ns	ns	ns				ns	ns
192	*Pcolce*	0.709	1.094	ns	0.906	ns	ns			ns	ns

#	Gene													
193	S100a4	1.215	0.655	ns	1.145	ns	ns						ns	ns
194	Prrx1	0.671	0.726	ns	ns	ns	ns						ns	ns
195	Fkbp10	0.727	1.014	ns	ns	ns	ns						ns	ns
196	Gpx8	ns	0.788	ns	ns	ns	ns						ns	ns
197	Col6a1	1.05	2.06	1.196	1.284	ns	ns						ns	ns
198	Cercam	ns	0.739	ns	ns	ns	ns						ns	ns
199	Pdgfrl	ns	1.125	ns	ns	ns	ns						ns	ns
200	Tgfb3	0.691	0.846	ns	ns	ns	ns						ns	ns
201	Homer2	ns	-0.655	ns	ns	ns	ns						ns	ns
202	Ecm1	0.603	1.183	ns	ns	ns	ns						ns	ns
203	Lum	ns	1.428	2.203	ns	ns	ns						ns	ns
204	Col5a2	1.038	1.53	1.435	1.408	ns	ns						ns	ns
205	Ssc5d	ns	2.256	1.229	ns	ns	ns						ns	ns
206	Ifitm5	ns	-0.669	ns	ns	ns	ns						ns	ns
207	Crabp2	2.132	2.925	ns	ns	ns	ns						ns	ns
208	Postn	1.856	1.925	1.167	ns	ns	ns						ns	ns
209	Dkk3	0.648	1.848	ns	ns	ns	ns						ns	ns
210	Cthrc1	1.935	2.337	0.894	1.548	ns	ns						ns	ns
211	Fap	ns	ns	1.734	ns	ns	ns						ns	ns
212	Cys1	ns	0.973	ns	ns	ns	ns						ns	ns
213	Fndc1	1.067	2.223	1.297	ns	ns	ns						ns	ns
214	Col3a1	2.037	2.522	2.017	1.976	ns	ns						ns	ns
215	Aspn	1.156	2.012	1.904	ns	ns	ns						ns	ns
216	Col2a1	ns	ns	1.607	ns	ns	ns						ns	ns
217	Nova1	ns	0.74	ns	ns	ns	ns	ns	ns	ns				
218	Ndufa4l2	ns	1.016	ns	ns	ns	ns	ns	ns	ns				
219	Avpi1	0.684	ns	ns	ns	ns	ns	ns	ns	ns				
220	Eln	1.406	1.648	ns	ns	ns	ns	ns	ns	ns				
221	Igfbp7	0.715	0.908	ns	ns	ns	ns	ns	ns	ns				
222	Medag	1.053	1.907	1.091	ns	ns	ns	ns	ns	ns				
223	Col22a1	ns	ns	1.352	ns								ns	ns
224	Ccl2	3.556	ns	ns	ns								ns
225	Spp1	ns	ns	1.481	ns			ns	ns				ns
226	Il6	2.588	ns	ns	ns			ns	ns	ns			
227	Fgl2	ns	ns	0.962	ns			ns	ns				
228	Ctss	1.084	ns	ns	ns			ns	ns			ns	
229	Aif1	0.735	ns	ns	ns			ns	ns			ns	
230	Fos	0.825	0.735	ns	ns						ns		ns	
231	Nr4a2	ns	1.283	ns	ns								ns	
232	Tnfaip6	2.258	1.985	ns	ns		ns						ns	
233	Pid1	0.778	ns	ns	ns			ns	ns				
234	Rcan1	0.674	ns	ns	ns			ns	ns	ns			ns
235	Slc7a2	ns	0.851	ns	ns			ns	ns	ns			ns
236	Srpx2	1.145	1.555	1.337	1.312			ns	ns	ns			ns
237	Ier3	0.854	0.63	ns	ns			ns	ns	ns			ns
238	Adssl1	ns	-0.674	ns	ns			ns	ns	ns	ns		ns
239	Baiap2	0.6	1.038	ns	ns			ns	ns	ns	ns		ns
240	Mmp3	2.156	2.506	3.554	2.618		ns	ns	ns			ns
241	Lrrc2	0.7	-0.772	ns	ns	ns					ns		
242	Sfrp1	2.301	1.988	ns	ns	ns					ns		
243	Csrp2	1.816	1.449	ns	ns	ns							ns	ns
244	Siglec1	0.674	ns	ns	ns	ns							ns	ns
245	Mepe	ns	ns	0.725	ns	ns							ns	ns
246	Ndc80	ns	ns	1.424	ns	ns							ns	ns
247	Plat	1.092	1.039	1.101	ns	ns							ns	ns
248	Ccl8	1.605	1.85	ns	ns	ns							ns	ns
249	Dmp1	ns	ns	1.668	ns	ns							ns	ns
250	Creb3l1	ns	ns	0.817	ns	ns							ns	ns
251	Atp6v0d2	ns	ns	1.881	ns	ns							ns	ns
252	Rab23	0.855	0.689	ns	ns	ns							ns	ns
253	Ppic	ns	1.035	ns	ns	ns							ns	ns
254	Slitrk6	ns	0.692	ns	ns	ns							ns	ns
255	Gja1	ns	ns	1.12	ns	ns							ns	ns
256	Tmem158	ns	0.625	ns	ns	ns							ns	ns
257	Alpl	ns	ns	0.701	ns	ns							ns	ns
258	Angptl1	1.19	2.48	1.591	ns	ns							ns	ns
259	Prss23	0.656	ns	ns	ns	ns							ns	ns
260	Angpt2	ns	ns	1.264	ns	ns							ns	ns
261	Itga11	ns	1.311	ns	ns	ns							ns	ns

#	Gene									
262	Bend6	0.909	0.598	ns	ns	ns			ns	ns
263	Tpbg	0.733	ns	ns	ns	ns			ns	ns
264	Col1a2	ns	ns	0.599	ns	ns			ns	ns
265	Gxylt2	ns	0.78	ns	ns	ns			ns	ns
266	Cdh2	ns	ns	0.869	ns	ns			ns	ns
267	Olfml2b	ns	0.711	ns	1.304	ns			ns	ns
268	Sgms2	ns	ns	0.905	ns	ns			ns	ns
269	Tmem119	ns	0.628	1.351	ns	ns			ns	ns
270	C1qtnf6	0.593	1.483	ns	ns	ns			ns	ns
271	Bicc1	0.735	0.908	ns	ns	ns			ns	ns
272	Lrrc17	1.637	0.971	ns	ns	ns			ns	ns
273	Thy1	1.076	1.321	1.121	1.335	ns			ns	ns
274	Ednra	ns	0.777	ns	ns	ns				ns
275	Mmp2	ns	1.715	1.752	1.46	ns				ns
276	Thbs2	1.204	1.893	1.006	ns	ns				ns
277	Nid2	ns	0.854	ns	ns	ns				ns
278	Lrrc15	0.852	1.961	ns	ns	ns				ns
279	Smpd3	ns	ns	0.921	ns	ns				ns
280	Aldh1l2	1.09	0.781	ns	ns				ns	
281	Cxcl14	1.057	ns	ns	1.255	ns	ns	ns		ns
282	Pamr1	-0.812	1.945	1.265	1.27	ns	ns	ns		ns
283	Kcne4	1.722	1.287	ns	ns	ns	ns	ns		ns
284	Spats2l	ns	0.696	ns	ns	ns	ns	ns	ns	
285	Emp1	1.017	1.212	0.903	ns	ns	ns	ns	ns	
286	Moxd1	ns	2.79	ns	ns	ns	ns	ns	ns	
287	Col5a3	1.043	1.457	1.122	ns	ns	ns	ns	ns	
288	Mfap5	1.355	1.881	ns	ns	ns	ns	ns	ns	
289	Igfbp5	ns	0.663	ns	ns	ns	ns	ns	ns	
290	Cyp1b1	ns	ns	0.775	ns	ns	ns	ns		
291	Sfrp4	ns	0.692	1.342	ns	ns	ns	ns		
292	Sh3pxd2b	ns	0.9	ns	ns	ns	ns	ns		ns
293	Cdh11	ns	ns	1.155	ns	ns	ns	ns		ns
294	Tmtc4	0.727	ns	ns	ns	ns	ns	ns		ns
295	Emilin2	ns	ns	ns	1.217	ns	ns	ns		ns
296	B3galnt1	0.95	0.95	ns	ns	ns	ns	ns		ns
297	Stab1	1.385	0.908	ns	ns	ns	ns	ns		ns
298	Itgbl1	0.624	1.408	ns	ns	ns	ns	ns		ns
299	Fabp5	0.74	ns	ns	ns	ns	ns	ns		ns
300	Tlr4	ns	ns	0.973	ns	ns	ns	ns		ns
301	Igf1	0.946	1.636	1.135	ns	ns	ns	ns		ns
302	C1qtnf3	1.563	3.683	3.789	ns	ns	ns	ns		ns
303	Vsig4	0.653	0.683	2.94	ns	ns	ns	ns		ns
304	C1qtnf2	0.786	1.441	ns	ns	ns	ns	ns		ns
305	Svep1	0.9	1.248	ns	ns	ns	ns	ns		ns
306	Twist1	ns	0.61	ns	ns	ns	ns	ns		ns
307	Anpep	1.356	1.66	1.16	ns	ns	ns	ns		ns
308	Ahr	0.859	ns	ns	ns	ns	ns	ns		ns
309	Ptn	0.729	1.634	ns	ns	ns	ns	ns		ns
310	Olfml3	0.783	ns	ns	ns	ns	ns	ns		ns
311	Col1a1	ns	ns	0.814	ns	ns	ns	ns		ns
312	Col4a2	ns	0.653	ns	ns	ns	ns	ns		ns
313	Lamb1	1.056	1.354	ns	ns	ns	ns	ns		ns
314	Ptx3	2.819	1.114	ns	ns	ns	ns	ns		ns
315	Serpinf1	ns	ns	0.771	ns	ns	ns	ns		ns
316	Nov	ns	1.09	0.733	ns		ns	ns	ns	ns
317	Meox2	0.713	0.779	ns	ns		ns	ns	ns	ns
318	Lrrn1	1.12	ns	ns	ns	ns	ns	ns	ns	
319	Mcam	ns	0.675	ns	ns	ns	ns	ns	ns	
320	Lama4	0.787	1.099	ns	ns	ns	ns	ns		
321	Pck1	-1.273	-0.866	ns	ns	ns			ns	ns
322	Mest	0.924	2.6	ns	ns	ns			ns	ns
323	Cidec	ns	-0.862	ns	ns	ns			ns	ns
324	Lpl	ns	-0.586	ns	ns	ns			ns	ns
325	Lair1	ns	ns	1.192	ns	ns			ns	ns
326	Nusap1	ns	ns	1.276	ns	ns			ns	ns
327	Itga7	1.205	ns	ns	ns	ns			ns	ns
328	Hmmr	ns	ns	1.203	ns	ns			ns	ns
329	Acacb	ns	-0.582	ns	ns	ns			ns	ns
330	Aspm	ns	ns	1.454	ns	ns			ns	ns

#	Gene											
331	Atf3	0.731	ns	ns	ns	ns						ns
332	Basp1	0.856	ns	ns	ns	ns						ns
333	Col5a1	1.335	1.927	1.279	1.118	ns	ns					
334	Inhba	0.922	0.857	1.451	ns	ns	ns					
335	Tnfrsf12a	1.435	ns	ns	ns	ns	ns					ns
336	Dcn	ns	0.676	1.023	ns	ns	ns					ns
337	Tnfrsf11b	ns	ns	1.298	ns	ns	ns					ns
338	Lox	1.492	1.241	ns	ns	ns	ns					ns
339	Adam12	1.023	1.141	ns	ns	ns	ns					ns
340	Thbs3	0.847	1.981	2.037	1.32	ns	ns					ns
341	Htra1	ns	1.341	0.855	1.197	ns	ns					ns
342	Fn1	0.664	1.597	2.158	1.55	ns	ns					ns
343	Comp	ns	0.988	1.087	0.837	ns	ns					ns
344	Crlf1	2.668	2.306	ns	ns	ns	ns					ns
345	Ogn	ns	1.129	ns	ns	ns	ns					ns
346	Dio2	ns	ns	1.947	ns	ns	ns				ns	
347	Susd5	ns	ns	1.392	ns	ns					ns	ns
348	Ibsp	ns	ns	1.863	ns	ns	ns					ns
349	Col9a1	-0.587	ns	ns	ns	ns	ns					ns
350	Mfap2	ns	1.56	ns	ns	ns	ns					ns
351	Sulf1	1.194	1.561	1.051	ns	ns	ns					ns
352	Col12a1	ns	1.428	1.059	ns	ns	ns					ns
353	Thbs4	1.074	1.174	ns	ns	ns	ns					ns
354	Cx3cr1	1.039	ns	ns	ns	ns						ns
355	Col6a3	1.165	2.133	1.652	1.256		ns				ns	ns
356	Col16a1	0.784	1.293	1.097	ns		ns					ns
357	Prelp	ns	1.106	1.44	ns	ns	ns	ns	ns			
358	Fmod	ns	1.025	ns	ns	ns	ns	ns	ns			
359	Vwa1	ns	0.863	-1.368	ns	ns		ns	ns			
360	Ltbp3	ns	1.006	ns	ns	ns		ns	ns			
361	F5	ns	ns	1.291	ns	ns		ns	ns			
362	Angptl4	1.959	0.833	ns	1.304	ns	ns					ns
363	Htra3	ns	1.127	ns	ns	ns	ns					ns
364	Ism1	ns	0.707	ns	ns	ns		ns	ns	ns		
365	Fgf7	0.847	ns	ns	ns	ns	ns	ns	ns			
366	Angptl7	ns	-0.722	ns	ns	ns		ns	ns	ns	ns	
367	Myot	ns	-0.704	ns	ns	ns		ns	ns	ns	ns	
368	Fzd9	ns	ns	-0.785	ns	ns		ns	ns	ns	ns	
369	Cytl1	-1.407	-1.502	ns	ns	ns		ns	ns	ns	ns	
370	Ppp1r3c	ns	-0.629	ns	ns	ns		ns	ns	ns	ns	
371	Slc38a3	ns	-0.625	ns	ns	ns		ns	ns	ns	ns	
372	Sobp	ns	ns	-1.04	ns	ns		ns	ns	ns	ns	
373	Metrn	ns	ns	-0.698	ns	ns		ns	ns	ns	ns	
374	Tdrp	ns	-0.636	ns	ns	ns	ns	ns	ns	ns		
375	Zswim7	ns	-0.593	ns	ns	ns	ns	ns	ns	ns		
376	Cpeb1	ns	ns	-1.183	ns	ns	ns	ns	ns	ns		
377	Slc47a1	-0.923	-0.962	ns	ns	ns	ns	ns	ns	ns		
378	Timp4	-0.961	-0.747	ns	ns	ns	ns			ns	ns	
379	Dgat2	-0.595	ns	ns	ns	ns	ns			ns	ns	
380	Slc2a4	ns	-0.642	ns	ns	ns	ns			ns	ns	
381	Mmrn1	ns	ns	1.099	ns	ns	ns			ns	ns	
382	Lyve1	ns	ns	1.111	ns	ns	ns			ns	ns	
383	Fasn	-1.247	ns	ns	ns	ns	ns			ns	ns	
384	Gpd1	-0.771	ns	ns	ns	ns	ns			ns	ns	
385	Rbp4	ns	0.682	ns	ns	ns	ns			ns	ns	
386	Thrsp	-1.394	-0.782	ns	ns	ns	ns			ns	ns	
387	Mlxipl	ns	-0.669	ns	ns	ns	ns			ns	ns	
388	Atp1a2	ns	-0.666	ns	ns	ns	ns			ns	ns	
389	Hspb7	1.193	-0.97	ns	ns	ns	ns			ns	ns	
390	Ppp1r1a	ns	-0.657	ns	ns	ns	ns			ns	ns	
391	Cryab	0.851	-0.635	ns	ns	ns	ns			ns	ns	
392	Pfkfb1	-0.872	-0.617	ns	ns	ns	ns			ns	ns	
393	Cenpf	ns	ns	1.558	ns	ns	ns			ns	ns	
394	Alpk3	ns	-0.831	ns	ns	ns	ns			ns	ns	
395	Ctf1	ns	ns	-1.838	ns	ns	ns			ns	ns	
396	Cdca5	ns	ns	ns	0.974	ns	ns			ns	ns	
397	Arhgap20	ns	ns	ns	-0.704	ns	ns			ns	ns	
398	Ampd1	-0.698	ns	ns	ns	ns	ns			ns	ns	
399	Casc5	ns	ns	1.323	ns	ns	ns			ns	ns	

Chapter 4: Molecular Susceptibility to Post Traumatic Osteoarthritis in Mice, Systems Biology Approach of Identifying Molecular Changes with Respect to Injury Through RNA Sequencing.

Post-traumatic osteoarthritis (PTOA) is a painful and debilitating disease that is caused by mechanical destabilization of the joint and injury to the articular cartilage; however the molecular and cellular mechanisms leading to cartilage degeneration due to trauma are not well understood. Despite high incidences of OA occurrences, current PTOA treatment options are limited, focusing on surgical procedures that restore the joint anatomy and reduce pain; hence, OA patients are anxiously awaiting the development of new pharmacologic interventions aimed at minimizing or preventing progressive tissue damage triggered by joint injury. Previously inflammation [51], irregular subchondral bone formation [52], and loss of response to mechanical responses [54, 55] in joints were demonstrated to lead to the development of OA. In the past decade, using human biopsy and animal OA models, new insights about joint OA pathogenesis were uncovered. To date, several studies have evaluated molecular changes associated with human arthritic joint tissues including: synovium [137], meniscus [138], cartilage [139], osteophytes [140] and subchondral bone [141]. Furthermore, some data has been generated using 3D tissue culture approaches and cartilage explants. However, the unique microenvironment of this "joint" disease including cartilage, bone, meniscus, ligaments, and synovium before and after trauma is hard to model *in vitro*; thus, animal models that resemble PTOA are vital in understanding the

molecular, physiological and structural changes within the joint in response to injury. Several studies revealed molecular changes associated with late stages of OA but only a few examined earlier molecular events because of clinical limitations. To date the method of discriminating asymptomatic OA tissues from age matched healthy controls is difficult. Instead, mouse models that mimic human OA have been used with great success to study OA pathogenesis and to identify putative molecular and genetic factors driving the progression of the disease [142, 143, 178].

Previously, we investigated (Chapter 2) Sclerostin (Sost), as a potential therapeutic to OA progression. By using a clinically relevant, whole-joint PTOA injury mouse model, in which ACL rupture was introduced through a single rapid mechanical overload [64], and observed that SOST overexpression presents a delay in a OA developing joint (Chapter 2). In addition to its preservation to overall cartilage integrity, a reduction of osteophytes was identified in transgenic animals. It had been well established that in injured joints, elevated levels of secreted catabolic enzymes accelerates OA progression [179, 180]. In our model, activated MMPs 2 (Gelatinase A) and 3 (Stromelysin-1) were reduced with respect to injury in joints overexpressing SOST (Chapter 2). Consistent with the transgenic data, the overall activated MMP levels were also reduced in *WT* injured joints when recombinant Sost protein was administered intra-articularly shortly after tibial compression (TC) injury. We also investigated the molecular analysis comparing injured and uninjured contralateral among *WTs* at various time points (1 day, 1-, 6-, and 12-weeks) post injury and revealed a variety of inflammatory triggers that

126

may also be responsible for OA advancements (Chapter 3). Tough we attempted to separate and computationally analyze transcriptional alterations in *WT* injured joints, as previously described in chapter 3, many more transcriptional alterations in *Sost KO* (*Sost^{KO}*) and *SOST* transgenic (*SOST^{TG}*) remain to be unveiled. Moreover the genetic susceptibility to OA developing joints remains to be explored. Here I present a few systems biology approaches for future OA research by utilizing the TC PTOA injury model and the RNA sequencing (RNASeq) analysis methodology previously described in chapters 2 and 3.

Computational Approach using RNA Sequencing to Identify Molecular Changes that parallels the progression of OA developing joints.

Though OA is commonly diagnosed by visible damage to the articular cartilage, more recent assessments of OA have been migrating to evaluate the entire joint, and perceive the disease as a multi factorial, multi cell-type phenotype [144, 145]. Through RNA sequencing (RNAseq) at various stages of OA development, a time-course analysis may uncover possible candidate biomarkers in tracking disease and potential therapeutics. To investigate the joint biology of PTOA developing knees, one direction is to explore the molecular differences in mice with varying OA susceptibility as comparison after injury. Since PTOA is a progressive disease that manifest over time, we hypothesize that PTOA does not occur as an immediate consequence of the injury itself, but rather the injury triggers a series of molecular events that promote cartilage degradation over time, therefore pharmacologically modifying the local articular environment immediately

post injury may prevent subsequent cartilage degradation and hinder the development of PTOA. By using a systematic gene expression analysis of injured joints immediately post trauma, in several strains of mice with varying susceptibility to PTOA we may be able to identify new candidate molecules that may be responsible for inducing cartilage degradation in PTOA.

In addition, systematic analysis of PTOA in mouse strains with varying susceptibility to cartilage degradation could also prove invaluable in determining what molecular events precede articular cartilage degradation, or prime the joint to sustain cartilage damage without triggering subsequent ECM degradation. Strains that are resistant to OA, such as MRL/MpJ, can be further explored to determine what molecular environment provides protection from cartilage degradation, subsequent to joint trauma. The MRL/MpJ mouse strain was previously shown to display the unique ability to mount a regenerative response against a wide range of injuries [181-183]. More recently this strain was demonstrated to be resistant to the development of OA (OA-resistant strain) following intraarticular fractures [181, 182]. Examination of these mice at 4- and 8- weeks post fracture revealed no differences in bone density or histological grading of cartilage generation between the injured and uninjured knee [181]. Despite the regenerative properties of this mouse strain, the specific genetic causes that explain the enhanced regenerative abilities of MRL/MpJ mice are still unknown [184]. In sharp contrast, the males of STR/ort strain (OA-susceptible strain) spontaneously develop OA resembling human-like cartilage lesions at 12-22 weeks of age. These mice display mild to severe loss of hyaline cartilage,

osteophyte formation, calcification and ossification of cruciate ligaments and chondroid metaplasia, in the absence of traumatic injury [185-187]. Since this initial discovery, a wide range of studies have been performed using this strain to better understand the development of OA; however, the etiology of osteoarthritis development in these mice is still unclear [188, 189]. In addition, genome-wide gene expression analysis of this strain in a PTOA model has not yet been performed. Although previous studies have examined the process of OA development in these murine strains in regards to inflammation and joint characteristics, no previous studies have systematically examined the differences in gene expression between these strains using a human-relevant PTOA-induced model.

The MRL/MpJ and STR/ort strains have yet to be examined using the TC OA injury model.   Histological evaluations suggest that the OA phenotype observed here are distinct from the previously reported intraarticular fractures and spontaneous development of OA [181, 185] (Fig 1A). At 12 weeks post injury, the MRL/MpJs showed very small evidence of joint disease, with a mild OA phenotype (scores ~2), while the STR/ort joints were severely compromised, displaying high grade OA phenotypes (scores of 6). Consistent with published reports on the STR/ort strain, the uninjured contralateral of these mice also displayed sing of OA (score~4). This degree of OA severity in the contralateral joint of STR/ort mice was more severe than other published results [190, 191], suggesting that environmental conditions our mice are housed in our animal care facility may also contribute to the development of the OA phenotype.   Because of this drastic

129

phenotype, it is important that the RNA is collected and captured at critical time points post injury. By sequencing RNA from injured and contralateral uninjured whole-joints at various time points (Fig 2A) we hope to identify transcripts altered in different stages of OA developing joint (Fig 2B). The $Sost^{KO}$ and $SOST^{TG}$ comparisons were initially purposed following the studies presented in chapters 2 and 3 (Bold Box), other ideal comparisons would include: 1) compare common genes in susceptible strains (STR/ort and $Sost^{KO}$, gray and orange stripes); 2) identify common genes in resistant strains (MRL/MpJ and $SOST^{TG}$, red and green stripes); and 3) common in susceptible but distinctly opposite in resistant strains between injured and contralateral joints (STR/ort and MRL/MpJ, purple and blue stripes) (Fig 2C). Ideally, the comparison between susceptible strains will indicate common genes reflecting advance cartilage degradation, bone turnover, and osteophyte formation. Conversely, the comparison between resistant strains may identify genes that play a role in vasculature, decrease activity of carbolic enzymes and/or inhibit inflammation. Lastly, the contrast between resistant and susceptible strains may highlight distinct pathways reflecting the contributions to OA advancement or delay. By examining gene expression differences among mouse strains that vary in OA susceptibility, this could detect potential biomarkers and therapeutic targets for the treatment of OA; i.e. determine the genetic factors that allow the MRL/MpJ mouse strain to be resistant to OA and the STR/ort strain to be susceptible to OA.

Genes that are differentially regulated between the STR/ort and MRL/MpJ will be further examined for their potential therapeutic application. The potential

130

candidates may be tested by administering either antibodies or competitive inhibitors to target surface receptors, receptor proteins, and/or secreted molecules. Receptors that have already been identified as being significantly upregulated in injured joints of mice, to determine if pharmacologic inhibition of these molecules blunts the inflammatory or the developing phase of PTOA. The predicted transcripts that are "more susceptible" or "less resistance" may be explored in cell specific knock out (KO) mice for further validations.

Chondrocyte Specific Conditional KO Mouse Models to Study PTOA developing Joint.

OA is considered a joint disease with multiple contributing tissues affecting the articular cartilage maintenance with response to injury. The cartilage integrity and homeostasis is primarily maintained by chondrocytes [22], however many contributing triggers stem from surrounding joint tissues possibly including the synovium and the underlining bone to trigger cartilage breakdown or maintenance. Although the articular cartilage (through chondrocytes) can modulate its own functional responses to load, their ability to modify and repair surrounding extracellular matrix is limited by comparison to bone [22]. Therefore, understanding the molecular mechanism or triggers involving matrix or cartilage synthesis is an important avenue to explore when understanding OA pathogenesis.

Bone morphogenic protein (BMP) signaling is very important in regulating bone formation [192]. BMPs are potent chemokines that induce bone and cartilage formation. During bone and cartilage development, BMPs regulate expression

and/or the function of several transcriptional factors through downstream activation of Smad transcription factors [192]. Genetic studies revealed Runx2, Osterix, and Sox9 all of which function downstream of BMPs, play an important role in bone and cartilage development [193]. These transcriptional factors in bone and cartilage have been previously supported by biochemical and cellular biology studies. Interestingly, BMPs are regulated by several negative feedback systems that appear necessary for bone and cartilage maintenance. Regulators include molecular antagonists and mutations in molecules that have been demonstrated to cause bone and cartilage defects. For example, noggin (Nog) KO mice display cartilage hyperplasia (overgrowth) during skeletal development leading to the loss of joint function (excessive BMPs activity), whereas transgenic mice overexpressing noggin in skeletal cells display severe osteopenia and bone fragility (reduced BMPs activity) [194]. Furthermore, BMPs signaling has been shown to be up-stream of Wnt signaling, that has also been shown to play critical roles in bone and cartilage homeostasis in the adult skeleton. Wnt has also been implicated in the process of cartilage degradation in OA. Potentially, Noggin and Gremlin play a role in cartilage formation in chondrocytes and affect PTOA, therefore it would be interesting to evaluate whether *nog* and/or *grem* deletion impacts the development of OA in traumatic models. Both global KOs of *grem* and *nog* are neonatal lethal in mice, where *grem* deletion causes abnormal limb formation and kidney failure [195-197], and *Nog* deletion causes a cartilage overgrowth and a cranial defect phenotypes [198-200]. In order to investigate the role of noggin (*nog*) and gremlin (*grem*) in PTOA, one would use tissue-specific

deletion of these alleles in the AC and test to see if they modulate the PTOA phenotype.

To evaluate the function of Nog or Grem in PTOA developing joints, we generated conditional null mice (cKO) by mating mice with either Nog or Grem was flanked by *loxP* sequence [201] with mice expressing the Cre recombinase under the collagen 2A (chondrocyte specific) promoter [202, 203]. Chondrocyte specific deletions of Nog (Nog^f/f; Col2-Cre) and Grem (Grem^f/f; Col2-Cre) have not yet been evaluated under TC OA injury model. At 12 weeks post injury, histological evaluation presented both cKO with severe OA phenotype (score between 5~6) in injured joints, while no obvious cartilage phenotype was observed in uninjured joints (Fig 3A). Utilizing the negative Cre ("No Cre") as the internal "*WT* controls" for the cKO genotypes, TC OA injury at 12 weeks presented severe OA phenotype among all genotypes (Fig 3B). Interestingly, both Cre positive genotypes still retain some cartilage left on the tibial surface (Fig 3A, black arrows), in comparison to Cre negative and WTs (Fig 1A, middle) and the femoral plateau appears minimally affected by injury. Though OA is severe in cKO mice, compared to the WT controls which display a complete erosion (score 6) of tibial cartilage surface, the chondrocyte specific KO of either *Nog* or *Grem* (score ~5) may present slight, but ultimately significant delay in OA development. These results are preliminary, a larger sample size and a shorter time post injury may present the necessary statistical relevance and hint at the differences between injured and uninjured strains.

Discussion and Concluding Remarks

In this chapter, we addressed a few of the current challenges and knowledge gaps in the studies in OA pathogenesis. Because OA diagnosis is primarily based on clinical symptoms and radiological changes in the joint (which have poor and resolution sensitivity), this chronic disease has a relatively long 'silent' period. Usually, many individuals developing OA are asymptomatic until significant joint damage has occurred [55], at which point the only available long term treatment options are limited to surgical intervention [56]. Since cartilage damage is irreversible, and currently no reliable markers can be used to predict OA or its progression, the identification and characterization of OA biomarkers for detection and tracking the progression of the disease combined with developing new pharmacologic interventions aimed to minimize cartilage damage triggered by joint injury, are vital scientific endeavors. By utilizing mouse strains that vary in PTOA susceptibility as a function of joint trauma we can now begin to systematically characterize the molecular events perturbed in PTOA, and the various contributions of specific molecular pathways. In addition, a compilation of a highly curated list of candidate molecules that could potentially be utilized as biomarkers or therapeutic targets of PTOA would further facilitate future studies.

Here I presented histological evaluation of distinct mouse strains that vary in OA susceptibility (Fig 1), where molecular analysis using these strains may aid in further understanding of the pathogenesis and the progression of this disease. By making various comparisons of RNA transcripts at various stages post injury

(Fig 2) we may be able to highlight potential targets for therapeutics or candidate biomarkers to track OA progression. After RNA Seq analysis among the MRL/MpJ and the STR/ort strains, cell specific cKOs may also be implemented to further investigate the mechanism of target genes in PTOA joints. Separating cell specific studies may be one of the most effective approaches to study individual contributions or bone, cartilage and synovial cells to PTOA since joints dependent on so many other surrounding tissues given its avascular microenvironment for chondrocytes. Therefore, KO in cell specific targets may not only reveal its role on cartilage/bone cells, it may also resolve other tissues/cell types contributing to cartilage maintenance and preventing integrity disruption. As is demonstrated in the Nog and the Grem cKO mice, where we can observe specific effect in cartilage post injury. Further investigation of existing KO mouse models is necessary to evaluate the similarities and differences in catabolic enzymes (i.e. MMPs or ADAMTS) altered that may cause OA advancement or delay in injured compared to uninjured joints.

The ultimate goal of OA research is to develop effective therapies that bring injured and genetically at risk patients close to a fully restored function of the joint without surgical interventions. Despite that many of the risk factors (trauma/aging) associated with the development of OA are well established, the pathogenesis of OA is still poorly understood. The molecular and genetic mechanisms contributing to cartilage degeneration have yet to be elucidated. Moreover, many asymptomatic individuals have developing OA and are unaware. Thus, the need to better understand pathogenesis of OA to identify potential therapeutic targets to minimize

cartilage degradation is critical. Simultaneously, we also need to establish a repertoire of candidate biomarkers that can be used to track the progression of the disease in asymptomatic patients. By utilizing the TC OA injury mouse model and taking a systems biology approach of analyzing molecular changes (whole joint) at various stages of OA developing joint using RNASeq. Our laboratory hopes to identify targets of early detection for OA developing patients and uncover possible therapeutic, such as secreted molecules. One potential may be the administration of recombinant Sclerostin proteins.

Figure 1. Histology of STR/ort and MRL/MpJ after tibial compression (TC) OA injury
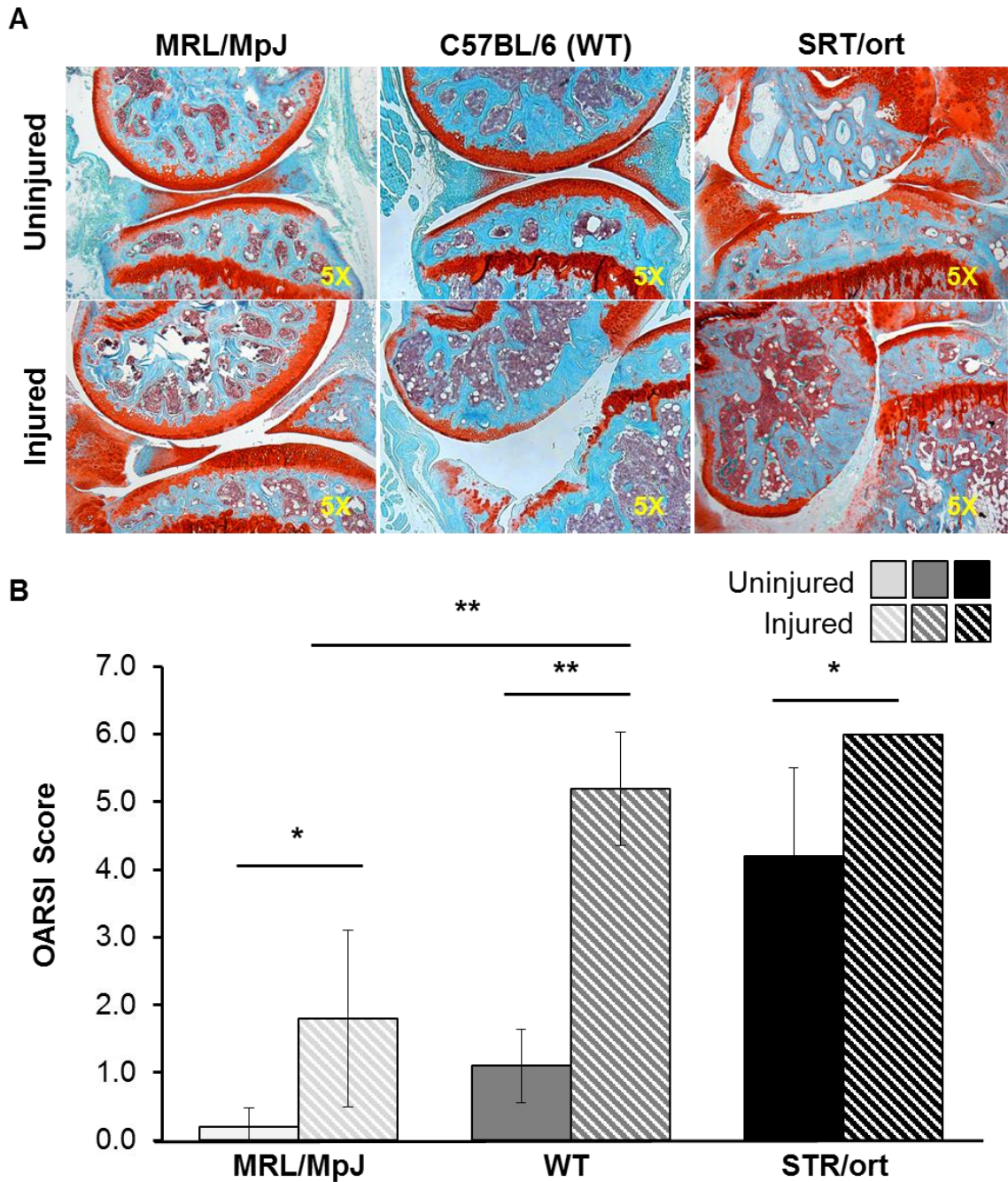
Figure 1. TC OA injury of MRL/Mpj and STR/ort. Ten week old MRL/MpJ and STR/ort male mice were injured and evaluated after 12 weeks post TC (12~14N) injury. (A) Safranin-O and Fast Green histological stains of uninjured contralateral

(top row) and injured (bottom row) joints. (B) OARSI scoring between genotypes comparing injured and uninjured joints using scales from normal (0~0.5), mild (1~2), moderate (3~4), and severe (5~6). Sample size of 5 for each genotype were used for OARSI scoring evaluation. * $p < 0.05$ and ** $p < 0.01$

Figure 2. **Model for competitive analysis to identify common genes associated with PTOA progression**
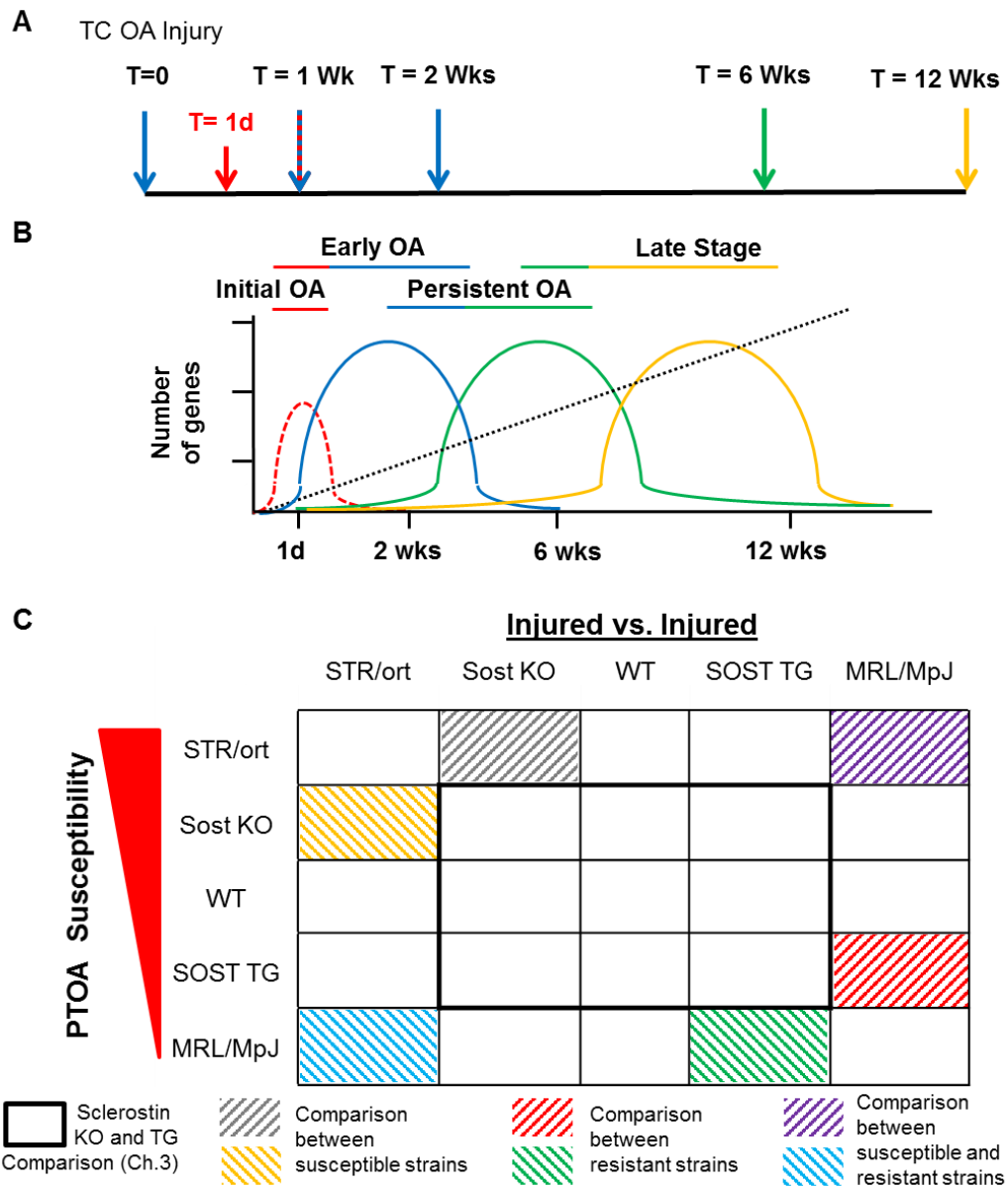
Figure 2. **Schematic of RNA comparison between strains varying in OA susceptibility.** Model for revealing common transcripts associated with PTOA progression. (A) Time line for sample collection for RNA and histology. (B) Broad overview to identify genes associated with different stages of OA progression. (C) Ideal comparison between OA susceptible and OA resistant strains. Bolded border is the ideal comparison for Wnt dependent change.

Figure 3. Histology of Gremlin and Noggin cKO after tibial compression (TC) OA injury
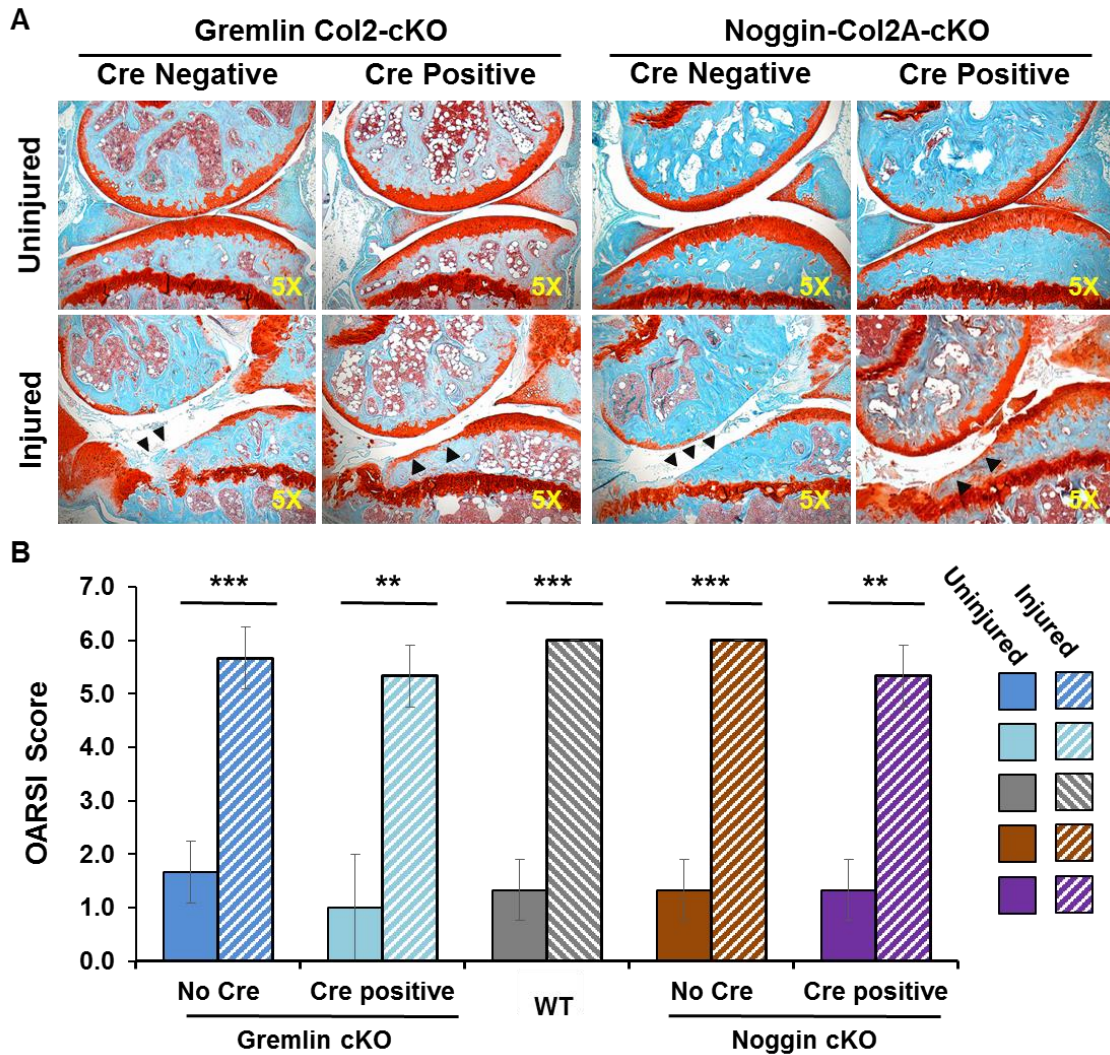
Figure 3. TC OA injury of Noggin and Gremlin cKO. Sixteen week old Nog and Grem male mice were injured and evaluated after 12 weeks post TC (12~14N) injury. (A) Safranin-O and Fast Green histological stains of uninjured contralateral (left knee) and injured (right knee) joints. (B) OARSI scoring between genotypes comparing injured and uninjured joints using scales from normal (0~0.5), mild (1~2), moderate (3~4), and severe (5~6). Sample size of 3 for cKO and 5 for WTs were used for OASRI scoring evaluation. ** $p < 0.01$ and *** $p < 0.001$

References

1. Garstang, S.V. and T.P. Stitik, *Osteoarthritis: epidemiology, risk factors, and pathophysiology.* Am J Phys Med Rehabil, 2006. **85**(11 Suppl): p. S2-11; quiz S12-4.
2. Lane, N.E., et al., *OARSI-FDA initiative: defining the disease state of osteoarthritis.* Osteoarthritis Cartilage. **19**(5): p. 478-82.
3. Caplazi, P., et al., *Mouse Models of Rheumatoid Arthritis.* Vet Pathol, 2015. **52**(5): p. 819-26.
4. Hunter, D.J., *Osteoarthritis.* Best Pract Res Clin Rheumatol, 2011. **25**(6): p. 801-14.
5. Yoo, J.H., et al., *A meta-analysis of the effect of neuromuscular training on the prevention of the anterior cruciate ligament injury in female athletes.* Knee Surg Sports Traumatol Arthrosc, 2010. **18**(6): p. 824-30.
6. Yucesoy, B., et al., *Occupational and genetic risk factors for osteoarthritis: a review.* Work, 2015. **50**(2): p. 261-73.
7. Sharma, L., *Osteoarthritis year in review 2015: clinical.* Osteoarthritis Cartilage, 2016. **24**(1): p. 36-48.
8. Bijlsma, J.W., F. Berenbaum, and F.P. Lafeber, *Osteoarthritis: an update with relevance for clinical practice.* Lancet, 2011. **377**(9783): p. 2115-26.
9. Pereira, D., et al., *The effect of osteoarthritis definition on prevalence and incidence estimates: a systematic review.* Osteoarthritis Cartilage, 2011. **19**(11): p. 1270-85.
10. Menkes, C.J., *Radiographic criteria for classification of osteoarthritis.* J Rheumatol Suppl, 1991. **27**: p. 13-5.
11. Altman, R.D., *Criteria for classification of clinical osteoarthritis.* J Rheumatol Suppl, 1991. **27**: p. 10-2.
12. Cutolo, M., et al., *Commentary on recent therapeutic guidelines for osteoarthritis.* Semin Arthritis Rheum, 2015. **44**(6): p. 611-7.
13. Zhang, W., et al., *OARSI recommendations for the management of hip and knee osteoarthritis, part I: critical appraisal of existing treatment guidelines and systematic review of current research evidence.* Osteoarthritis Cartilage, 2007. **15**(9): p. 981-1000.
14. Castellsague, J., et al., *Individual NSAIDs and upper gastrointestinal complications: a systematic review and meta-analysis of observational studies (the SOS project).* Drug Saf, 2012. **35**(12): p. 1127-46.
15. Jordan, K.M., et al., *EULAR Recommendations 2003: an evidence based approach to the management of knee osteoarthritis: Report of a Task Force of the Standing Committee for International Clinical Studies Including Therapeutic Trials (ESCISIT).* Ann Rheum Dis, 2003. **62**(12): p. 1145-55.
16. Bannuru, R.R., et al., *Relative efficacy of hyaluronic acid in comparison with NSAIDs for knee osteoarthritis: a systematic review and meta-analysis.* Semin Arthritis Rheum, 2014. **43**(5): p. 593-9.

17. Kahan, A., et al., *Long-term effects of chondroitins 4 and 6 sulfate on knee osteoarthritis: the study on osteoarthritis progression prevention, a two-year, randomized, double-blind, placebo-controlled trial.* Arthritis Rheum, 2009. **60**(2): p. 524-33.

18. Michel, B.A., et al., *Chondroitins 4 and 6 sulfate in osteoarthritis of the knee: a randomized, controlled trial.* Arthritis Rheum, 2005. **52**(3): p. 779-86.

19. Henrotin, Y., M. Marty, and A. Mobasheri, *What is the current status of chondroitin sulfate and glucosamine for the treatment of knee osteoarthritis?* Maturitas, 2014. **78**(3): p. 184-7.

20. Mahajan, A., S. Verma, and V. Tandon, *Osteoarthritis.* J Assoc Physicians India, 2005. **53**: p. 634-41.

21. Sanchez-Adams, J., et al., *The mechanobiology of articular cartilage: bearing the burden of osteoarthritis.* Curr Rheumatol Rep, 2014. **16**(10): p. 451.

22. Goldring, M.B. and S.R. Goldring, *Articular cartilage and subchondral bone in the pathogenesis of osteoarthritis.* Ann N Y Acad Sci, 2010. **1192**: p. 230-7.

23. Zuscik, M.J., et al., *Regulation of chondrogenesis and chondrocyte differentiation by stress.* J Clin Invest, 2008. **118**(2): p. 429-38.

24. Staines, K.A., V.E. Macrae, and C. Farquharson, *Cartilage development and degeneration: a Wnt Wnt situation.* Cell Biochem Funct, 2012. **30**(8): p. 633-42.

25. Dong, S., et al., *MicroRNAs regulate osteogenesis and chondrogenesis.* Biochem Biophys Res Commun, 2012. **418**(4): p. 587-91.

26. Kirk, M.D. and A.J. Kahn, *Extracellular matrix synthesized by clonal osteogenic cells is osteoinductive in vivo and in vitro: role of transforming growth factor-beta 1 in osteoblast cell-matrix interaction.* J Bone Miner Res, 1995. **10**(8): p. 1203-8.

27. Yoneda, T., *[Mechanism and strategy for treatment of cancer metastasis to bone].* Gan To Kagaku Ryoho, 2011. **38**(6): p. 877-84.

28. Barna, M. and L. Niswander, *Visualization of cartilage formation: insight into cellular properties of skeletal progenitors and chondrodysplasia syndromes.* Dev Cell, 2007. **12**(6): p. 931-41.

29. Sandell, L.J., et al., *Alternatively spliced type II procollagen mRNAs define distinct populations of cells during vertebral development: differential expression of the amino-propeptide.* J Cell Biol, 1991. **114**(6): p. 1307-19.

30. Oberlender, S.A. and R.S. Tuan, *Expression and functional involvement of N-cadherin in embryonic limb chondrogenesis.* Development, 1994. **120**(1): p. 177-87.

31. Bi, W., et al., *Haploinsufficiency of Sox9 results in defective cartilage primordia and premature skeletal mineralization.* Proc Natl Acad Sci U S A, 2001. **98**(12): p. 6698-703.

32. Dusad, A., et al., *Impact of Total Knee Arthroplasty as Assessed Using Patient-Reported Pain and Health-Related Quality of Life Indices:*

Rheumatoid Arthritis Versus Osteoarthritis. Arthritis Rheumatol, 2015. **67**(9): p. 2503-11.

33. Spencer, J.A., et al., *Direct measurement of local oxygen concentration in the bone marrow of live animals.* Nature, 2014. **508**(7495): p. 269-73.

34. Li, L., et al., *Hedgehog signaling is involved in the BMP9-induced osteogenic differentiation of mesenchymal stem cells.* Int J Mol Med, 2015. **35**(6): p. 1641-50.

35. Barbero, A., et al., *Age related changes in human articular chondrocyte yield, proliferation and post-expansion chondrogenic capacity.* Osteoarthritis Cartilage, 2004. **12**(6): p. 476-84.

36. Towler, D.A., *The osteogenic-angiogenic interface: novel insights into the biology of bone formation and fracture repair.* Curr Osteoporos Rep, 2008. **6**(2): p. 67-71.

37. Goldring, S.R., *The role of bone in osteoarthritis pathogenesis.* Rheum Dis Clin North Am, 2008. **34**(3): p. 561-71.

38. Bhosale, A.M. and J.B. Richardson, *Articular cartilage: structure, injuries and review of management.* Br Med Bull, 2008. **87**: p. 77-95.

39. Loeser, R.F., *Aging and osteoarthritis: the role of chondrocyte senescence and aging changes in the cartilage matrix.* Osteoarthritis Cartilage, 2009. **17**(8): p. 971-9.

40. Sanchez, C., et al., *Mechanical loading highly increases IL-6 production and decreases OPG expression by osteoblasts.* Osteoarthritis Cartilage, 2009. **17**(4): p. 473-81.

41. Raizman, I., et al., *Articular cartilage subpopulations respond differently to cyclic compression in vitro.* Tissue Eng Part A, 2009. **15**(12): p. 3789-98.

42. Hall, A.C., J.P. Urban, and K.A. Gehl, *The effects of hydrostatic pressure on matrix synthesis in articular cartilage.* J Orthop Res, 1991. **9**(1): p. 1-10.

43. Monfort, J., et al., *Decreased metalloproteinase production as a response to mechanical pressure in human cartilage: a mechanism for homeostatic regulation.* Arthritis Res Ther, 2006. **8**(5): p. R149.

44. Lomas, C., et al., *Cyclic mechanical load causes global translational arrest in articular chondrocytes: a process which is partially dependent upon PKR phosphorylation.* Eur Cell Mater, 2011. **22**: p. 178-89.

45. Leong, D.J. and H.B. Sun, *Mechanical loading: potential preventive and therapeutic strategy for osteoarthritis.* J Am Acad Orthop Surg, 2014. **22**(7): p. 465-6.

46. Tanimoto, K., et al., *Modulation of hyaluronan catabolism in chondrocytes by mechanical stimuli.* J Biomed Mater Res A, 2010. **93**(1): p. 373-80.

47. Loeser, R.F., et al., *Basic fibroblast growth factor inhibits the anabolic activity of insulin-like growth factor 1 and osteogenic protein 1 in adult human articular chondrocytes.* Arthritis Rheum, 2005. **52**(12): p. 3910-7.

48. Tran-Khanh, N., et al., *Aged bovine chondrocytes display a diminished capacity to produce a collagen-rich, mechanically functional cartilage extracellular matrix.* J Orthop Res, 2005. **23**(6): p. 1354-62.

49. Kempson, G.E., *Relationship between the tensile properties of articular cartilage from the human knee and age.* Ann Rheum Dis, 1982. **41**(5): p. 508-11.

50. Kamada, H., et al., *Age-related differences in the accumulation and size of hyaluronan in alginate culture.* Arch Biochem Biophys, 2002. **408**(2): p. 192-9.

51. Joosten, L.A., et al., *Interleukin-18 promotes joint inflammation and induces interleukin-1-driven cartilage destruction.* Am J Pathol, 2004. **165**(3): p. 959-67.

52. van Osch, G.J., et al., *Relation of ligament damage with site specific cartilage loss and osteophyte formation in collagenase induced osteoarthritis in mice.* J Rheumatol, 1996. **23**(7): p. 1227-32.

53. Kamekura, S., et al., *Osteoarthritis development in novel experimental mouse models induced by knee joint instability.* Osteoarthritis Cartilage, 2005. **13**(7): p. 632-41.

54. Glasson, S.S., et al., *Deletion of active ADAMTS5 prevents cartilage degradation in a murine model of osteoarthritis.* Nature, 2005. **434**(7033): p. 644-8.

55. Glasson, S.S., T.J. Blanchet, and E.A. Morris, *The surgical destabilization of the medial meniscus (DMM) model of osteoarthritis in the 129/SvEv mouse.* Osteoarthritis Cartilage, 2007. **15**(9): p. 1061-9.

56. Ma, H.L., et al., *Osteoarthritis severity is sex dependent in a surgical mouse model.* Osteoarthritis Cartilage, 2007. **15**(6): p. 695-700.

57. Schenker, M.L., et al., *Pathogenesis and prevention of posttraumatic osteoarthritis after intra-articular fracture.* J Am Acad Orthop Surg, 2014. **22**(1): p. 20-8.

58. Little, C.B. and M.M. Smith, *Animal Models of Osteoarthritis* Current Rheumatology Reviews, 2008. **4**(3).

59. van der Kraan, P.M., et al., *Development of osteoarthritic lesions in mice by "metabolic" and "mechanical" alterations in the knee joints.* Am J Pathol, 1989. **135**(6): p. 1001-14.

60. van der Kraan, P.M., et al., *The effect of low sulfate concentrations on the glycosaminoglycan synthesis in anatomically intact articular cartilage of the mouse.* J Orthop Res, 1989. **7**(5): p. 645-53.

61. Poulet, B., et al., *Characterizing a novel and adjustable noninvasive murine joint loading model.* Arthritis Rheum, 2011. **63**(1): p. 137-47.

62. Christiansen, B.A., et al., *Non-invasive mouse models of post-traumatic osteoarthritis.* Osteoarthritis Cartilage, 2015. **23**(10): p. 1627-38.

63. Furman, B.D., et al., *Joint degeneration following closed intraarticular fracture in the mouse knee: a model of posttraumatic arthritis.* J Orthop Res, 2007. **25**(5): p. 578-92.

64. Christiansen, B.A., et al., *Musculoskeletal changes following non-invasive knee injury using a novel mouse model of post-traumatic osteoarthritis.* Osteoarthritis Cartilage, 2012. **20**(7): p. 773-82.

65. Ko, F.C., et al., *In vivo cyclic compression causes cartilage degeneration and subchondral bone changes in mouse tibiae.* Arthritis Rheum, 2013. **65**(6): p. 1569-78.

66. Lockwood, K.A., et al., *Comparison of loading rate-dependent injury modes in a murine model of post-traumatic osteoarthritis.* J Orthop Res, 2014. **32**(1): p. 79-88.

67. Dahlberg, L., et al., *Cartilage metabolism in the injured and uninjured knee of the same patient.* Ann Rheum Dis, 1994. **53**(12): p. 823-7.

68. Tonge, D.P., M.J. Pearson, and S.W. Jones, *The hallmarks of osteoarthritis and the potential to develop personalised disease-modifying pharmacological therapeutics.* Osteoarthritis Cartilage, 2014. **22**(5): p. 609-21.

69. Swagerty, D.L., Jr. and D. Hellinger, *Radiographic assessment of osteoarthritis.* Am Fam Physician, 2001. **64**(2): p. 279-86.

70. Glasson, S.S., et al., *The OARSI histopathology initiative - recommendations for histological assessments of osteoarthritis in the mouse.* Osteoarthritis Cartilage, 2010. **18 Suppl 3**: p. S17-23.

71. Tocchi, A. and W.C. Parks, *Functional interactions between matrix metalloproteinases and glycosaminoglycans.* FEBS J, 2013. **280**(10): p. 2332-41.

72. Sorokin, L., *The impact of the extracellular matrix on inflammation.* Nat Rev Immunol, 2010. **10**(10): p. 712-23.

73. Ishiguro, N., T. Kojima, and A.R. Poole, *Mechanism of cartilage destruction in osteoarthritis.* Nagoya J Med Sci, 2002. **65**(3-4): p. 73-84.

74. Khokha, R., A. Murthy, and A. Weiss, *Metalloproteinases and their natural inhibitors in inflammation and immunity.* Nat Rev Immunol, 2013. **13**(9): p. 649-65.

75. Page-McCaw, A., A.J. Ewald, and Z. Werb, *Matrix metalloproteinases and the regulation of tissue remodelling.* Nat Rev Mol Cell Biol, 2007. **8**(3): p. 221-33.

76. Haller, J.M., et al., *Intraarticular Matrix Metalloproteinases and Aggrecan Degradation Are Elevated After Articular Fracture.* Clin Orthop Relat Res, 2015. **473**(10): p. 3280-8.

77. Martignetti, J.A., et al., *Mutation of the matrix metalloproteinase 2 gene (MMP2) causes a multicentric osteolysis and arthritis syndrome.* Nat Genet, 2001. **28**(3): p. 261-5.

78. Mosig, R.A., et al., *Loss of MMP-2 disrupts skeletal and craniofacial development and results in decreased bone mineralization, joint erosion and defects in osteoblast and osteoclast growth.* Hum Mol Genet, 2007. **16**(9): p. 1113-23.

79. Mudgett, J.S., et al., *Susceptibility of stromelysin 1-deficient mice to collagen-induced arthritis and cartilage destruction.* Arthritis Rheum, 1998. **41**(1): p. 110-21.

80.   Heilpern, A.J., et al., *Matrix metalloproteinase 9 plays a key role in lyme arthritis but not in dissemination of Borrelia burgdorferi.* Infect Immun, 2009. **77**(7): p. 2643-9.

81.   Chen, J., et al., *Estrogen via estrogen receptor beta partially inhibits mandibular condylar cartilage growth.* Osteoarthritis Cartilage, 2014. **22**(11): p. 1861-8.

82.   Murphy, G. and H. Nagase, *Reappraising metalloproteinases in rheumatoid arthritis and osteoarthritis: destruction or repair?* Nat Clin Pract Rheumatol, 2008. **4**(3): p. 128-35.

83.   Raducanu, A. and A. Aszódi, *Knock-Out Mice in Osteoarthritis Research* Current Rheumatology Reviews, 2008. **4**(3).

84.   Nelson, W.J. and R. Nusse, *Convergence of Wnt, beta-catenin, and cadherin pathways.* Science, 2004. **303**(5663): p. 1483-7.

85.   Moon, R.T., *Wnt/beta-catenin pathway.* Sci STKE, 2005. **2005**(271): p. cm1.

86.   Moon, R.T., et al., *WNT and beta-catenin signalling: diseases and therapies.* Nat Rev Genet, 2004. **5**(9): p. 691-701.

87.   Baron, R. and M. Kneissel, *WNT signaling in bone homeostasis and disease: from human mutations to treatments.* Nat Med, 2013. **19**(2): p. 179-92.

88.   Bodine, P.V., et al., *A small molecule inhibitor of the Wnt antagonist secreted frizzled-related protein-1 stimulates bone formation.* Bone, 2009. **44**(6): p. 1063-8.

89.   Morvan, F., et al., *Deletion of a single allele of the Dkk1 gene leads to an increase in bone formation and bone mass.* J Bone Miner Res, 2006. **21**(6): p. 934-45.

90.   Li, X., et al., *Targeted deletion of the sclerostin gene in mice results in increased bone formation and bone strength.* J Bone Miner Res, 2008. **23**(6): p. 860-9.

91.   Kramer, I., et al., *Parathyroid hormone (PTH)-induced bone gain is blunted in SOST overexpressing and deficient mice.* J Bone Miner Res, 2010. **25**(2): p. 178-89.

92.   Loots, G.G., et al., *Genomic deletion of a long-range bone enhancer misregulates sclerostin in Van Buchem disease.* Genome Res, 2005. **15**(7): p. 928-35.

93.   Gong, Y., et al., *LDL receptor-related protein 5 (LRP5) affects bone accrual and eye development.* Cell, 2001. **107**(4): p. 513-23.

94.   Little, R.D., et al., *A mutation in the LDL receptor-related protein 5 gene results in the autosomal dominant high-bone-mass trait.* Am J Hum Genet, 2002. **70**(1): p. 11-9.

95.   Boyden, L.M., et al., *High bone density due to a mutation in LDL-receptor-related protein 5.* N Engl J Med, 2002. **346**(20): p. 1513-21.

96.   Cui, Y., et al., *Lrp5 functions in bone to regulate bone mass.* Nat Med, 2011. **17**(6): p. 684-91.

97.   van Dinther, M., et al., *Anti-Sclerostin antibody inhibits internalization of Sclerostin and Sclerostin-mediated antagonism of Wnt/LRP6 signaling.* PLoS One, 2013. **8**(4): p. e62295.

98.   Li, X., et al., *Sclerostin binds to LRP5/6 and antagonizes canonical Wnt signaling.* J Biol Chem, 2005. **280**(20): p. 19883-7.

99.   Brunkow, M.E., et al., *Bone dysplasia sclerosteosis results from loss of the SOST gene product, a novel cystine knot-containing protein.* Am J Hum Genet, 2001. **68**(3): p. 577-89.

100.   Balemans, W., et al., *Identification of a 52 kb deletion downstream of the SOST gene in patients with van Buchem disease.* J Med Genet, 2002. **39**(2): p. 91-7.

101.   Krause, C., et al., *Distinct modes of inhibition by sclerostin on bone morphogenetic protein and Wnt signaling pathways.* J Biol Chem, 2010. **285**(53): p. 41614-26.

102.   Collette, N.M., et al., *Targeted deletion of Sost distal enhancer increases bone formation and bone mass.* Proc Natl Acad Sci U S A, 2012. **109**(35): p. 14092-7.

103.   Collette, N.M., et al., *Genetic evidence that SOST inhibits WNT signaling in the limb.* Dev Biol, 2010. **342**(2): p. 169-79.

104.   Balemans, W., et al., *The binding between sclerostin and LRP5 is altered by DKK1 and by high-bone mass LRP5 mutations.* Calcif Tissue Int, 2008. **82**(6): p. 445-53.

105.   Ke, H.Z., et al., *Sclerostin and Dickkopf-1 as therapeutic targets in bone diseases.* Endocr Rev, 2012. **33**(5): p. 747-83.

106.   Lewiecki, E.M., *New targets for intervention in the treatment of postmenopausal osteoporosis.* Nat Rev Rheumatol, 2011. **7**(11): p. 631-8.

107.   Goldring, M.B., *Chondrogenesis, chondrocyte differentiation, and articular cartilage metabolism in health and osteoarthritis.* Ther Adv Musculoskelet Dis, 2012. **4**(4): p. 269-85.

108.   Lodewyckx, L., F.P. Luyten, and R.J. Lories, *Genetic deletion of low-density lipoprotein receptor-related protein 5 increases cartilage degradation in instability-induced osteoarthritis.* Rheumatology (Oxford), 2012. **51**(11): p. 1973-8.

109.   Joiner, D.M., et al., *Heterozygosity for an inactivating mutation in low-density lipoprotein-related receptor 6 (Lrp6) increases osteoarthritis severity in mice after ligament and meniscus injury.* Osteoarthritis Cartilage, 2013. **21**(10): p. 1576-85.

110.   Weng, L.H., et al., *Inflammation induction of Dickkopf-1 mediates chondrocyte apoptosis in osteoarthritic joint.* Osteoarthritis Cartilage, 2009. **17**(7): p. 933-43.

111.   Oh, H., C.H. Chun, and J.S. Chun, *Dkk-1 expression in chondrocytes inhibits experimental osteoarthritic cartilage destruction in mice.* Arthritis Rheum, 2012. **64**(8): p. 2568-78.

112. Thysen, S., F.P. Luyten, and R.J. Lories, *Loss of Frzb and Sfrp1 differentially affects joint homeostasis in instability-induced osteoarthritis.* Osteoarthritis Cartilage, 2015. **23**(2): p. 275-9.
113. Chan, B.Y., et al., *Increased chondrocyte sclerostin may protect against cartilage degradation in osteoarthritis.* Osteoarthritis Cartilage, 2011. **19**(7): p. 874-85.
114. Roudier, M., et al., *Sclerostin is expressed in articular cartilage but loss or inhibition does not affect cartilage remodeling during aging or following mechanical injury.* Arthritis Rheum, 2013. **65**(3): p. 721-31.
115. Corr, M., *Wnt-beta-catenin signaling in the pathogenesis of osteoarthritis.* Nat Clin Pract Rheumatol, 2008. **4**(10): p. 550-6.
116. Ma, B., et al., *WNT signaling and cartilage: of mice and men.* Calcif Tissue Int, 2013. **92**(5): p. 399-411.
117. Karlsson, C., et al., *Genome-wide expression profiling reveals new candidate genes associated with osteoarthritis.* Osteoarthritis Cartilage, 2010. **18**(4): p. 581-92.
118. Bouaziz, W., et al., *Loss of sclerostin promotes osteoarthritis in mice via beta-catenin-dependent and -independent Wnt pathways.* Arthritis Res Ther, 2015. **17**: p. 24.
119. Dejour, H., et al., *Arthrosis of the knee in chronic anterior laxity.* Orthop Traumatol Surg Res, 2014. **100**(1): p. 49-58.
120. Panzer, S., et al., *3-T MRI assessment of ostephyte formation in patients with unilateral anterior cruciate ligament injury and reconstruction.* Skeletal Radiol, 2012. **41**(12): p. 1597-604.
121. Zhu, M., et al., *Activation of beta-catenin signaling in articular chondrocytes leads to osteoarthritis-like phenotype in adult beta-catenin conditional activation mice.* J Bone Miner Res, 2009. **24**(1): p. 12-21.
122. Hwang, S.G., et al., *Regulation of beta-catenin signaling and maintenance of chondrocyte differentiation by ubiquitin-independent proteasomal degradation of alpha-catenin.* J Biol Chem, 2005. **280**(13): p. 12758-65.
123. Itin, P.H., B. Keseru, and V. Hauser, *Syndactyly/brachyphalangy and nail dysplasias as marker lesions for sclerosteosis.* Dermatology, 2001. **202**(3): p. 259-60.
124. Nobrega, M.A., et al., *Scanning human gene deserts for long-range enhancers.* Science, 2003. **302**(5644): p. 413.
125. Gerwin, N., et al., *The OARSI histopathology initiative - recommendations for histological assessments of osteoarthritis in the rat.* Osteoarthritis Cartilage, 2010. **18 Suppl 3**: p. S24-34.
126. Yee, C.S., et al., *Sclerostin antibody treatment improves fracture outcomes in a Type I diabetic mouse model.* Bone, 2016. **82**: p. 122-34.
127. Bouxsein, M.L., et al., *Guidelines for assessment of bone microstructure in rodents using micro-computed tomography.* J Bone Miner Res, 2010. **25**(7): p. 1468-86.
128. Schmieder, R. and R. Edwards, *Quality control and preprocessing of metagenomic datasets.* Bioinformatics, 2011. **27**(6): p. 863-4.

129. Trapnell, C., L. Pachter, and S.L. Salzberg, *TopHat: discovering splice junctions with RNA-Seq.* Bioinformatics, 2009. **25**(9): p. 1105-11.

130. Trapnell, C., et al., *Transcript assembly and quantification by RNA-Seq reveals unannotated transcripts and isoform switching during cell differentiation.* Nat Biotechnol, 2010. **28**(5): p. 511-5.

131. Huang da, W., B.T. Sherman, and R.A. Lempicki, *Systematic and integrative analysis of large gene lists using DAVID bioinformatics resources.* Nat Protoc, 2009. **4**(1): p. 44-57.

132. Tchetverikov, I., et al., *MMP protein and activity levels in synovial fluid from patients with joint injury, inflammatory arthritis, and osteoarthritis.* Ann Rheum Dis, 2005. **64**(5): p. 694-8.

133. Tetlow, L.C., D.J. Adlam, and D.E. Woolley, *Matrix metalloproteinase and proinflammatory cytokine production by chondrocytes of human osteoarthritic cartilage: associations with degenerative changes.* Arthritis Rheum, 2001. **44**(3): p. 585-94.

134. Glasson, S.S., *In vivo osteoarthritis target validation utilizing genetically-modified mice.* Curr Drug Targets, 2007. **8**(2): p. 367-76.

135. Reppe, S., et al., *Methylation of bone SOST, its mRNA, and serum sclerostin levels correlate strongly with fracture risk in postmenopausal women.* J Bone Miner Res, 2015. **30**(2): p. 249-56.

136. Mabey, T., et al., *Plasma and synovial fluid sclerostin are inversely associated with radiographic severity of knee osteoarthritis.* Clin Biochem, 2014. **47**(7-8): p. 547-51.

137. Lambert, C., et al., *Gene expression pattern of cells from inflamed and normal areas of osteoarthritis synovial membrane.* Arthritis Rheumatol, 2014. **66**(4): p. 960-8.

138. Sun, Y., et al., *Analysis of meniscal degeneration and meniscal gene expression.* BMC Musculoskelet Disord, 2010. **11**: p. 19.

139. Ramos, Y.F., et al., *Genes involved in the osteoarthritis process identified through genome wide expression analysis in articular cartilage; the RAAK study.* PLoS One, 2014. **9**(7): p. e103056.

140. Klinger, P., et al., *The Transient Chondrocyte Phenotype in Human Osteophytic Cartilage: A Role of Pigment Epithelium-Derived Factor?* Cartilage, 2013. **4**(3): p. 249-55.

141. Chou, C.H., et al., *Genome-wide expression profiles of subchondral bone in osteoarthritis.* Arthritis Res Ther, 2013. **15**(6): p. R190.

142. Fang, H. and F. Beier, *Mouse models of osteoarthritis: modelling risk factors and assessing outcomes.* Nat Rev Rheumatol, 2014. **10**(7): p. 413-21.

143. Little, C.B. and D.J. Hunter, *Post-traumatic osteoarthritis: from mouse models to clinical trials.* Nat Rev Rheumatol, 2013. **9**(8): p. 485-97.

144. Kapoor, M., et al., *Role of proinflammatory cytokines in the pathophysiology of osteoarthritis.* Nat Rev Rheumatol, 2011. **7**(1): p. 33-42.

145. Wieland, H.A., et al., *Osteoarthritis - an untreatable disease?* Nat Rev Drug Discov, 2005. **4**(4): p. 331-44.

146. Christiansen, B.A., et al., *Musculoskeletal changes following non-invasive knee injury using a novel mouse model of post-traumatic osteoarthritis.* Osteoarthritis Cartilage, 2012.

147. Bateman, J.F., et al., *Transcriptomics of wild-type mice and mice lacking ADAMTS-5 activity identifies genes involved in osteoarthritis initiation and cartilage destruction.* Arthritis Rheum, 2013. **65**(6): p. 1547-60.

148. Loeser, R.F., et al., *Microarray analysis reveals age-related differences in gene expression during the development of osteoarthritis in mice.* Arthritis Rheum, 2012. **64**(3): p. 705-17.

149. Liao, Y., G.K. Smyth, and W. Shi, *featureCounts: an efficient general purpose program for assigning sequence reads to genomic features.* Bioinformatics, 2014. **30**(7): p. 923-30.

150. Law, C.W., et al., *voom: Precision weights unlock linear model analysis tools for RNA-seq read counts.* Genome Biol, 2014. **15**(2): p. R29.

151. Smyth, G.K., *Linear models and empirical bayes methods for assessing differential expression in microarray experiments.* Stat Appl Genet Mol Biol, 2004. **3**: p. Article3.

152. Ritchie, M.E., et al., *limma powers differential expression analyses for RNA-sequencing and microarray studies.* Nucleic Acids Res, 2015. **43**(7): p. e47.

153. Gentleman, R.C., et al., *Bioconductor: open software development for computational biology and bioinformatics.* Genome Biol, 2004. **5**(10): p. R80.

154. Loeser, R.F., et al., *Disease progression and phasic changes in gene expression in a mouse model of osteoarthritis.* PLoS One, 2013. **8**(1): p. e54633.

155. Irizarry, R.A., et al., *Exploration, normalization, and summaries of high density oligonucleotide array probe level data.* Biostatistics, 2003. **4**(2): p. 249-64.

156. Harrow, J., et al., *GENCODE: the reference human genome annotation for The ENCODE Project.* Genome Res, 2012. **22**(9): p. 1760-74.

157. Kaimal, V., et al., *ToppCluster: a multiple gene list feature analyzer for comparative enrichment clustering and network-based dissection of biological systems.* Nucleic Acids Res, 2010. **38**(Web Server issue): p. W96-102.

158. Shannon, P., et al., *Cytoscape: a software environment for integrated models of biomolecular interaction networks.* Genome Res, 2003. **13**(11): p. 2498-504.

159. Christiansen, B.A., et al., *Non-Invasive Mouse Models of Post-Traumatic Osteoarthritis.* Osteoarthritis Cartilage, 2015.

160. Gardiner, M.D., et al., *Transcriptional analysis of micro-dissected articular cartilage in post-traumatic murine osteoarthritis.* Osteoarthritis Cartilage, 2015. **23**(4): p. 616-28.

161. Scanzello, C.R., et al., *Fibronectin splice variation in human knee cartilage, meniscus and synovial membrane: observations in osteoarthritic knee.* J Orthop Res, 2015. **33**(4): p. 556-62.

162. Jiao, Q., et al., *Cartilage oligomeric matrix protein and hyaluronic acid are sensitive serum biomarkers for early cartilage lesions in the knee joint.* Biomarkers, 2015: p. 1-6.

163. Wei, T., et al., *Analysis of early changes in the articular cartilage transcriptisome in the rat meniscal tear model of osteoarthritis: pathway comparisons with the rat anterior cruciate transection model and with human osteoarthritic cartilage.* Osteoarthritis Cartilage, 2010. **18**(7): p. 992-1000.

164. Echtermeyer, F., et al., *Syndecan-4 regulates ADAMTS-5 activation and cartilage breakdown in osteoarthritis.* Nat Med, 2009. **15**(9): p. 1072-6.

165. Seemayer, C.A., et al., *Cartilage destruction mediated by synovial fibroblasts does not depend on proliferation in rheumatoid arthritis.* Am J Pathol, 2003. **162**(5): p. 1549-57.

166. Zhang, H., X. Chen, and M.R. Sairam, *Novel genes of visceral adiposity: identification of mouse and human mesenteric estrogen-dependent adipose (MEDA)-4 gene and its adipogenic function.* Endocrinology, 2012. **153**(6): p. 2665-76.

167. Sohaskey, M.L., et al., *Osteopotentia regulates osteoblast maturation, bone formation, and skeletal integrity in mice.* J Cell Biol, 2010. **189**(3): p. 511-25.

168. Baird, A.E., et al., *Genome-wide association study identifies genomic regions of association for cruciate ligament rupture in Newfoundland dogs.* Anim Genet, 2014. **45**(4): p. 542-9.

169. Snelling, S., et al., *A gene expression study of normal and damaged cartilage in anteromedial gonarthrosis, a phenotype of osteoarthritis.* Osteoarthritis Cartilage, 2014. **22**(2): p. 334-43.

170. Murayama, M.A., et al., *CTRP3 plays an important role in the development of collagen-induced arthritis in mice.* Biochem Biophys Res Commun, 2014. **443**(1): p. 42-8.

171. Bushby, K.M., J. Collins, and D. Hicks, *Collagen type VI myopathies.* Adv Exp Med Biol, 2014. **802**: p. 185-99.

172. Watanabe, T., et al., *Dnm3os, a non-coding RNA, is required for normal growth and skeletal development in mice.* Dev Dyn, 2008. **237**(12): p. 3738-48.

173. Steck, E., et al., *Regulation of H19 and its encoded microRNA-675 in osteoarthritis and under anabolic and catabolic in vitro conditions.* J Mol Med (Berl), 2012. **90**(10): p. 1185-95.

174. Goncalves, C.M., et al., *Molecular cloning and analysis of SSc5D, a new member of the scavenger receptor cysteine-rich superfamily.* Mol Immunol, 2009. **46**(13): p. 2585-96.

175. Yoshida, H., et al., *KIAA1199, a deafness gene of unknown function, is a new hyaluronan binding protein involved in hyaluronan depolymerization.* Proc Natl Acad Sci U S A, 2013. **110**(14): p. 5612-7.
176. Balakrishnan, L., et al., *Differential proteomic analysis of synovial fluid from rheumatoid arthritis and osteoarthritis patients.* Clin Proteomics, 2014. **11**(1): p. 1.
177. Yang, X., et al., *KIAA1199 as a potential diagnostic biomarker of rheumatoid arthritis related to angiogenesis.* Arthritis Res Ther, 2015. **17**: p. 140.
178. Lorenz, J. and S. Grassel, *Experimental osteoarthritis models in mice.* Methods Mol Biol, 2014. **1194**: p. 401-19.
179. Martel-Pelletier, J., D.J. Welsch, and J.P. Pelletier, *Metalloproteases and inhibitors in arthritic diseases.* Best Pract Res Clin Rheumatol, 2001. **15**(5): p. 805-29.
180. van den Berg, W.B., *Osteoarthritis year 2010 in review: pathomechanisms.* Osteoarthritis Cartilage, 2011. **19**(4): p. 338-41.
181. Ward, B.D., et al., *Absence of posttraumatic arthritis following intraarticular fracture in the MRL/MpJ mouse.* Arthritis Rheum, 2008. **58**(3): p. 744-53.
182. Rajnoch, C., et al., *Regeneration of the ear after wounding in different mouse strains is dependent on the severity of wound trauma.* Dev Dyn, 2003. **226**(2): p. 388-97.
183. Clark, L.D., R.K. Clark, and E. Heber-Katz, *A new murine model for mammalian wound repair and regeneration.* Clin Immunol Immunopathol, 1998. **88**(1): p. 35-45.
184. Ueno, M., et al., *Accelerated wound healing of alkali-burned corneas in MRL mice is associated with a reduced inflammatory signature.* Invest Ophthalmol Vis Sci, 2005. **46**(11): p. 4097-106.
185. Mason, R.M., et al., *The STR/ort mouse and its use as a model of osteoarthritis.* Osteoarthritis Cartilage, 2001. **9**(2): p. 85-91.
186. Walton, M., *Degenerative joint disease in the mouse knee; radiological and morphological observations.* J Pathol, 1977. **123**(2): p. 97-107.
187. Kyostio-Moore, S., et al., *STR/ort mice, a model for spontaneous osteoarthritis, exhibit elevated levels of both local and systemic inflammatory markers.* Comp Med, 2011. **61**(4): p. 346-55.
188. Aigner, T., et al., *Large-scale gene expression profiling reveals major pathogenetic pathways of cartilage degeneration in osteoarthritis.* Arthritis Rheum, 2006. **54**(11): p. 3533-44.
189. Watters, J.W., et al., *Inverse relationship between matrix remodeling and lipid metabolism during osteoarthritis progression in the STR/Ort mouse.* Arthritis Rheum, 2007. **56**(9): p. 2999-3009.
190. Staines, K.A., et al., *Endochondral growth defect and deployment of transient chondrocyte behaviours underlie osteoarthritis onset in a natural murine model.* Arthritis Rheumatol, 2015.

191. Kumagai, K., et al., *Spontaneously developed osteoarthritis in the temporomandibular joint in STR/ort mice.* Biomed Rep, 2015. **3**(4): p. 453-456.

192. Beederman, M., et al., *BMP signaling in mesenchymal stem cell differentiation and bone formation.* J Biomed Sci Eng, 2013. **6**(8A): p. 32-52.

193. Nishimura, R., et al., *Regulation of bone and cartilage development by network between BMP signalling and transcription factors.* J Biochem, 2012. **151**(3): p. 247-54.

194. Rosen, V., *BMP and BMP inhibitors in bone.* Ann N Y Acad Sci, 2006. **1068**: p. 19-25.

195. Gazzerro, E., et al., *Conditional deletion of gremlin causes a transient increase in bone formation and bone mass.* J Biol Chem, 2007. **282**(43): p. 31549-57.

196. Khokha, M.K., et al., *Gremlin is the BMP antagonist required for maintenance of Shh and Fgf signals during limb patterning.* Nat Genet, 2003. **34**(3): p. 303-7.

197. Myers, M., et al., *Loss of gremlin delays primordial follicle assembly but does not affect female fertility in mice.* Biol Reprod, 2011. **85**(6): p. 1175-82.

198. Brunet, L.J., et al., *Noggin, cartilage morphogenesis, and joint formation in the mammalian skeleton.* Science, 1998. **280**(5368): p. 1455-7.

199. Stottmann, R.W., et al., *The BMP antagonist Noggin promotes cranial and spinal neurulation by distinct mechanisms.* Dev Biol, 2006. **295**(2): p. 647-63.

200. Tylzanowski, P., L. Mebis, and F.P. Luyten, *The Noggin null mouse phenotype is strain dependent and haploinsufficiency leads to skeletal defects.* Dev Dyn, 2006. **235**(6): p. 1599-607.

201. Stafford, D.A., et al., *Cooperative activity of noggin and gremlin 1 in axial skeleton development.* Development, 2011. **138**(5): p. 1005-14.

202. Akiyama, H., et al., *The transcription factor Sox9 has essential roles in successive steps of the chondrocyte differentiation pathway and is required for expression of Sox5 and Sox6.* Genes Dev, 2002. **16**(21): p. 2813-28.

203. Ovchinnikov, D.A., et al., *Col2a1-directed expression of Cre recombinase in differentiating chondrocytes in transgenic mice.* Genesis, 2000. **26**(2): p. 145-6.